

Spring 4-5-2013

When Does A Stream Gain The Ability To Create Its Own Channel? A Field Study In Northwest Georgia On The Conasauga River

Roy H. Srymanske
rsrymanske

Follow this and additional works at: https://scholarworks.gsu.edu/geosciences_theses

Recommended Citation

Srymanske, Roy H., "When Does A Stream Gain The Ability To Create Its Own Channel? A Field Study In Northwest Georgia On The Conasauga River." Thesis, Georgia State University, 2013.
https://scholarworks.gsu.edu/geosciences_theses/57

This Thesis is brought to you for free and open access by the Department of Geosciences at ScholarWorks @ Georgia State University. It has been accepted for inclusion in Geosciences Theses by an authorized administrator of ScholarWorks @ Georgia State University. For more information, please contact scholarworks@gsu.edu.

WHEN DOES A STREAM GAIN THE ABILITY TO CREATE ITS OWN CHANNEL?

A FIELD STUDY IN NORTHWEST GEORGIA ON THE CONASAUGA RIVER

by

ROY SRYMANSKE

Under the Direction of Dr. Seth Rose

ABSTRACT

Rivers are said to be self-shaping when a stream is able to create its own morphological features. This occurs when bankfull Shields stress (τ_{bf}^*) is greater than reference Shields stress (τ_r^*). Shields stress in the channel is affected during upstream progression by the height and width of the water decreasing, the slope becoming steeper, and the bed material becoming coarser. Bankfull Shields stress decreased progressing upstream while reference Shields stress increased due to increased slope. The self-shaping portions of the Conasauga occur in areas where the relative roughness of the bed material is fully submerged or greater than 5. Once the relative submergence is no longer fully submerged the stream channel no longer produces enough bankfull Shields stress to overcome the reference Shields stress. This occurs about midway through the study. This study allows better classification of streams using Shields stress and better understanding of channel processes for hydrologic engineering.

INDEX WORDS: Geology, Shield stress, Gravel bed mountain streams

WHEN DOES A STREAM GAIN THE ABILITY TO CREATE ITS OWN CHANNEL?
A FIELD STUDY IN NORTHWEST GEORGIA ON THE CONASAUGA RIVER

by

ROY SRYMANSKE

A Thesis Submitted in Partial Fulfillment of the Requirements for the Degree

Master of Science

in the College of Arts and Sciences

Georgia State University

2013

Copyright by
Roy Hill Srymanske
2013

WHEN DOES A STREAM GAIN THE ABILITY TO CREATE ITS OWN CHANNEL?

A FIELD STUDY IN NORTHWEST GEORGIA ON THE CONASAUGA RIVER

by

ROY SRYMANSKE

Committee Chair: Dr. Seth Rose

Committee: Dr. Jordan Clayton

Dr. Daniel Deocampo

Electronic Version Approved:

Office of Graduate Studies

College of Arts and Sciences

Georgia State University

May 2013

TABLE OF CONTENTS

LIST OF TABLES	v
LIST OF FIGURES	vi
LIST OF ABBREVIATIONS	xii
1. INTRODUCTION.....	1
2. INTRODUCTION TO THE PROBLEM	3
3. LITERATURE REVIEW	5
4. RESEARCH QUESTION	16
5. SETTING.....	18
6. METHODS	20
<i>6.1 OVERVIEW</i>	20
<i>6.2 SPECIFIC METHODOLOGY</i>	20
7. RESULTS	27
8. DISCUSSION	77
9. CONCLUSIONS	89
REFERENCES.....	91

LIST OF TABLES

Table 1. Elementary classification of alluvial river channels and riverine landscapes (excerpt from Church, 2006 Table 1).....	10
Table 2. Measurements of D_{90} and D_{50} , bankfull Shields stress (τ_{bf}^*), and reference Shields stress (τ_r^*) for all cross-section. No data is presented for cross-section 6 due to the lack of grain size data resulting from high slope and bedrock surface at the cross-section.	70
Table 3. Measurements of D_{90} , D_{50} , slope, width, height, and submergence. No grain size or submergence data is presented for cross-section 6 due to the lack of grain size data resulting from high slope and bedrock surface at the cross-section.	74
Table 4. Values for grain size dependent bankfull Shields stress, slope dependent bankfull Shields stress, and ratios for comparison between the different methods. No data is presented for cross-section 6 due to the lack of grain size data resulting from high slope and bedrock surface at the cross-section.....	79

LIST OF FIGURES

Figure 1. Relationship between bankfull and reference Shields stress for forty five headwater streams (from Mueller et al. 2005, Fig. 6).	4
Figure 2. Relationship between bankfull discharge (\hat{Q}) and channel width (\hat{B}) (Parker et al., 2007, Figure 3.21).	11
Figure 3. Relationship between bankfull discharge (\hat{Q}) and height of the water at bankfull (\hat{H}) (Parker et al., 2007, Figure 3.20)	12
Figure 4. Relationship between bankfull discharge (\hat{Q}) and channel bed slope (S) (Parker et al., 2007, Figure 3.22).	12
Figure 5. Relationship between bankfull discharge (\hat{Q}) and bankfull Shields stress (τ_{bf50}^*) (Parker et al., 2007, Figure 3.23)	12
Figure 6. Relationship between dimensionless critical Shields stress (τ_c^*) and relative roughness given by H/D_{50} (from Lenzi et al., 2006, Figure 4).	13
Figure 7. Map showing the study area, the Conasauga River drainage, and the trail system used to access the river. The X represents the location of the initial benchmark for the longitudinal survey.....	19
Figure 8. Longitudinal profile of the study area with the most downstream cross section located on the left of the figure, cross-section 1 is located at 0 meters and is 600 meters downstream from the intersection of the Conasauga River and Trail 90.	27
Figure 9. Cross-section 1, the red line represents bankfull conditions.	28
Figure 10. B axis distribution for cross-section 1.	29
Figure 11. Photo of cross-section 1, view is downstream.	29
Figure 12. Cross-section 2, the red line represents bankfull conditions.....	30

Figure 13.	B axis distribution of cross-section 2.....	30
Figure 14.	Photo of cross-section 2, view is downstream.	31
Figure 15.	Cross-section 3, red line represents bankfull conditions.	31
Figure 16.	B axis distribution of cross-section 3.....	32
Figure 17.	Photo of cross-section 3, view is downstream.	32
Figure 18.	Cross-section 4 is bisected by an island and splits the flow of the river into 2 channels, the red line represents the bankfull conditions in the downstream facing left channel and the green line represents the bankfull conditions in the downstream facing right channel. ..	33
Figure 19.	B axis distribution of cross-section 4 for both channels.	33
Figure 20.	Photo of downstream facing right channel on cross-section 4, view is upstream. .	34
Figure 21.	Photo of island in cross-section 4, view downstream.	34
Figure 22.	Photo of downstream facing left channel on cross-section 4, view upstream.	35
Figure 23.	Cross-section 5, the red line represents bankfull conditions.....	35
Figure 24.	B axis distribution of cross-section 5.....	36
Figure 25.	Photo of cross-section 5, view is downstream.	36
Figure 26.	Cross-section 6, the red line represents bankfull conditions.....	37
Figure 27.	Photo of cross-section 6, view is upstream.	37
Figure 28.	Cross-section 7, Trail 90 crosses Conasauga River on this cross-section, red line represents bankfull conditions.	38
Figure 29.	B axis distribution of cross-section 7.....	38
Figure 30.	Photo of cross-section 7, view is downstream.	39
Figure 31.	Cross-section 8, red line represents bankfull conditions.	39
Figure 32.	B axis distribution of cross-section 8.....	40

Figure 33.	Photo of cross-section 8, view is upstream.....	40
Figure 34.	Cross-section 9, the red line represents bankfull conditions.....	41
Figure 35.	B axis distribution of cross-section 9.....	41
Figure 36.	Photo of cross-section 9, view is upstream.....	42
Figure 37.	Cross-section 10, the red line represents bankfull conditions.....	42
Figure 38.	B axis distribution of cross-section 10.....	43
Figure 39.	Photo of cross-section 10, view is upstream.....	43
Figure 40.	Cross-section 11, the red line represents bankfull conditions.....	44
Figure 41.	B axis distribution of cross-section 11.....	44
Figure 42.	Photo of cross-section 11, view is upstream.....	45
Figure 43.	Cross-section 12, the red line represents bankfull conditions.....	45
Figure 44.	B axis distribution of cross-section 12.....	46
Figure 45.	Photo of cross-section 12, view is upstream.....	46
Figure 46.	Cross-section 13, the red line represents bankfull conditions.....	47
Figure 47.	B axis distribution of cross-section 13.....	47
Figure 48.	Photo of cross-section 13, view is downstream.....	48
Figure 49.	Cross-section 14, the red line represents bankfull conditions.....	48
Figure 50.	B axis distribution of cross-section 14.....	49
Figure 51.	Photo of cross-section 14, view is upstream.....	49
Figure 52.	Cross-section 15, the red line represents bankfull conditions.....	50
Figure 53.	B axis distribution of cross-section 15.....	50
Figure 54.	Photo of cross-section 15, view is upstream and the tree at the bottom of the frame is above bankfull stage.....	51

Figure 55.	Cross-section 16, the red line represents bankfull conditions.....	51
Figure 56.	B axis distribution of cross-section 16.....	52
Figure 57.	Photo of cross-section 16, view is upstream.....	52
Figure 58.	Cross-section 17, the red line represents bankfull conditions.....	53
Figure 59.	B axis distribution of cross-section 17.....	53
Figure 60.	Photo of cross-section 17, view is upstream.....	54
Figure 61.	Cross-section 18, the red line represents bankfull conditions.....	54
Figure 62.	B axis distribution of cross-section 18.....	55
Figure 63.	Photo of cross-section 18, view is upstream.....	55
Figure 64.	Cross-section 19, the red line represents bankfull conditions.....	56
Figure 65.	B axis distribution of cross-section 19.....	56
Figure 66.	Photo of cross-section 19, view is upstream.....	57
Figure 67.	Cross-section 20, red line represents bankfull conditions.	57
Figure 68.	B axis distribution of cross-section 20.....	58
Figure 69.	Photo of cross-section 20, view is upstream.....	58
Figure 70.	Cross-section 21, the red line represents bankfull conditions.....	59
Figure 71.	B axis distribution of cross-section 21.....	59
Figure 72.	Photo of cross-section 21, view is upstream.....	60
Figure 73.	Cross-section 22, the red line represents bankfull conditions.....	60
Figure 74.	B axis distribution of cross-section 22.....	61
Figure 75.	Photo of cross-section 22, view is upstream.....	61
Figure 76.	Cross-section 23, the red line represents bankfull conditions.....	62
Figure 77.	B axis distribution of cross-section 23.....	62

Figure 78.	Photo of cross-section 23, view is downstream.	63
Figure 79.	Cross-section 24, the red line represents bankfull conditions.....	63
Figure 80.	B axis distribution of cross-section 24, the red line represents the D_{90} grain size and the green line represents the D_{50} grain size.....	64
Figure 81.	Photo of cross-section 24, view is downstream.	64
Figure 82.	Cross-section 25, the red line represents bankfull conditions.....	65
Figure 83.	B axis distribution of cross-section 25.....	65
Figure 84.	Photo of cross-section 25, view is downstream.	66
Figure 85.	Cross-section 26, the red line represents bankfull conditions.....	66
Figure 86.	B axis distribution of cross-section 26.....	67
Figure 87.	Photo of cross-section 26, view is downstream.	67
Figure 88.	Cross-section 27, the red line represents bankfull conditions.....	68
Figure 89.	B axis distribution of cross-section 27.....	68
Figure 90.	Photo of cross-section 27, view is downstream.	69
Figure 91.	Height of the water at bankfull conditions at each cross-section.....	71
Figure 92.	Slope of the channel at each cross-section.....	71
Figure 93.	Width of the channel at each cross-section.....	72
Figure 94.	D_{90} and D_{50} measurements at each cross-section.....	72
Figure 95.	Relative submergence of the D_{90} and D_{50} at each cross-section.....	73
Figure 96.	Bankfull Shields stress (τ_{bf}^*) verses slope.....	74
Figure 97.	Graphical representation of the ratio between bankfull Shields stress (τ_{bf}^*) and reference Shields stress (τ_r^*) by cross-section.....	76

Figure 98. Difference between bankfull Shields stress (τ_{bf}^*) and reference Shields stress (τ_r^*) at each cross-section...	76
Figure 99. Grain size dependent bankfull Shields stress (τ_{bf}^*) versus slope dependent bankfull Shields stress (τ_{bf}^*) calculation.....	80
Figure 100. Relationship between grain size bankfull Shields stress (τ_{bf}^*) and reference Shields stress (τ_r^*) and 1:1 reference line.....	82
Figure 101. Relationship between grain size bankfull Shields stress (τ_{bf}^*) and reference Shields stress (τ_r^*) with points classed above and below cross-section 14 (midpoint on longitudinal survey) and 1:1 reference line.....	82
Figure 102. Relationship between τ_r^* and height/ D_{90} or height/ D_{50}	84
Figure 103. H/D_{90} for each cross-section showing greater than or less than 5.	85
Figure 104. H/D_{50} for each cross-section showing greater than or less than 5.	85
Figure 105. Forces acting upon a single submerged particle are the hydrodynamic drag force F_D , the longitudinal component of the weight $W \sin \alpha$, and the seepage force S_e , and in the normal direction to the flow, the grain is subject to the normal weight component $W \cos \alpha$, the buoyancy B , and the hydrodynamic lift force F_L (from Gregoretti, 2008, Figure 2).....	87

LIST OF ABBREVIATIONS

τ	Shear stress exerted by the fluid
τ_{bf}^*	Bankfull Shields stress
τ_c^*	Critical Shields stress
τ_r^*	Reference Shields stress
τ_{bf50}^*	Bankfull Shields stress calculated with the D_{50}
ρ	Density of Water
ρ_s	Grain Density
g	Gravitational acceleration
D_i	Grain Size for the i th grain size
Kg	Kilogram
N	Newton
m	meter
s	Second
H	Height of the water at bankfull
B	width of the water at bankfull
Q	Discharge
H/D_i	Relative Roughness

1. INTRODUCTION

This study was conducted in the headwaters of the Conasauga River located in the Cohutta Wilderness Area, Georgia, USA. The stream channel data was gathered by measuring cross-sections, conducting a longitudinal survey, and surface sediment size analysis for evaluation of the channel thus allowing the channel to be classified as self-shaping or non-self-shaping. Streams are considered to be self-shaping once they are capable of producing their own morphological features.

Mueller et al. (2005), Church (2006), Buffington et al. (1997), and Ferguson (2012), as well as many others, have found that self-shaping streams are capable of creating their own morphological features when the bankfull Shields stress is capable of full, or nearly full, mobilization of the bed. At this point active transport becomes responsible for the morphological features of the river. Mueller et al.'s (2005) study identified that bankfull Shields stress (τ_{bf}^*) is slightly greater than reference Shields stress (τ_r^*) in self-shaping rivers.

Reference Shields stress (τ_r^*) is the calculated, or observed, amount of Shields stress imposed that produces a non-zero amount sediment transportation (Buffington et al., 1997). Reference Shields stress is not the only way to define sediment when sediment transportation begins to take place. Critical Shields stress (τ_c^*) which is used to define incipient motion can also be used to determine if sediment transportation is occurring. Incipient motion is when grains or clast on the channel bed first begin to move. There are four ways to determine when first movement occurs (Buffington et al., 1997). The first method to determine incipient motion is extrapolation from a measured bed load transport rates to zero or low reference value (Shields, 1936; Day, 1980; Parker et al., 1982; Buffington et al., 1997). The second method to determine incipient is by visual observation (Gilbert, 1914; Kramer, 1935; Yalin et al., 1979; Buffington et

al., 1997). The third method to determine incipient motion is the development of competence functions, which relate shear stress to the largest mobile grain size and can be used to establish the critical shear stress for a given grain size (Andrews, 1983; Carling, 1983; Komar, 1987a; Buffington et al., 1997). Finally the fourth method to determine incipient motion is by theoretical calculation (White, 1940; Wiberg et al., 1987; Jiang et al., 1993; Buffington et al., 1997). Reference Shields stress (τ_r^*) is analogous to the critical shear stress (τ_c^*) and can be used in its place in other bed load transport equations (Pitlick et al., 2009).

Bankfull Shields stress (τ_{bf}^*) on the other hand is the amount of stress that is acting upon the grains of the bed at bankfull conditions (Buffington et al., 1997). The amount of bankfull Shields stress on a grain size of interest is dependent upon the size of that grain, depth of the water at bankfull, and the slope of the channel. If the amount of stress present on a given grain size at bankfull conditions (bankfull Shields stress) is greater than the amount of stress needed to produce a minimum amount of transportation (reference Shields stress) for that given grain size movement of that grain size and smaller could occur. Therefore, streams that are said to be self-shaping can then be characterized by having a greater amount of bankfull Shields stress than reference Shields stress, meaning movement could occur at bankfull conditions just as Mueller et al. (2005) have shown.

In channels that are considered to be non-self-shaping the amount of Shields stress that is produced at bankfull flows is less than the reference Shields stress of the bed material. Reference Shields stress is when sediment transportation becomes non-zero and movement of sediment within the channel begins. Streams where reference Shields stress is likely higher than the bankfull Shields stress would be headwater streams, where the bed material is large in size, and the stream is not capable of producing large amounts of bankfull Shields stress. In these settings

the relationship shown by Mueller et al. (2005) would not be observed, the reference Shields stress would be greater than bankfull Shields stress and the stream would not be considered self-shaping.

This study aims to find the upper bounds of this relationship, where τ_{bf}^* is slightly greater than τ_r^* , and the relationship breaks down suggesting that the channel is transitioning to a non-alluvial state. This transition to a non-alluvial state would take place once the amount of bankfull Shields stress becomes less than the amount of reference Shields stress for the channel. In this scenario sediment transportation would not be possible due to the lack of stress on the grains from the water in the channel. Without transportation of the sediment occurring there is no way that the stream could be said to be self-shaping resulting in a non-alluvial state.

2. INTRODUCTION TO THE PROBLEM

Streams that are considered to be self-shaping produce greater amounts of bankfull Shields stress (τ_{bf}^*) than the reference Shields stress (τ_r^*) of the channel. Mueller et al. (2005) show a clear relationship between τ_r^* and τ_{bf}^* for rivers that are considered to be self-shaping, as seen in Figure 1. Figure 1 was produced from a study of 45 streams showing the amount of bankfull and reference Shields stress for each stream. Once the bankfull Shields stress becomes greater than the reference Shields stress sediment movement begins to occur and the stream can begin to adjust its channel features becoming a self-shaping stream. This relationship is consistent throughout Mueller et al.'s (2005) data set and in other studies (Buffington et al., 1997; Ferguson, 2012). Once a stream becomes self-shaping it is able to adjust the channel and form alluvial features within the stream. Before the stream is capable of making these adjustments the features within the channel are controlled by the material that makes up the

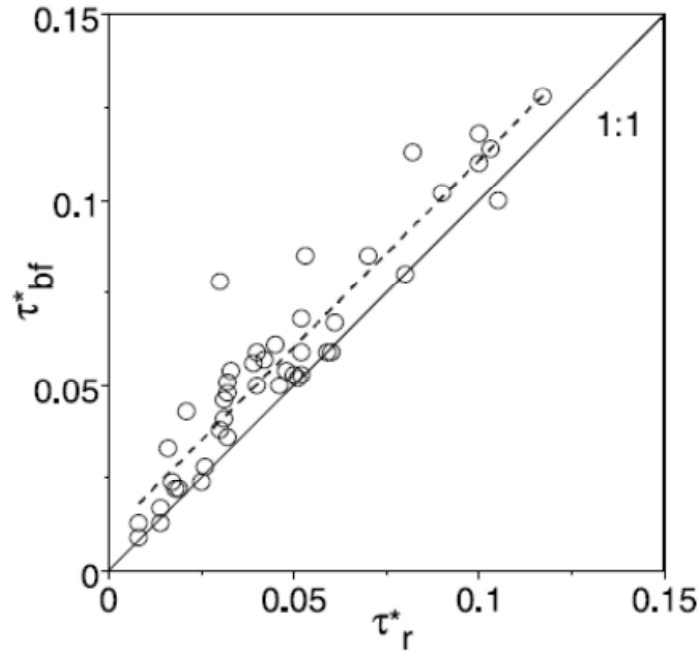


Figure 1. Relationship between bankfull and reference Shields stress for forty five headwater streams (from Mueller et al. 2005, Fig. 6).

channel. By using the relationship between bankfull and reference Shields stress, classification of streams into alluvial and non-alluvial states can be conducted. When using the relationship between bankfull Shields stress and reference Shields stress, the chances that bedload transport occurring can be better understood. Mueller et al. (2005) relate that estimates of bedload transport are used in the analysis of many different problems in hydrology such as, calculation of environmental maintenance flows, calculation of sediment loads, development of channel evolution models, and also can aid in yielding a better understanding of the effects of watershed disturbance and river management.

However, the Mueller et al. (2005) study does not include any mountain streams that are in transitional or non-alluvial phases, such as headwater locations. Mountain streams, which at some locations that I hope to identify in this study, transition to a non-alluvial state where the

bankfull Shields stress (τ_{bf}^*) is less than reference Shields stress (τ_r^*). Transitional areas may also fluctuate between bankfull Shields stress (τ_{bf}^*) and reference Shields stress (τ_r^*) being greater than one another at different locations within the transitional zone. Progressing from reaches that are considered to be self-shaping into reaches that are not self-shaping would change the relationship between bankfull Shields stress (τ_{bf}^*) and reference Shields stress (τ_r^*) and would plot differently than Figure 1. At some point this relationship will break down and the amount of bankfull Shields stress (τ_{bf}^*) will be lower than the amount of reference Shields stress (τ_r^*) or the scattering of points, when plotted like Figure 1, would increase when the stream transitions from an alluvial to a non-alluvial state.

3. LITERATURE REVIEW

In most research the streams are classified into different types of streams based on the bed material (gravel, sand, etc) and the setting where they occur (mountain, low slope, etc) (Schumm, 1963; Church, 2006). Also there is considerable interest regarding when the bed material within the stream begins to move (Buffington et al., 1997). Streams where most of the material in the bed does not move are considered to be non-alluvial. In contrast, streams that can move larger amounts of bed material are said to be alluvial.

The sediment grain size distribution found within the beds of rivers is rarely uniform; streams are termed “gravel-bed streams” if the mean or median size of the bed material is in the gravel range, which is greater than 2 mm and less than 46 mm (Parker et al., 2007). Gravel-bed rivers and streams can be further classified as being jammed, threshold, transitional, and labile channels (Schumm, 1963). Jammed channels consist of alluvial deposits that are often unmoved, whereas labile channels are completely self-shaping and consist mostly of sand and fine

sediment. Threshold and transitional channels occur between jammed and labile channels. A major way to differentiate between the different channel types is the characteristic Shield stress of the different stream types (Schumm, 1963).

In order to understand the arrangement of Schumm's classification scheme of different stream types Shields stress must first be understood. Shields stress represents the dimensionless amount of force exerted by a fluid, which can be either air or water, to cause movement of sediment (in this case) that is in the contact surface between the sediment and water (Shields, 1936). Equation 1 is the Shields stress equation:

$$\tau^* = \frac{\tau}{(\rho_s - \rho)(g)(D_i)} \quad (1)$$

where τ is the amount of shear stress exerted by the fluid in N/m^2 , ρ_s represents sediment density in kg/m^3 of the bed sediment, ρ represents the density of water in kg/m^3 , g is acceleration due to gravity in m/s^2 , D_i represents bed sediment diameter of interest in meters, and τ^* is the amount of non-dimensional Shields stress (Buffington et al., 1997). Dimensionless parameters are used in order to maintain generality in the data; this allows the equations and their results to be transferable across scales (Pitlick et al., 2009). Equation 1 can be modified to calculate the critical Shields stress of the sediment by using the critical boundary shear stress value to predict sediment movement in the stream channel and non-dimensionalize the amount of energy exerted on the grains (Buffington et al., 1997). The critical Shields stress (τ_c^*) is the amount of shear stress needed to begin sediment transport (Meyer et al., 1948; Engelund et al., 1976; Luque et al., 1976; Parker, 1990; Buffington et al., 1997; Wilcock et al. 2003; Lamb et al., 2008;).

The equation for Shields stress, Equation 1, uses τ as term when determining the amount of Shields stress for a given clast size but does not present a method for determining τ . There are several ways that the amount of boundary shear stress can be determined.

$$\tau = \rho g H S \quad (2)$$

Equation 2 is the DuBoys equation, which is a representation of the total boundary shear stress for a given location. In Equation 2, g is gravitational acceleration in m/s^2 , H is the stream depth in meters, and S is the energy slope (DuBoys, 1879). With the boundary shear stress the critical Shields stress can be calculated. The DuBoys equation (Equation 2) is limited to estimate only the amount of shear stress at a given location. The DuBoys equation does not take into account bed forms present within the channel and starts to break down in locations with high channel roughness (Garde et al., 2000). Equation 1, which derives the dimensionless Shields stress, is used to maintain consistency in the data when measuring shear stress along a stream channel where different bed forms occur or when presenting measured data between different streams in different areas (Mueller et al., 2005).

As stated above critical shear stress is the shear stress exerted on a clast when that clast starts to move. Bankfull shear stress is the amount of shear stress exerted on a clast at bankfull conditions. These two types of stress, bankfull shear stress and critical shear stress, are very different. The amount of critical Shields stress, at bankfull, needed to initiate clast movement for given sediment sizes within a channel can be calculated using Equation 1 and Equation 2 (Thompson et al. 2008). This is done by taking the height of the water at bankfull and the slope of the channel being studied in Equation 2 to calculate the shear stress on the channel. Then using the diameter and density of the sediment that is being studied, along with the amount of shear stress from Equation 1 in Equation 2 to calculate the dimensionless bankfull Shields. This

does not necessarily mean that the clast will be moved at these conditions. Various mechanisms affect the movement of a clast inhibit its movement, such as sheltering, packing, sorting, and grain arrangement on the bed surface (Buffington et al., 1997; Clayton, 2010).

Clast size must also be considered because of its importance in scaling the transport rate and defining thresholds for motion (Mueller and Pitlick, 2005). The most common way to refer to a given grain size is by referring the D_i size, where D is the diameter of the sediment or grain in meters and i indicates the percent finer than of the given diameter. In other words a D_{50} would be the diameter that 50 percent of the sample is finer than. The reference size most commonly used when talking about sediment movement is the D_{50} , but the use of the D_{90} has been proposed as a more meaningful measurement for analysis of streams with gravel sized grains (greater than 2 mm and less than 46 mm measured in the median axis) regarding its shaping ability (Reid et al., 1984, 1986; Petit, 1994; Lenzi et al., 2006).

The study of sediment transport in gravel bed streams is not a new area of research. These streams are often categorized as a single thread, alluvial gravel bed rivers that often have a surface D_{50} grain size greater than 25mm (Mueller and Pitlick, 2005). Typical mountain streams have a slope range from about 0.02 to 0.05 (Mueller et al., 2005). Mountain streams have surface D_{50} grain size greater than 25mm; this study largely focuses on significantly coarser grains present in transitional channel areas. Grain size in mountain streams can be greatly affected by sediment from landslides and debris flows, and these events will dominate sediment supply and force changes in channel gradient and grain size (Grant et al., 1990; Montgomery et al., 1997; Brummer et al., 2003; Mueller and Pitlick, 2005). Other factors influencing mountain stream morphology are the surrounding valley slope and the boundary materials of the channel being either coarse or non-alluvial (Jarrett, 1984, 1990; Grant et al., 1990; Rice et al., 1996;

Buffington et al., 1997; Wohl et al., 2005; Comiti et al., 2007; Wohl, 2007; Reid et al., 2010). As distance from the headwaters increases, fluvial sediment transport starts to dominate and the channel morphology reflects the movement of water and sediment (Emmett, 1975; Pizzuto, 1992; Whiting et al., 1999; Mueller and Pitlick, 2005). Before this transitional point channel form is dominated by the bed material and does not reflect the movement of water and sediment. The bed material, slope of the channel, height of the water, and width of the stream all play a role in the change from the non-alluvial to the alluvial state.

Calculating the Shields number for different channels yields different results based on the differences in height, slope, and bed material that can help lead to a classification system for different channels. Schumm (1963) proposed a classification scheme that gives a characteristic bankfull Shields number for each of different stream types. Church (2006) used Schumm's (1963) work to summarize the different characteristics that are found within higher gradient non-self-shaping mountain streams and lower gradient self-shaping streams. These classifications range from jammed channels that consist of mostly cobbles and gravel with a Shield's number of 0.04 as shown in Table 1, to a labile channel which is a sandy channel bed with a Shields number >1.0 (Church, 2006). Table 1 demonstrates this aspect as stream classifications changes from one to the next. The Shields number, which is associated with channel forming flows, also increases with each classification change. The sediment type in the channel also becomes finer going through the classification scheme. As sediment becomes finer the Shield number also increases, this results in an increased mobility of all sizes (Parker et al., 2007). This fining of sediment in the downstream direction directly affects the Shields stress due to the D_i value becoming smaller which increases the total amount of Shields stress calculated when using Equation 1.

Table 1. Elementary classification of alluvial river channels and riverine landscapes (excerpt from Church, 2006 Table 1).

Type/characteristic Shield's number	Sediment Type	Sediment transport regime	Channel morphology	Channel Stability
Jammed channel 0.04+	Cobble or boulder-gravel	Bed load dominated; low total transport, subject to debris flows	Step-pools or boulder cascades; low multiple of largest boulder size	Stable for long periods of time with throughput of bed load finer than structure- forming clast
Threshold channel up to 0.04+	Cobble-gravel	Bed load dominated; partial transport regime	Cobble-gravel channel bed; single thread or highly structured bed	Relatively stable for extended periods, but subject to major floods causing lateral channel instability and avulsion
Threshold channel up to 0.15	Sandy-gravel to cobble-gravel	Bed load dominated, but possibly high suspended load, partial to full mobility	Gravel to sandy- gravel; single to thread to braided	Subject to avulsion and frequent channel shifting
Transitional channel 0.15 - 1.0	Sand to fine- gravel	Mixed load, high proportion moves in suspension, full mobility with sandy bedforms	Mainly single thread, irregularly sinuous to meandered	Single-thread channels, irregular lateral instability or progressive meanders
Labile channel >1.0	Sandy channel bed, fine-sand to silt banks	Suspension dominated	Single thread, meandered with point bar development; significant levees	Single-thread, highly sinuous channel

The further downstream from the headwaters the river's ability to be self-shaping increases due to the sediment load becoming finer along with the increases in depth, width, and discharge of the stream, slope of the stream channel also becomes lower (Parker et al., 2007; Reid et al., 2010). As these variables, which are used to estimate rates of sediment transport, increase the amount of sediment transport capacity also increases (Mueller and Pitlick, 2005). As shown by Parker et al. (2007) the increase in discharge results from moving down a given watershed and with this increase in discharge the width, height, slope, and Shields stress of that stream also increase. Figures 2 and 3 both show that as bankfull discharge increases the width and the height of the water also increase. Figure 4 shows that as bankfull discharge increases the

slope of the stream decreases. And as a result of the width and height increasing and the channel slope decreasing the bankfull Shields stress on the D_{50} (τ_{bf50}^*) increases as predicted by Equation 1 as seen in Figure 5. Figures 2, 3, 4, and 5 all show the relationship between the measured parameters and the increase in bankfull discharge the further downstream from the headwaters the measurements are taken.

In conjunction with these parameters the transport rate and the reference Shields stress may also be used to learn about river channels (Mueller et al., 2005). When the channel increases in size, becomes less steep, and fining of the sediment within the stream the amount of Shields stress within the channel is influenced (Mueller et al., 2005). As a stream progresses from the headwaters, bankfull shear stress (τ) that is exerted on the bed would increase due to τ becoming

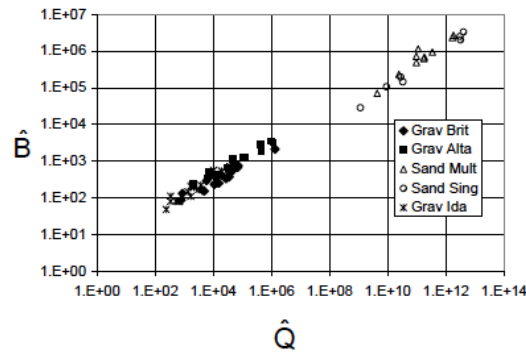


Figure 2. Relationship between bankfull discharge (\hat{Q}) and channel width (\hat{B}) (Parker et al., 2007, Figure 3.21)

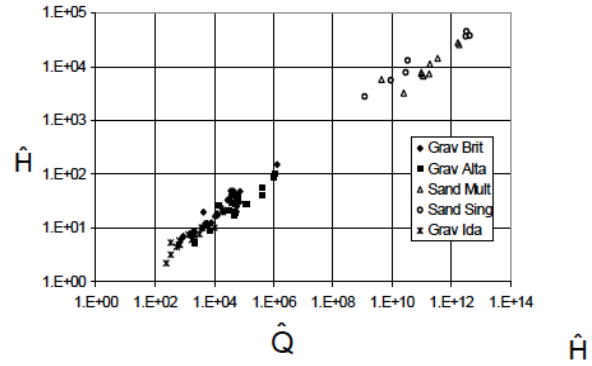


Figure 3. Relationship between bankfull discharge (\hat{Q}) and height of the water at bankfull (\hat{H}) (Parker et al., 2007, Figure 3.20)

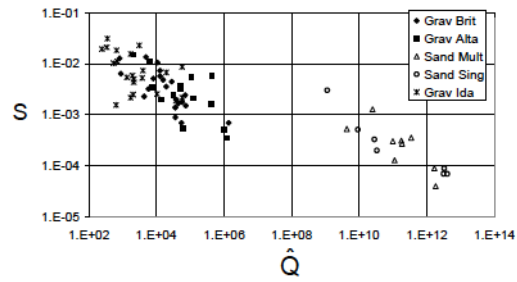


Figure 4. Relationship between bankfull discharge (\hat{Q}) and channel bed slope (S) (Parker et al., 2007, Figure 3.22)

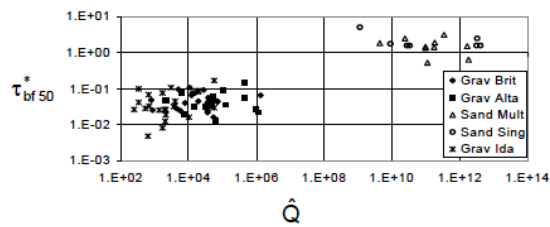


Figure 5. Relationship between bankfull discharge (\hat{Q}) and bankfull Shields stress (τ_{bf50}^*) (Parker et al., 2007, Figure 3.23)

larger in Equation 2 with an increase in height and a relatively small decrease in slope, leading to a greater shear stress (τ) in Equation 1. The amount of bankfull Shields stress (τ_{bf}^*), given by Equation 1, would also become larger due to a larger τ divided by a smaller denominator in response to a reduction in the grain size. Figure 5 shows the relationship between bankfull discharge and the bankfull Shields stress (τ_{bf50}^*) and shows that as discharge increases so does the amount of bankfull Shields stress. This is due to the links between increases in height, width, sediment size, slope of the channel, and bankfull discharge when used in Equation 1 to calculate the Shields stress of the channel. This downstream increase in bankfull Shields stress (τ_{bf}^*) determines what sediment sizes will move when compared to the critical Shields stress (τ_c^*) for the stream.

Another key aspect that determines the amount of Shields stress on a grain is the relative roughness of a given D_i in the stream, in this case the D_{90} , to describe the self-shaping ability of a stream. The influence of submergence in shallow flows and the increasing stability of clast have

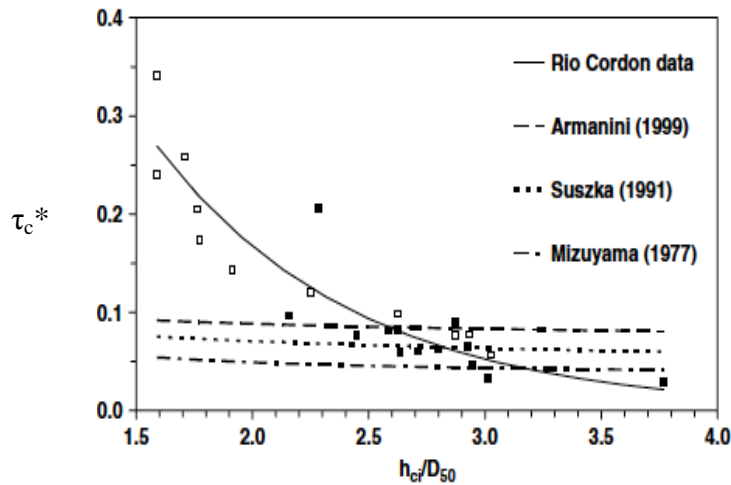


Figure 6. Relationship between dimensionless critical Shields stress (τ_c^*) and relative roughness given by H/D_{50} (from Lenzi et al., 2006, Figure 4).

been demonstrated in the past (Neill, 1967; Ashida et al., 1973; Bathurst et al., 1983, 1987; Misri et al., 1983; Bettess, 1984; Suszka, 1991; Wiberg and Smith, 1991; Armanini, 1999; Lenzi et al., 2006). Relative roughness is expressed as H/D_i where H is the height of the water and D_i is the diameter of the sediment of interest, both must be in the same units of measurement. The depth within a channel increases as discharge increases, relative roughness decreases, and the ability to entrain larger grains allowing for motion due to τ_c^* becoming smaller is shown in Figure 6 (Lenzi et al., 2006). As grains on the bed of the channel are increasingly submerged more force acts upon it due to the bed grains no longer being obstacles to flow, the resulting effect of lowering the amount of total force needed to move a given clast with a fluid (Ferguson, 2012). Sorting also plays another a role in clast movement within a channel in conjunction with submergence. Surface sorting of the grains plays a direct role in the ability of the clast to move (Clayton, 2010). Also the amount of flow resistance for a channel with known slope and grain size distribution is affected by the arrangement of the grains on the surface (Ferguson, 2012). Local sorting of the coarse grained sizes can promote sheltering of clast on the channel surface and local poor coarse grained sorting can promote mobilization of clast within the channel (Clayton, 2010). For this study the amount of sheltering of grains on the channel bed does not play as important of a role as the grain sorting within the channel, since this study is only focusing on the ability of a stream to be self-shaping and not the actual amount of movement of grains within the channel. The very large grains in the study are not of interest in this study because they are colluvial are not a result of sorting by the stream.

In the headwaters of a stream the channel morphology is controlled by the material that makes up the bed due to the lack of ability of the stream to shape its own channel. This lack of ability to shape the channel is due to the small size of the stream producing low amounts of shear

stress in Equation 2. As progression away from the headwaters occurs, down the channel, the size and slope of the stream changes as the sediment becomes finer. This increases the amount of Shields stress in the channel and also increases the ability of a river to move the grains within the channel. Therefore a river's ability to become more self-shaping increases downstream from their headwaters and varies along the channel due to the change in the previously mentioned parameters. At some point along the river channel the dimensionless Shields stress that is present at bankfull is going to become very close to the amount of Shields stress that is necessary to mobilize the D_{90} sediment load in the channel as shown in Figure 1 (Mueller et al., 2005). Figure 1 also shows that in most cases channel morphology is adjusted so that bankfull flows produce bankfull Shields stress (τ_{bf}^*) is slightly above the amount of that is needed to move sediment in the channel at a particular location (Mueller et al., 2005; Parker et al., 2007; Pitlick, 2009).

However, not all mountain streams have been adjusted to create the amount of shear stress needed for D_{90} mobilization (Thompson et al. 2008). Movement of clast is highly intermittent in streams or rivers with coarse bed material (Ferguson, 2012). There is a distinction between self-shaping and non-self-shaping channels in the literature as shown by Buffington et al. (1997), Mueller et al. (2005), Church (2006), Parker et al. (2007), and Pitlick (2009). A jammed channel or a threshold channel, as seen in Table 1, would fall into the category of a non-self-shaping stream since these channels do not create the amount of shear stress needed to mobilize the D_{90} grain sizes. In these kinds of channels the clasts on the channel bed control the morphology of the stream. In contrast, a labile channel and some transitional channels can be classified as self-shaping because of the ability to mobilize the D_{90} grain size within the channel. In channels where the D_{90} is capable of being mobilized by bankfull flows the morphology of the

channel is controlled by the shear stress and not the clast in the stream making these streams self-shaping.

4. RESEARCH QUESTION

As shown above, there is a vast body of knowledge about self-shaping rivers and streams that occupy low slope areas. Also many other studies have been conducted on streams with a gradient above 0.03 and their ability to move sediment and clast in their channel (Lenzi et al., 2006). However, very little work has been completed to determine the point a stream becomes self-shaping and if the measurements of H, B, Q, and S establish a relationship or a constant ratio? On Schumm's stream classification chart this would be the transition between a Threshold channel with a Shields number up to 0.04+, and a Threshold channel with a Shields number up to 0.15 shown in Table 1. Between these two classifications streams move from partial mobilization of the bed material to almost full mobilization of the bed material. The channel also becomes less static between these two classifications and changes regularly. The change between these two classifications is the point at which a channel becomes self-shaping. Not only would this be relevant for Table 1 it would also be relevant for Figure 1. The relationship in Figure 1 would start to break down and the τ_r^* would start to become greater than the τ_{bf}^* . The scatter of the graph would also increase and no longer be constrained to the narrow range shown in Figure 1. Plotted points would fall below the 1:1 reference line showing that τ_{bf}^* would be less than τ_r^* . In this situation sediment transport would likely only occur when discharge leaves the normal channel area spilling onto the flood plain. To better understand this relationship more work needs to be completed in this area and this study aims to help fill in those gaps.

This study essentially aims to find the upper bounds for this relationship, where the relationship between τ_r^* and τ_{bf}^* increases scatter distribution, if plotted on Figure 1, and suggests that the channels is transitioning to a non-alluvial state. This project is based on the assumption that at some point the linear relationship in Figure 1 will break down as the channel changes into a non-alluvial channel and the bankfull Shields stress will no longer be greater than the reference Shields stress. The research question is at what distance downstream from the headwaters and under what measurements of slope, height, width, and size of the bed material will the trend be established and maintained throughout the watershed? This study aims to answer that question and add to the body of knowledge associated with mountain streams and higher order self-shaping streams.

Proposed conditions that will be exhibited when a stream becomes self-shaping will be: a change in slope where the stream becomes less steep, the discharge becomes sufficiently large, and bankfull conditions sufficiently submerge clast deep enough to promote movement from the shear stress exerted upon them. Once all of these conditions are met, the channel is capable of producing sufficient amounts of Shields stress to produce movement of grains within the channel. Before these conditions are met, grains within the channel control the morphology of the stream. By using Equation 1 to calculate bankfull Shields stress (τ_{bf}^*) and comparing it to the reference Shields stress (τ_r^*) the point where a non-alluvial stream becomes an alluvial stream can be determined. Downstream from this point the relationship between bankfull and reference Shields stress will match Figure 1 and upstream from this point the relationship between bankfull and reference Shields stress will not match Figure 1.

5. SETTING

The study was conducted on the Conasauga River watershed, in the Cohutta Wilderness Area, as shown in Figure 7. The site was selected to contrast the sites used in the Mueller et al. (2005) and regional variations of this location. Figure 7 shows the study area and trail system used to access the river channel. Trail 90 (Chestnut Lead Trail) is the primary access trail for this portion of the river. The Cohutta Wilderness Area was used for the study location since it has never been developed and was last logged between 1915 and 1935. The area has since had 76 years to recover from the logging. The Conasauga River's drainage basin is located east of the Cartersville Fault and is part of the Blue Ridge Mountains comprised mostly of metamorphic rocks. The rock unit exposed at the surface in this area is the Ocoee Supergroup. The rock types of the Ocoee Supergroup are primarily metagraywacke, slate, phylolite, and quartzite of Precambrian age (Sutton, 1991; Goode et al., 2010). These rock types found within this region influence the methods used to gather data regarding the channel and the clast within it. The rock units within the study area are mainly bedded or foliated units that produce thin tabular bed material. This area of Georgia receives about 1.5 meters of precipitation a year, most of which is seasonal (University of Georgia, 2013). Most of the river is shallow with relatively wide channels compared to its depth. In the upper Conasauga watershed the predominant vegetation types are mountain laurel, rhododendron, white pine, hemlock, hickory, and poplar trees (Goode et al., 2010). Ground cover is fairly sparse due to the dense canopy and mainly consists of moss, ferns, and predominantly leaf litter.

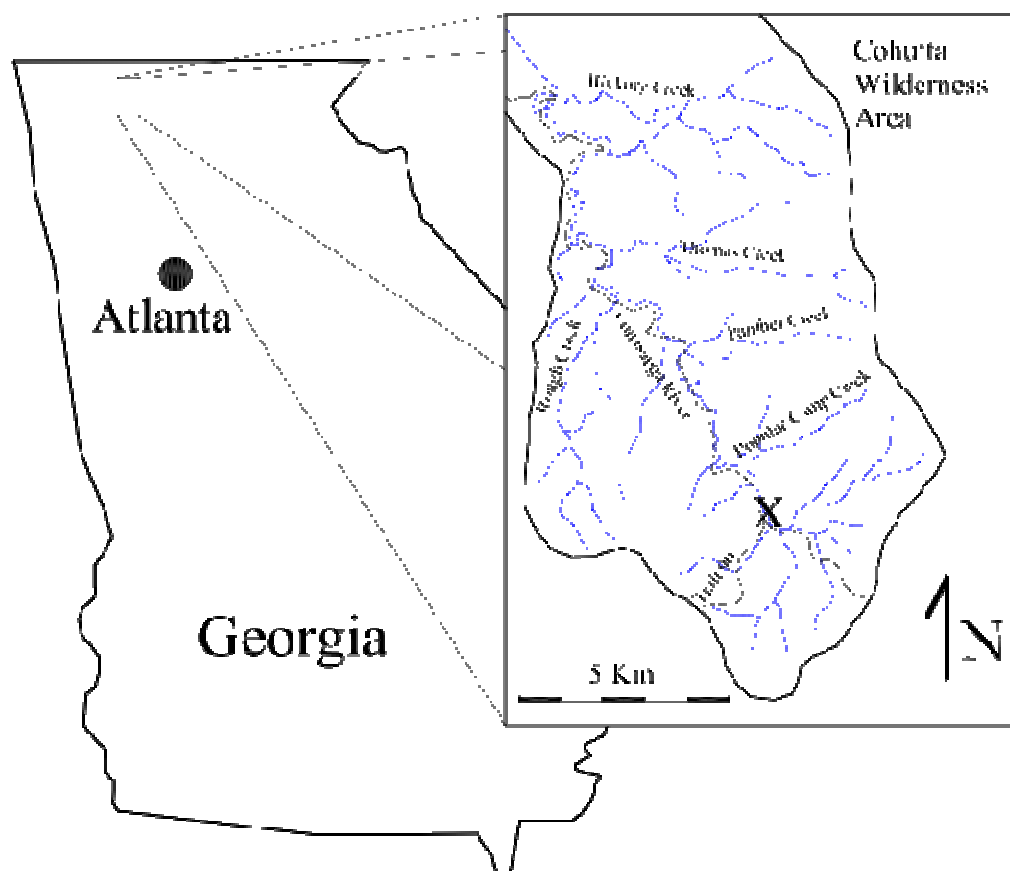


Figure 7. Map showing the study area, the Conasauga River drainage, and the trail system used to access the river. The X represents the location of the initial benchmark for the longitudinal survey.

6. METHODS

6.1 OVERVIEW

Direct measurements of the streambed for cross-sections and bankfull topography were measured along the channel every 100 meters. I placed the first cross-section 600 meters downstream of the intersection of Trail 90 and the Conasauga River. Between each of the cross-sections measurements were taken to create a longitudinal profile of the study reach. At each of the cross-section measurements for channel width, bankfull height, and channel slope were also taken. Surface sediment measurements were taken as well at each cross-section to determine the D_{50} and D_{90} values of the bed material. These measurements provided help determining the size distribution of clast within the stream channel.

After the determining the D_{50} and D_{90} values for each cross-section Equation 1 and Equation 2 are used to calculate the bankfull Shields stress (τ_{bf}^*) at each cross-section. Measurements were also taken at each of the cross-section to help calculate the reference Shields stress (τ_r^*) at each of the cross-section locations. The measurements of bankfull and reference Shields stress allow the location to be classified as either self-shaping or non-self-shaping.

6.2 SPECIFIC METHODOLOGY

I placed the first cross-section 600 meters downstream of the terminus of Trail 90 and then I placed cross-section stations upstream from that point in increments of 100 meters. Trail 90 was used to access the study area and provides a set reference point for the stream reach that is being studied. The cross-sections are taken at 100 meter increments in order to find the transition between alluvial and non-alluvial regimes more precisely. Also the initial benchmark

at the terminus of Trail 90 is a dead tree stump in a secure location away from the channel. The initial benchmark is used to reference the entire measured channel for a longitudinal survey. The elevation of the initial benchmark is determined with the use of a handheld GPS. The location of the initial benchmark is represented approximately by the X on Figure 7.

To gather elevation data throughout the channel a simple survey level was used with a measuring rod. The level is used to gather elevation data of points in relation to the initial benchmark by using standard surveying procedures while conducting the longitudinal survey. The level is also used for measuring cross-sectional elevations in relation to the longitudinal survey.

The longitudinal survey is used to delineate features of the stream accurately (Harrelson et al., 1994). The procedure for completing the longitudinal survey is contained in Harrelson et al. (1994) and was conducted as follows. Starting in the stream channel 600 meters downstream from trail 90, cross-section 1 was placed and measured. From this point the cross-sections are advanced upstream from here at 100 meter increments. From the initial cross-section a tape measure is laid on the centerline of the channel. Elevation measurements of the channel centerline are then made every unit of channel width at point 0. One unit of channel width is equivalent to the width of the channel at point 0. For example, if the channel is 6 meters wide at point 0, every six meters a channel centerline elevation is taken. In areas where the curvature of the stream does not allow for measurements being channel width apart the curve is broken down into to smaller segments and recorded as their position on the survey.

Surveying of cross-sections along the channel is conducted at 100 meter intervals along the longitudinal survey. Cross-sections are locations for measuring channel form, particle size, and particle distribution within the channel. Cross-section data is gathered by using the

procedure described by Harrelson et al. (1994). Cross-sections are measured from floodplain to floodplain across the channel starting on the downstream facing left side of the channel. The cross-section ends were higher than bankfull elevation in the floodplain due to the importance of bankfull elevation in this study. At each cross-section a tape is stretched across the channel and used as a reference for surveying. The instrument is set up off the cross-section and to one side along the cross-section plane for measurement of the cross-section.

A benchmark for each cross-section is also established at each location to aid in the gathering of survey data. This benchmark for the cross-sections is a large distinct boulder on the edge of the channel picked out for easy reference at each cross-section location on the longitudinal survey. This enables the cross-section to be tied into the longitudinal survey as a whole and allow for elevations on the cross-section to be truly representative of the actual elevation. Elevations on the cross-sections are taken at each half-meter interval in conjunction with surface sediment measurements. Also at each cross-section other important measurements of bankfull elevation, floodplain elevation, other items of interest, and the edge of the water are measured.

Before ending each cross-section, the survey is ended by measuring the benchmark again to see if there was any change in instrument height from any unintended contact with the instrument or other outside influences. After this a measurement of channel slope at the location is also taken. This was done by measuring the elevation of the water upstream and downstream of the cross-section incorporating at least one entire step or riffle pool sequence if present at the cross-section's location (Harrelson et al., 1994). Measurement of the distance from the cross-section to the location of water elevation is measured to the nearest 0.1 meter. If there is no step

or riffle sequence present the measurement is then taken 20 meters upstream and downstream of cross-section to determine slope of the channel.

At each cross-section bankfull height is also measured. Bankfull height is used in this study to find the bankfull Shields stress acting on the sediment in the channel and relates it to the ability of the river to be self shaping (Mueller et al, 2005). Bankfull indicators used in this study are change in vegetation, change in slope of the bank, a change in bank materials, bank undercutting, and stain lines (Harrelson et al. 1994). The bankfull in this environment was most represented by the change in bank slope and bank materials. The change in bank materials went from the unconsolidated large grain size clast in the channel to root stabilized finer grain sediments out of influence of the stream. By using these methods the bankfull depth, width, and slope of the channel are measured at each cross-section.

Surface sediment measurements are collected at each cross-section along with the other channel measurements. The Wolman (1954) pebble count procedure is used to evaluate the grain size distribution of the channel. At each cross-section sampling was conducting by picking up the first pebble that is at the toe of your wader once entering the channel. This pebble is then measured for the size of its axes; due to the nature of many clasts being flat and wide, tabular in nature, all three axes were measured. All pebble axis measurements are taken at 90 degrees from each other. The shortest axis is referred to as the C axis, the longest axis is referred to as the A axis, and the B axis measurement is the median axis. In this study environment the C axis was typically the thickness of the clasts. The B axis is used to determine median amount of stress acting on the grain. After measuring the pebble another step is taken and the first pebble at the toe of the wader is measured. This is repeated all the way across the channel until the other bankfull elevation. Grains were measured with a hand held metric measuring stick that was large

enough to accommodate very coarse grains. Very coarse grains were present at the surface of the channel; however, most of them were buried in fine sediment. If a large, partially buried grain was to be measured it was removed from the sediment and measured according to the methodology described. Very large non-alluvial clasts were not measured since they are not representative of the stream channel. These were identified by the size of the clast and the presence of moss or other vegetation growing on them above bankfull indicators.

To accurately measure the size distribution of pebbles in the channel there must be at least 100 pebbles measured (Wolman, 1954). The first sampling transect follows the cross-section. Due to the width of the channel the remaining samples are completed in a zigzag pattern, progressing upstream and downstream from the cross-section, within the stream channel until the appropriate numbers of samples were taken. To make sure that only representative sampling is conducted for the cross-section grain size measurements were only taken a maximum of 5 meters upstream or downstream from the cross-section. This amount of space allows for the proper number of grains to be measured and still be representative of the surface sediment at the cross-section.

After completing the cross-sections and the pebble counts the data is used to gain information about the stream channel and sediment distribution. Equation 2, the Dubois equation, allows for calculation of the boundary shear stress at the cross-section. In this calculation the slope is measured at the cross-section the height of the water is an average height of the water in the channel at the cross-section. The cross-section data allows and the shear stress from Equation 2 allow the calculation of the Shields stress at that cross-section by using Equation 1 in conjunction. The sediment size of interest, the D_i , in Equation 1 is determined from

the size distribution graphs and then used to calculate the Shields stress for that grain size of interest.

The pebble counts are used to determine size distribution of clast within the channel. After completing a size distribution analysis the D_{90} , the sediment diameter that is larger than 90 percent of the sediment in sample, value can be determined for the channel. The D_{90} value is used instead of the D_{50} because it will be more useful to describe the shaping ability of the stream (Reid et al., 1984, 1986; Petit, 1994; Lenzi et al., 2006). The D_{50} value is also considered to help relate this work to other work that has previously been completed. After determining the D_{90} and D_{50} of the channel, Equation 2 is used to calculate the bankfull shear stress of the channel at the given cross-section by using the bankfull measurements for height of the water and width of the stream. Equation 3 is then used to calculate the amount of bankfull Shields stress on the grain size of interest.

$$\tau_{bf}^* = \frac{\tau_{bf}}{(\rho_s - \rho)(g)(D_i)} \quad (3)$$

Using the product of Equation 2 the amount of shear stress at bankfull the bankfull Shields stress (τ_{bf}^*) is then calculated using Equation. This is meaningful because the amount of τ_{bf}^* exerted on clast can then be compared to τ_r^* needed to produce movement of clast in the channel. The reference Shields stress (τ_r^*) is the amount of Shields stress needed to initiate a pre-determined minimal amount of sediment movement (Mueller et al., 2005).

Due to the intermittent nature and lack of predictability of high flows within the stream and the time frame of the study bed load measurements were not taken during this study. Due to the lack of bed load data τ_r^* cannot be calculated directly. In Mueller et al. (2005) measurements of flow, slope, and sediment size are used to develop a relationship for the reference Shields

stress (τ_r^*) for 45 mountain streams. In this study τ_r^* is calculated by Equation 4, which uses the slope of the channel, S, to determine the reference Shields stress at a particular location (Mueller et al., 2005).

$$\tau_r^* = (2.18S + 0.021) \quad (4)$$

Equation 4 is an empirical equation that was generated from a large data set of 45 different streams from in different locations to develop this reference Shields stress equation (Mueller et al., 2005). Most of the streams, 34 of 45, are located in mountainous areas of Idaho, of those 45 streams 21 are underlain by intrusive igneous rocks of the Idaho batholith and the remaining 11 streams are located in western North America in areas of mixed lithology (Mueller et al., 2005). The study area for this study is located in the Appalachian Mountains in North Georgia in less steep terrain than the streams used in the Mueller et al. (2005) study.

The term τ_r^* is analogous to the critical shear stress (τ_c^*) and can be used in its place in other bed load transport equations (Pitlick et al., 2009). Reference Shields Stress (τ_r^*) is used to describe thresholds of motion in studies where the actual bedload data is absent. Whereas, critical Shields stress (τ_c^*) is the actual measurement of incipient motion of bed material. Gathering actual movement data in this study was not possible due to the inconsistent flows of the stream, therefore, τ_r^* is used to describe the threshold of sediment transportation within the channel. In this study τ_r^* was used in place of τ_c^* in order to make the comparison of τ_r^* and τ_{bf}^* as used within the Mueller et al. (2005) study.

Once the τ_{bf}^* and the τ_r^* are calculated for the cross-sections they were placed on to a graph similar to Figure 2. The main goal of this study is to establish at what conditions the trend of τ_{bf}^* of being slightly higher than τ_r^* and then continue to be maintained throughout the watershed (Mueller et al., 2005).

7. RESULTS

A longitudinal profile for the study area was also completed and is shown in Figure 8. The elevation of the initial benchmark was determined with a handheld GPS to be 752 meters (plus or minus 3 meters) above sea level. The profile is 2.6 kilometers in length from cross-section 1 to cross-section 27. The cross-section names in the photographs are different than the names that appear on the cross-section labels. This is due to a change in nomenclature from the original field visits for ease of presentation the data. Not all of the data could be gathered during one field visit to the study area. However, during the period of time between field visits no high flow events occurred in the channel as observed by the Mill Creek gage number 02384540 operated by the USGS which is the closest gage to the watershed. The data obtained is therefore consistent throughout the study area due to the absence of high flows in the study area.

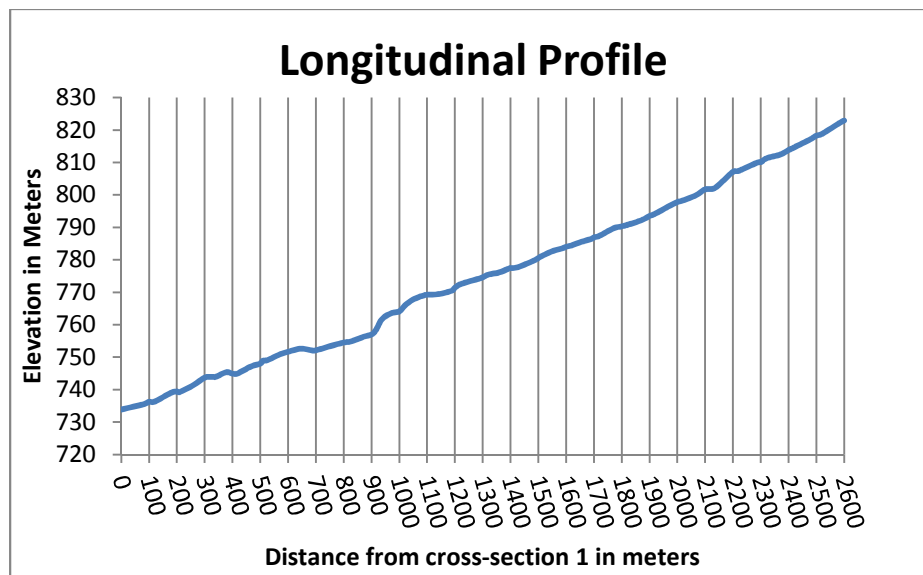


Figure 8. Longitudinal profile of the study area with the most downstream cross section located on the left of the figure, cross-section 1 is located at 0 meters and is 600 meters downstream from the intersection of the Conasauga River and Trail 90.

In total 27 cross-sections were completed with accompanying pebble counts for size distribution data. Cross-section 6 was the only cross-section without an accompanying pebble count, that cross-section occurs in an area with relatively high slope and consists of a bedrock channel with no overlying unconsolidated material within the channel. The cross-sections, accompanying size distribution graphs, and photographs of cross-sections are found in Figures 9 through Figures 90. Cross-section 4 was the only cross-section to contain an island in the study reach.

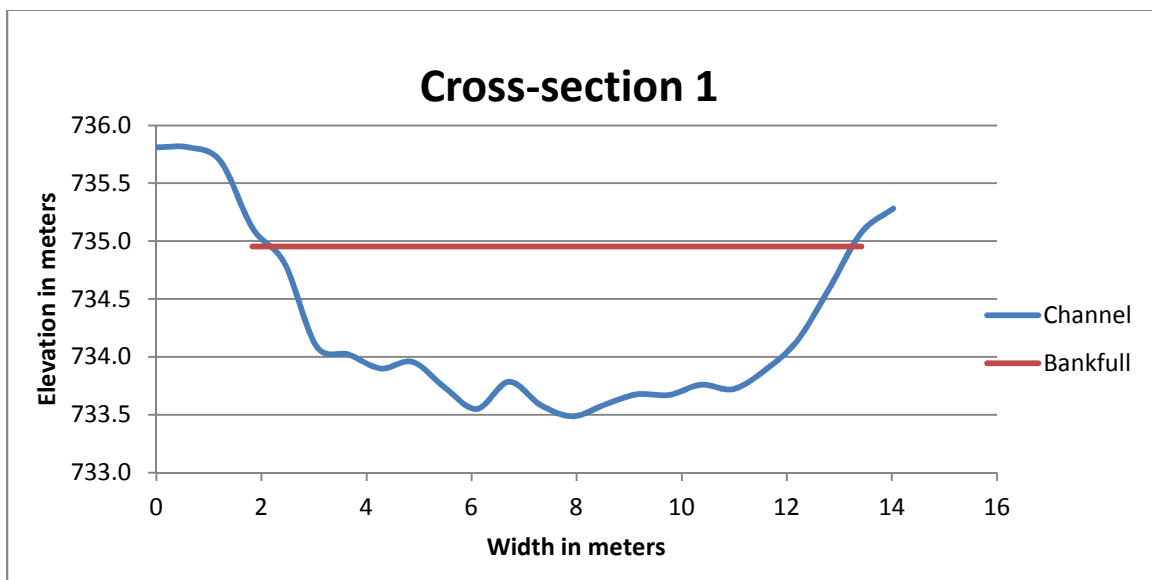


Figure 9. Cross-section 1, the red line represents bankfull conditions.

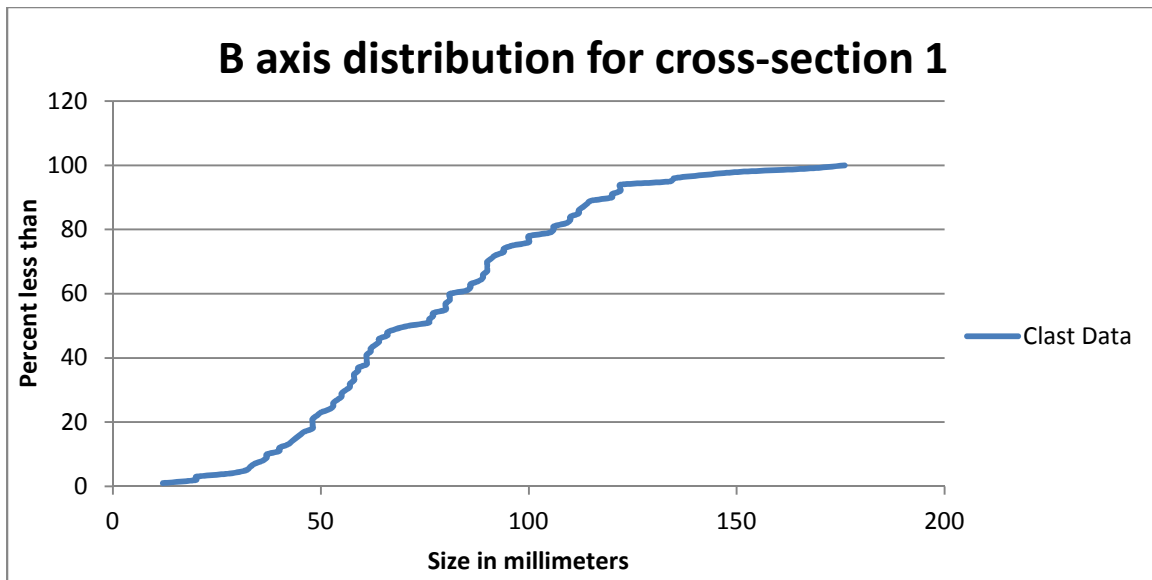


Figure 10. B axis distribution for cross-section 1.

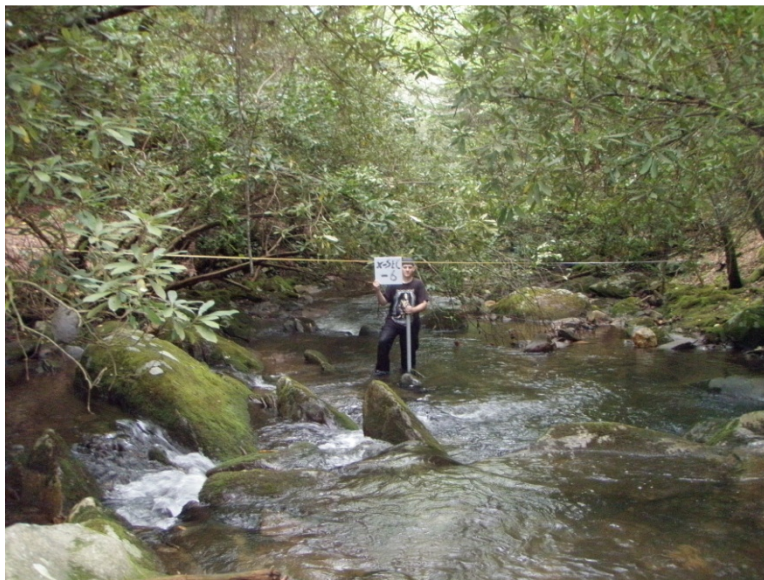


Figure 11. Photo of cross-section 1, view is downstream.

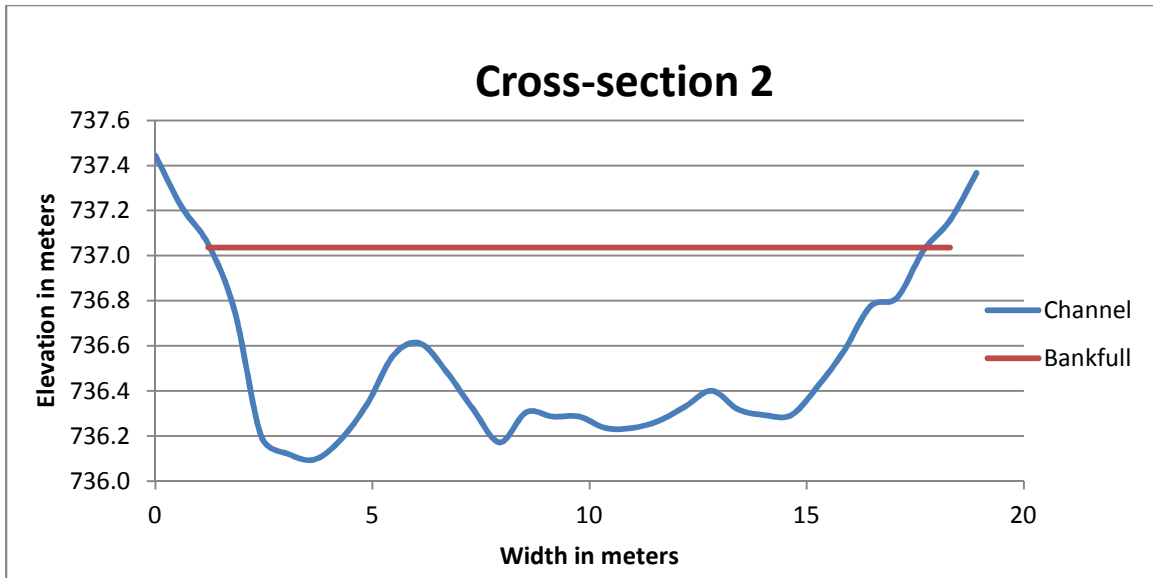


Figure 12. Cross-section 2, the red line represents bankfull conditions.

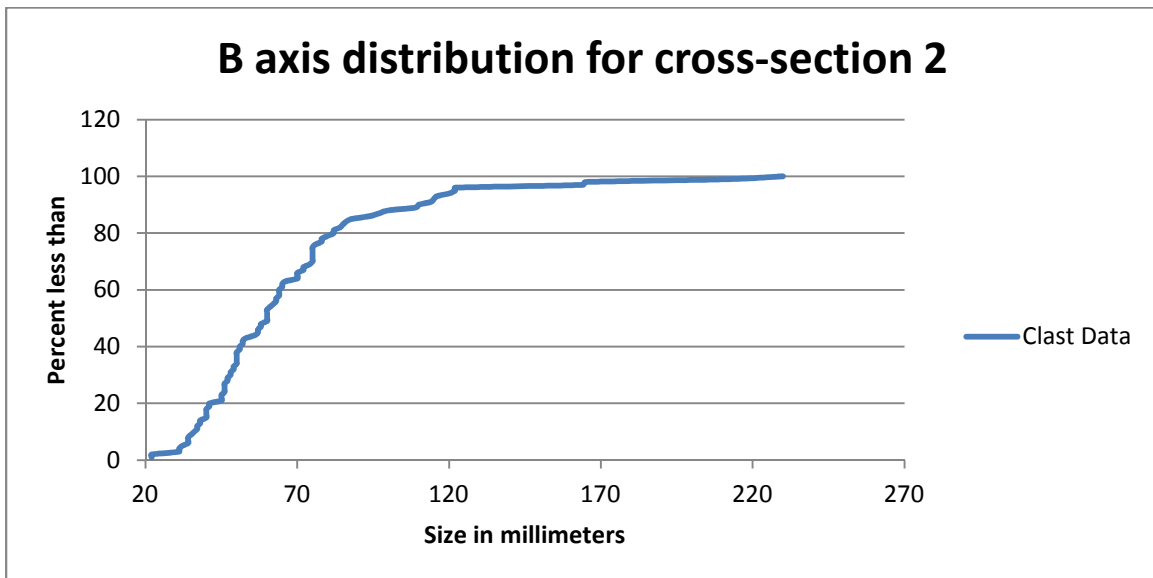


Figure 13. B axis distribution of cross-section 2.



Figure 14. Photo of cross-section 2, view is downstream.



Figure 15. Cross-section 3, red line represents bankfull conditions.

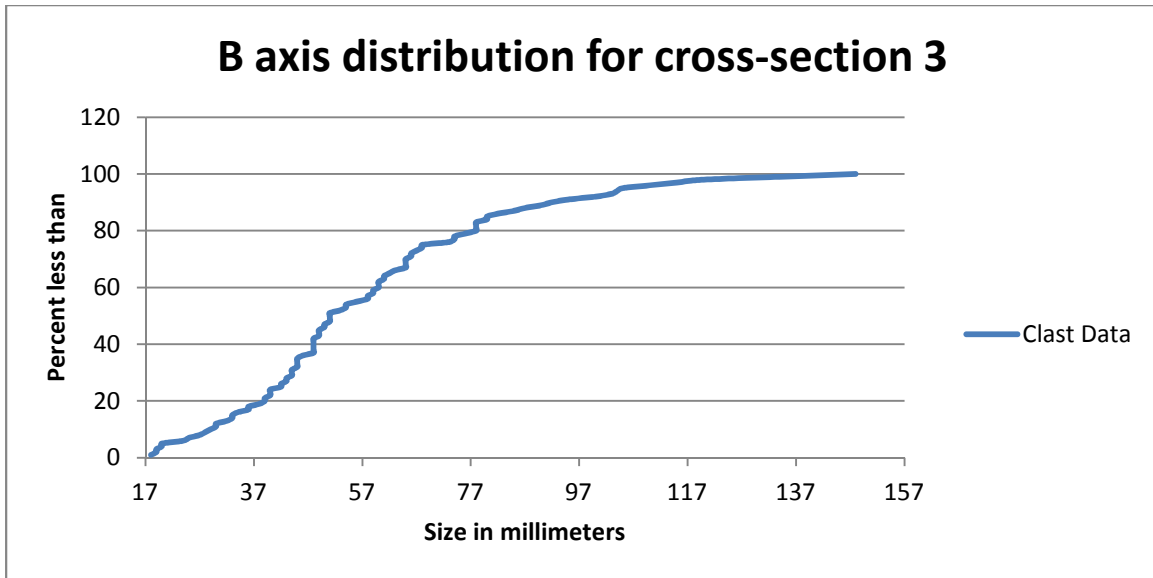


Figure 16. B axis distribution of cross-section 3.



Figure 17. Photo of cross-section 3, view is downstream.

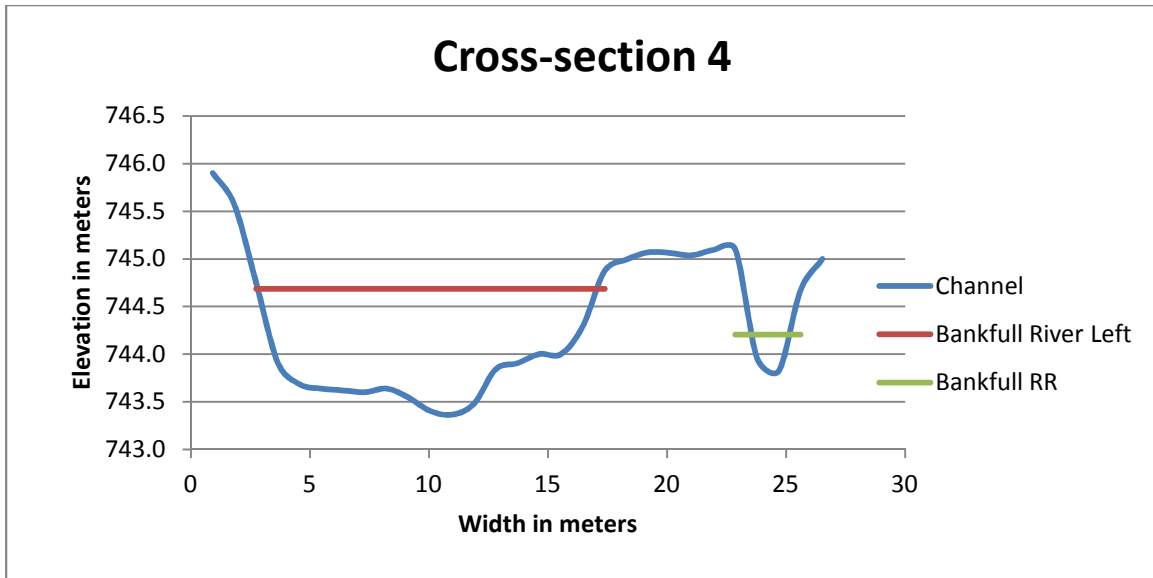


Figure 18. Cross-section 4 is bisected by an island and splits the flow of the river into 2 channels, the red line represents the bankfull conditions in the downstream facing left channel and the green line represents the bankfull conditions in the downstream facing right channel.

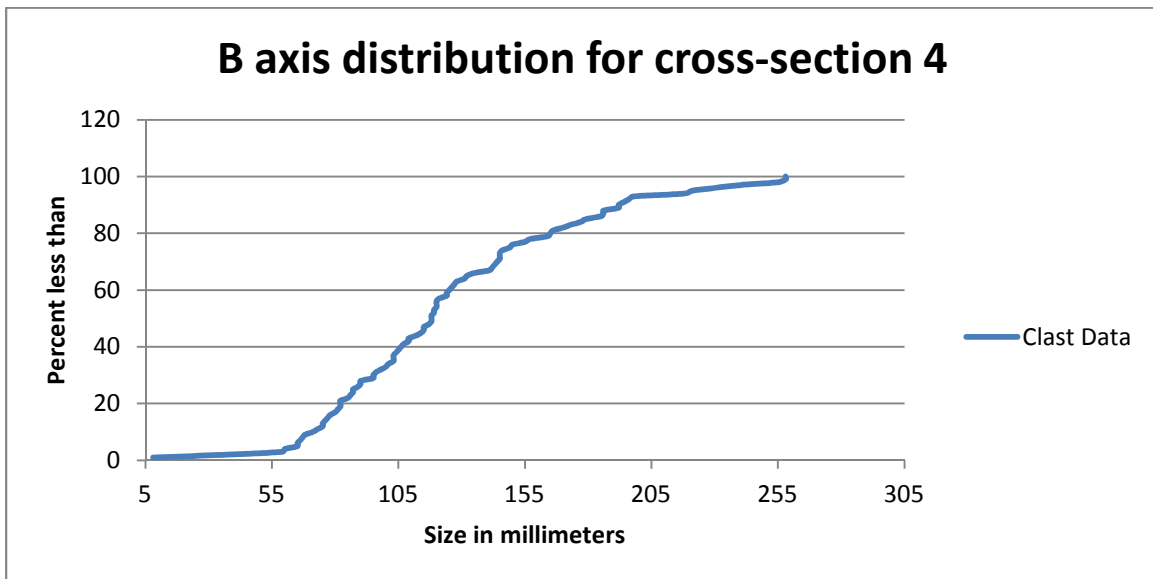


Figure 19. B axis distribution of cross-section 4 for both channels.



Figure 20. Photo of downstream facing right channel on cross-section 4, view is upstream.



Figure 21. Photo of island in cross-section 4, view downstream.



Figure 22. Photo of downstream facing left channel on cross-section 4, view upstream.

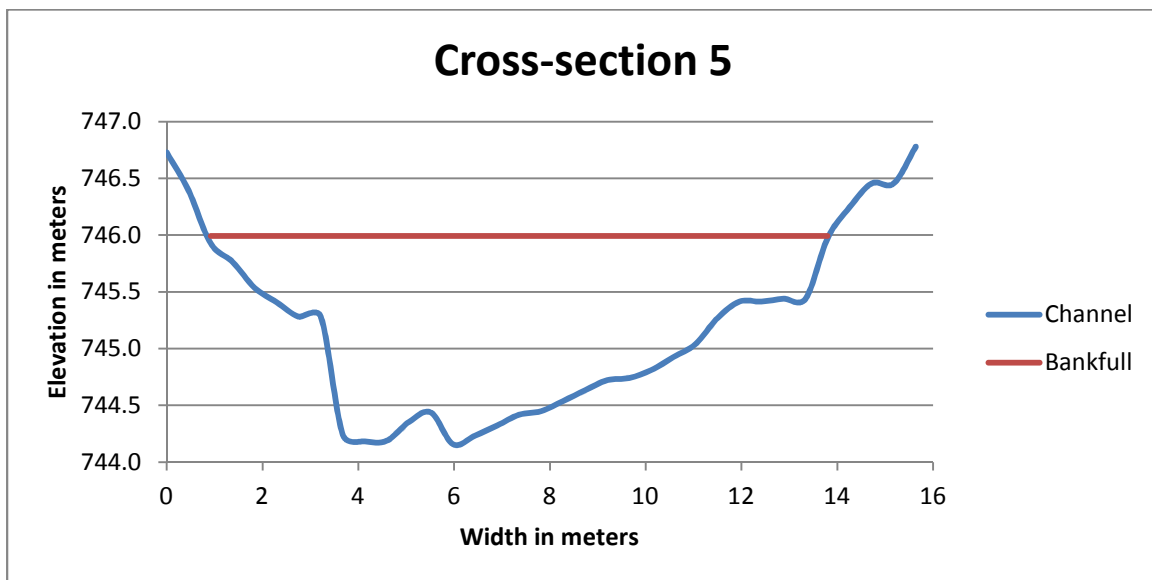


Figure 23. Cross-section 5, the red line represents bankfull conditions.

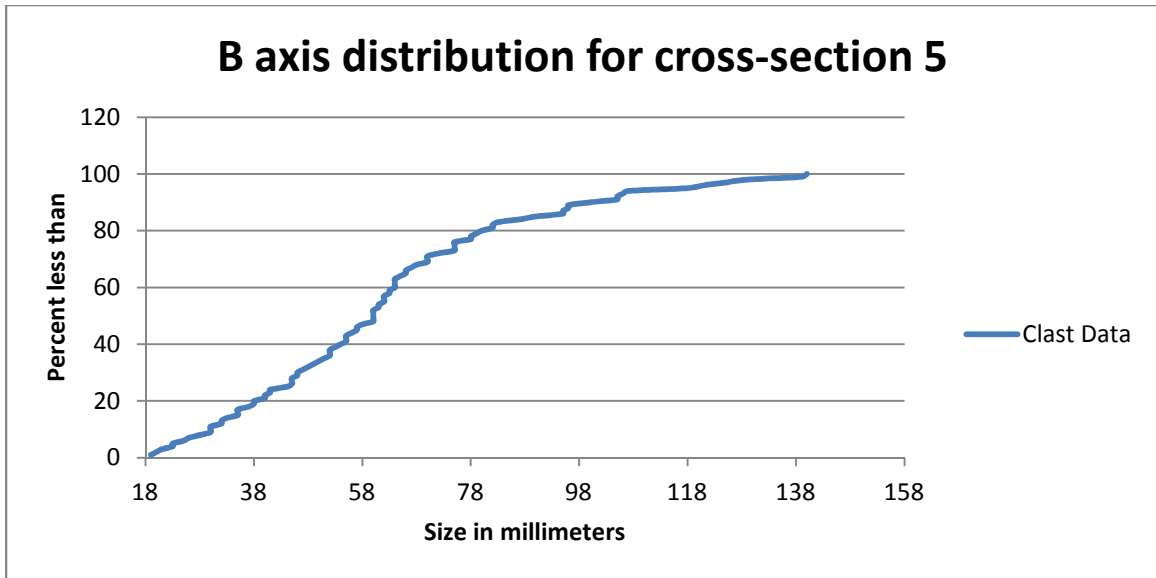


Figure 24. B axis distribution of cross-section 5.



Figure 25. Photo of cross-section 5, view is downstream.

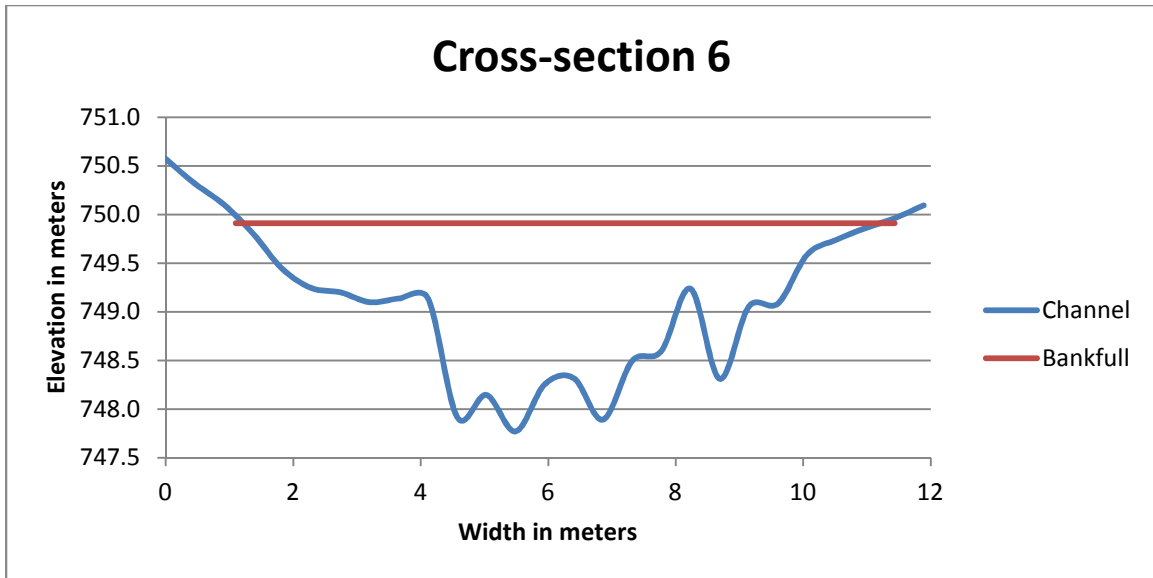


Figure 26. Cross-section 6, the red line represents bankfull conditions.



Figure 27. Photo of cross-section 6, view is upstream.

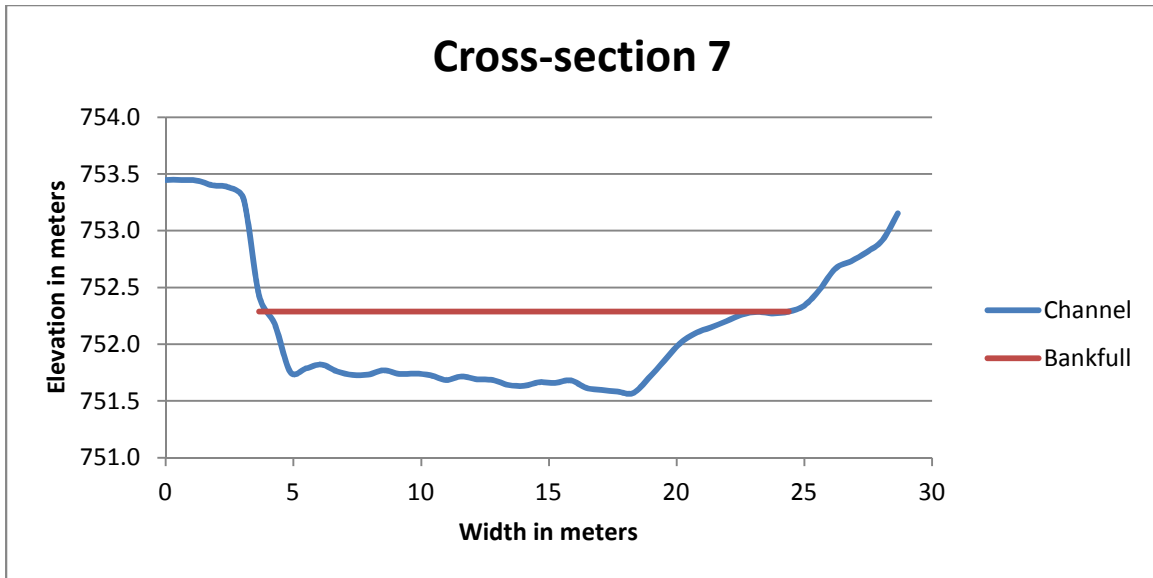


Figure 28. Cross-section 7, Trail 90 crosses Conasauga River on this cross-section, red line represents bankfull conditions.

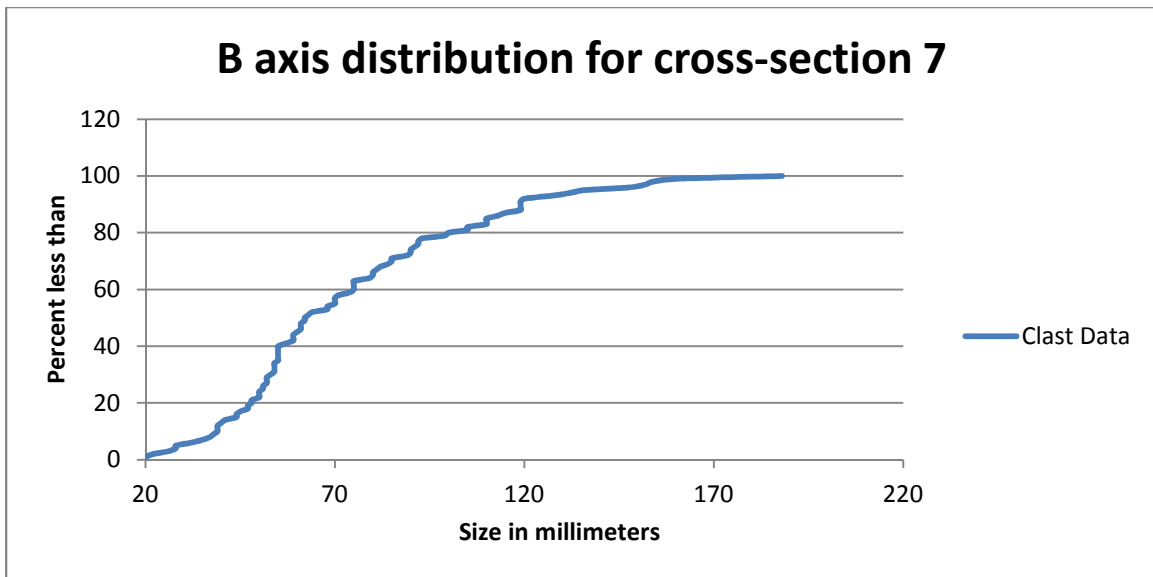


Figure 29. B axis distribution of cross-section 7.



Figure 30. Photo of cross-section 7, view is downstream.

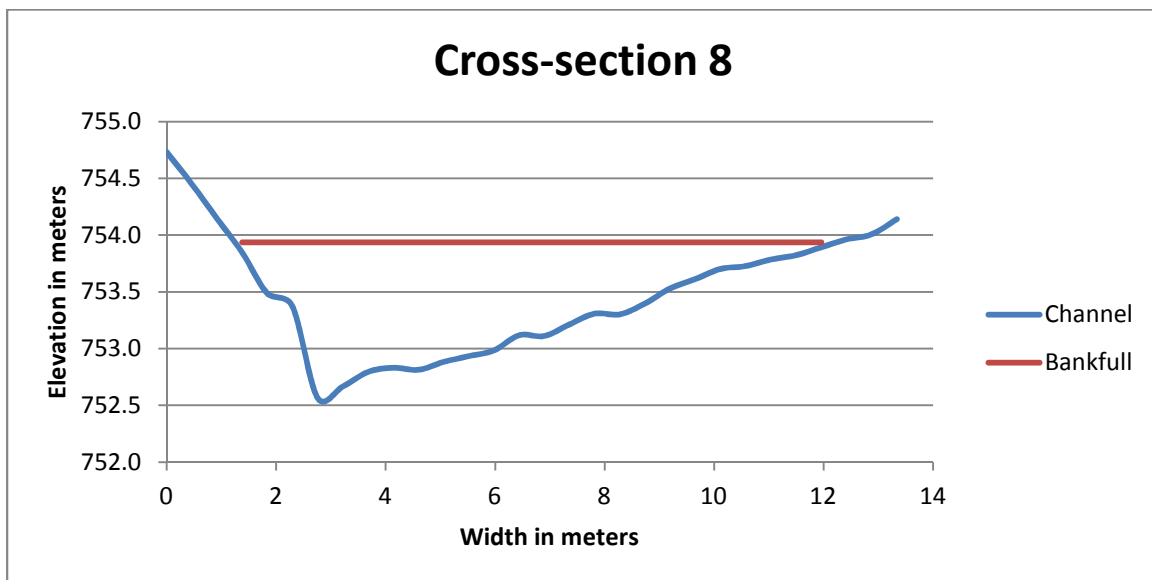


Figure 31. Cross-section 8, red line represents bankfull conditions.

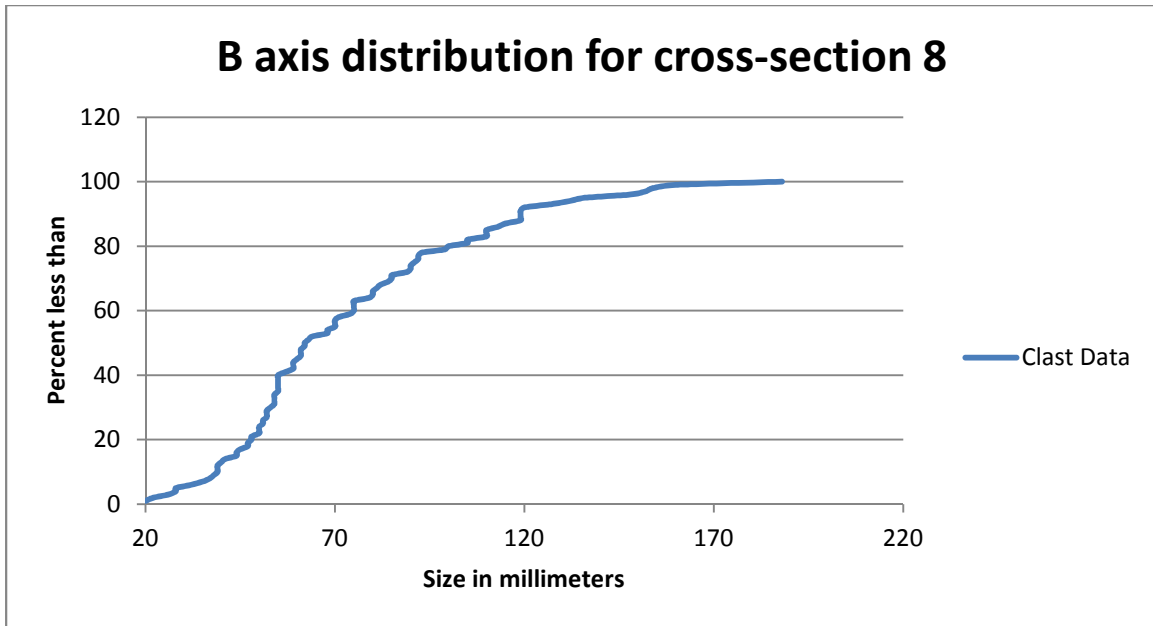


Figure 32. B axis distribution of cross-section 8.



Figure 33. Photo of cross-section 8, view is upstream.

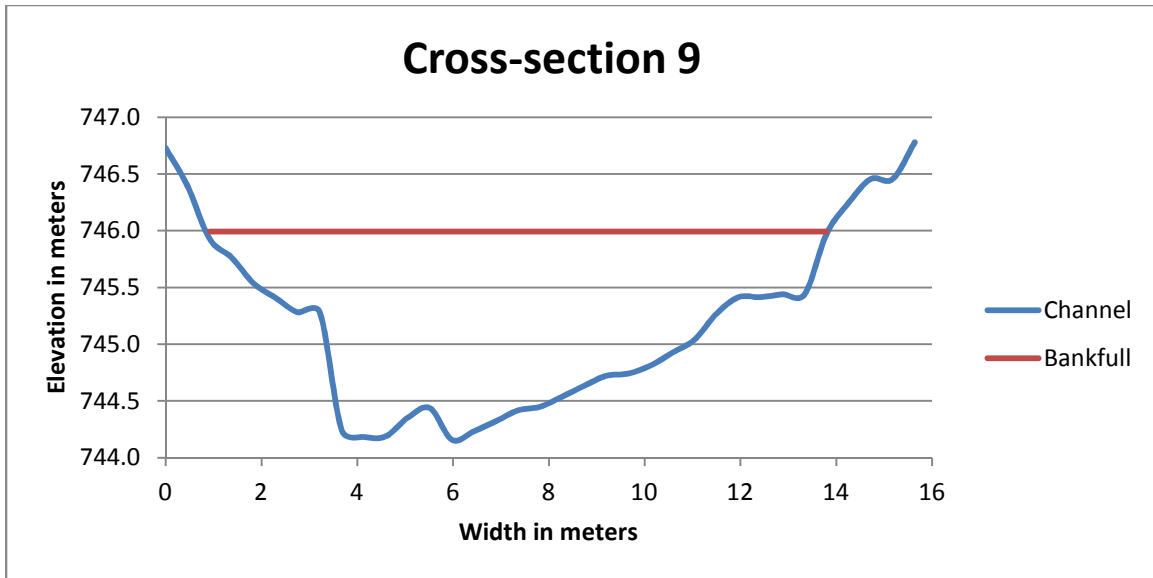


Figure 34. Cross-section 9, the red line represents bankfull conditions.

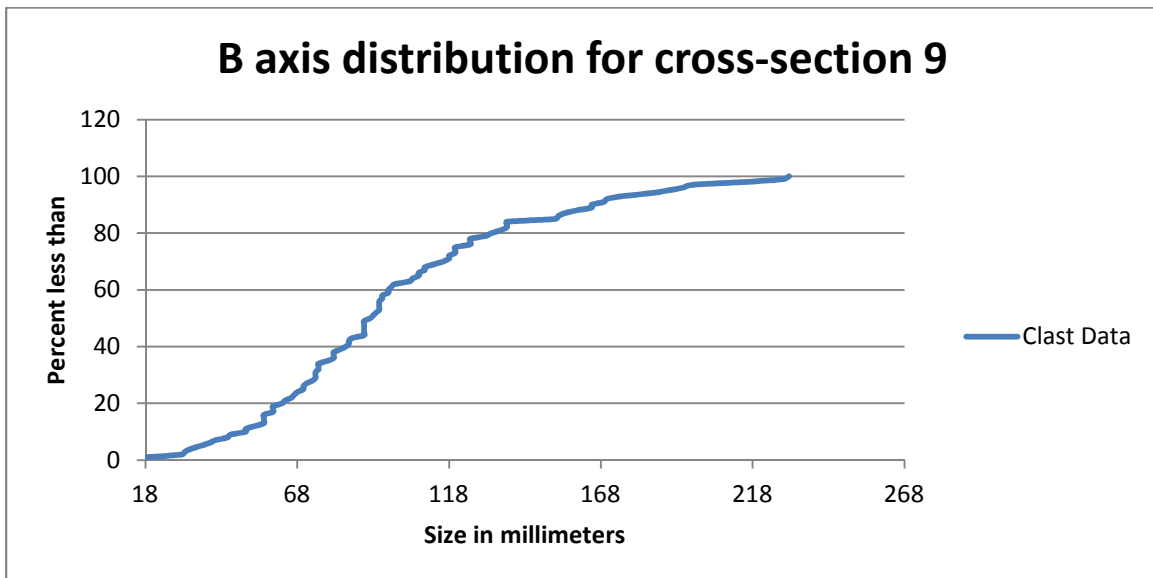


Figure 35. B axis distribution of cross-section 9.



Figure 36. Photo of cross-section 9, view is upstream.

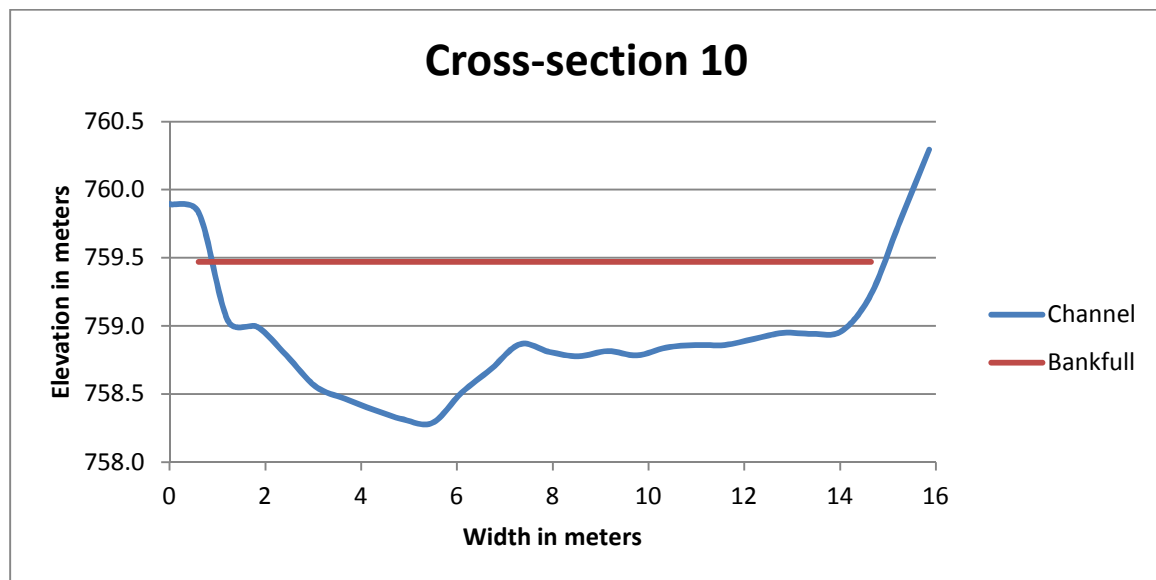


Figure 37. Cross-section 10, the red line represents bankfull conditions.

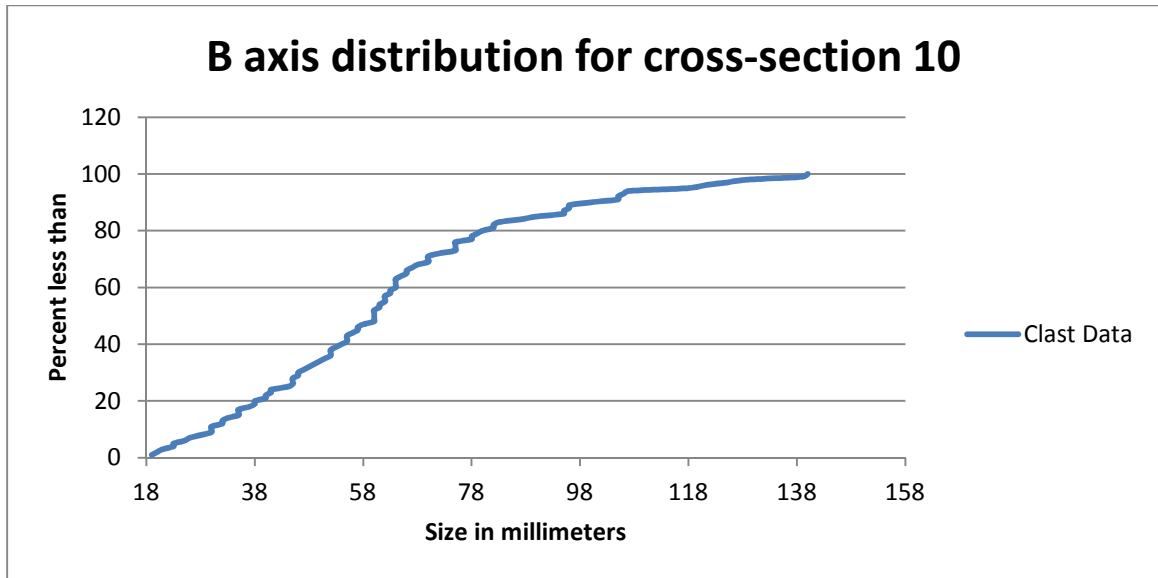


Figure 38. B axis distribution of cross-section 10.



Figure 39. Photo of cross-section 10, view is upstream.

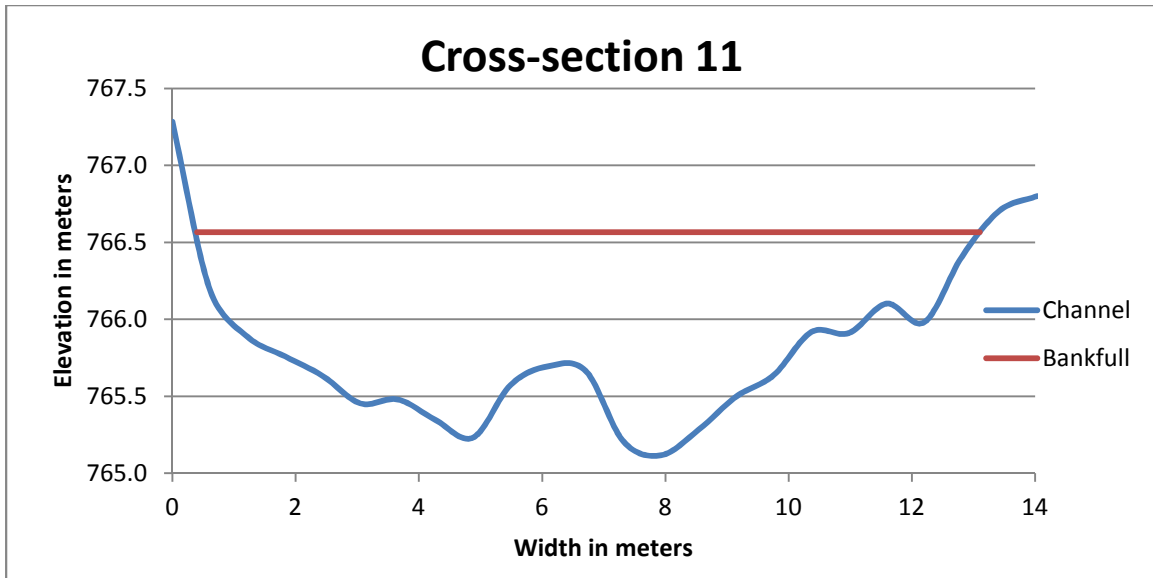


Figure 40. Cross-section 11, the red line represents bankfull conditions.

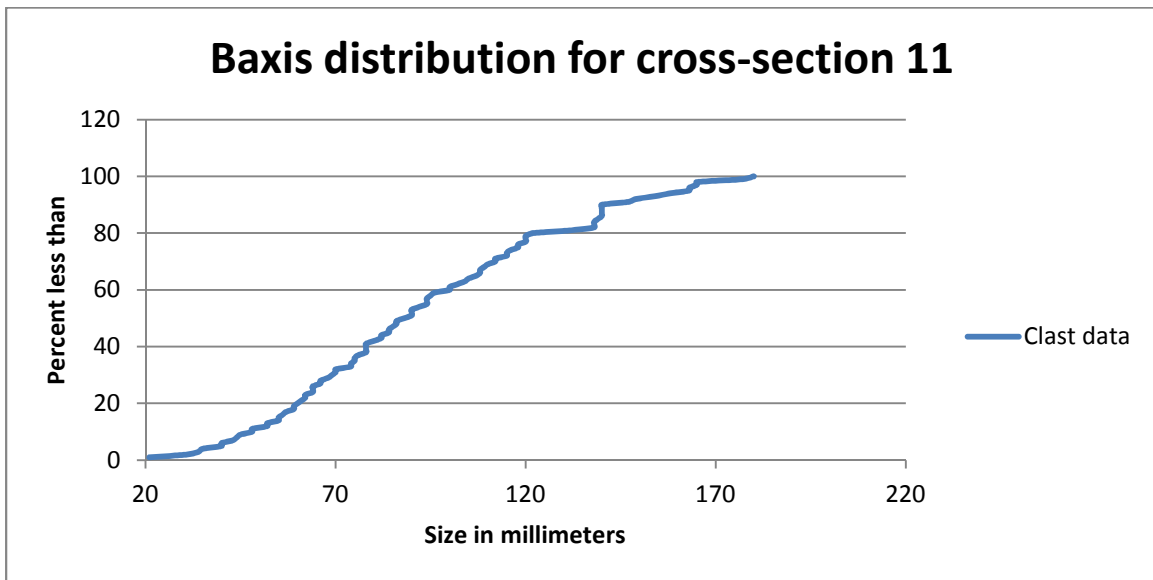


Figure 41. B axis distribution of cross-section 11.



Figure 42. Photo of cross-section 11, view is upstream.

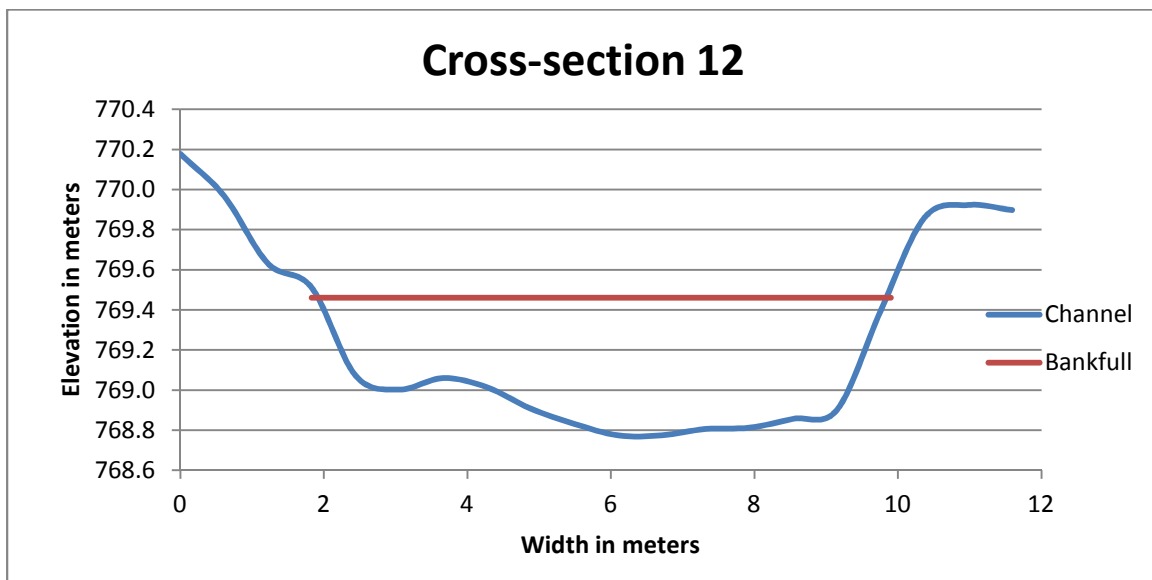


Figure 43. Cross-section 12, the red line represents bankfull conditions.

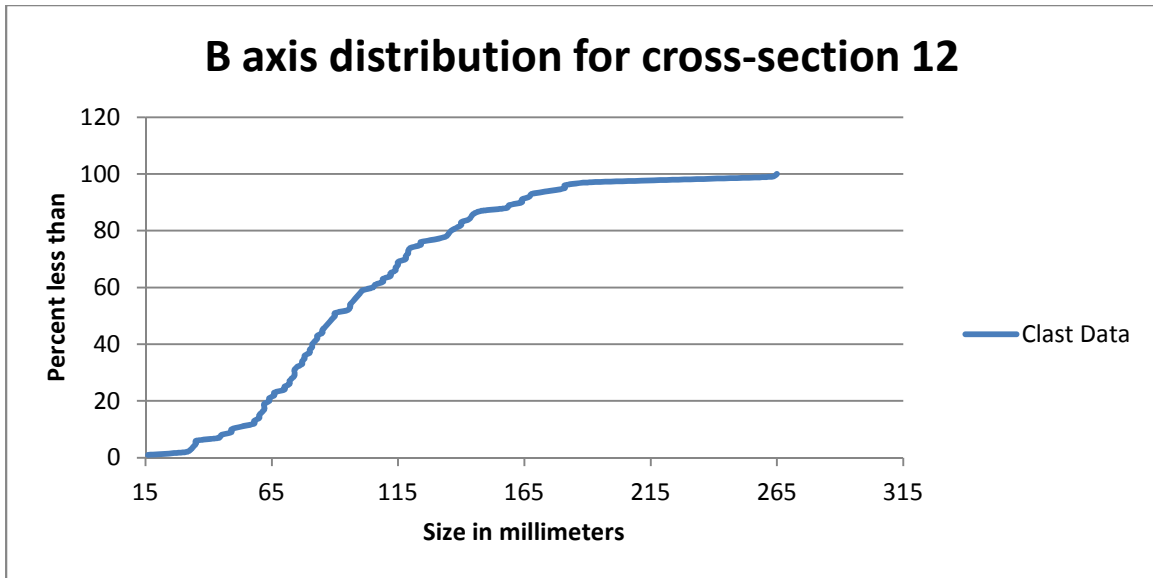


Figure 44. B axis distribution of cross-section 12.



Figure 45. Photo of cross-section 12, view is upstream.

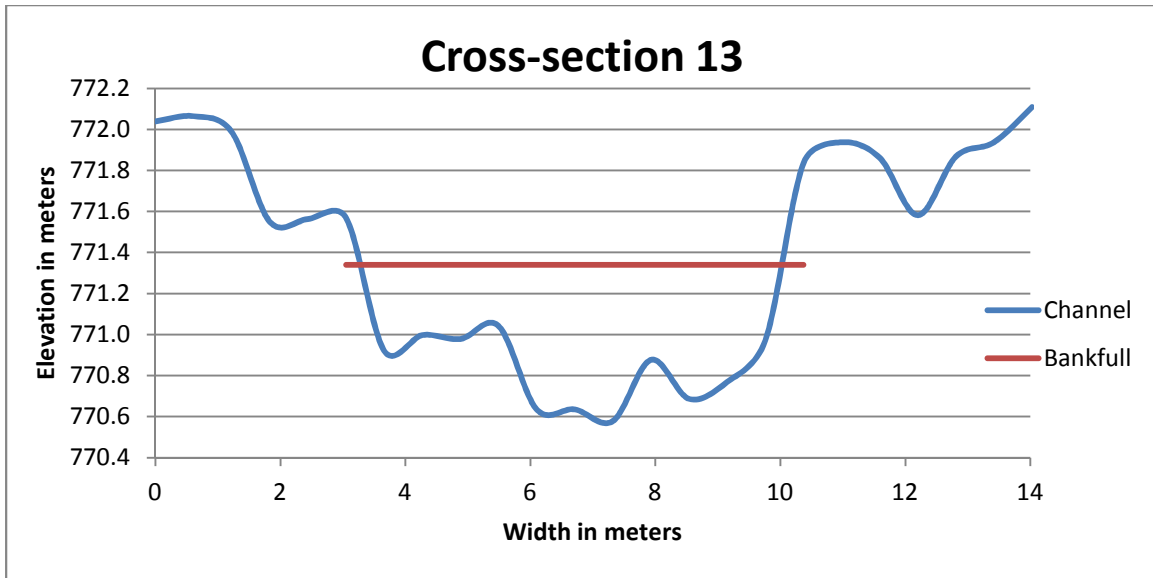


Figure 46. Cross-section 13, the red line represents bankfull conditions.

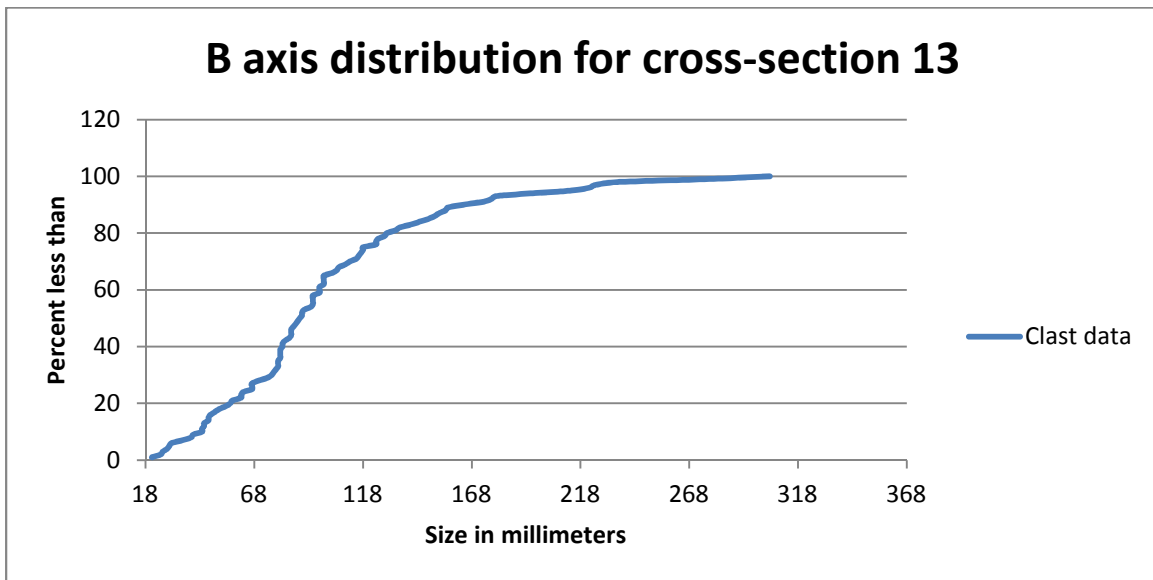


Figure 47. B axis distribution of cross-section 13.



Figure 48. Photo of cross-section 13, view is downstream.

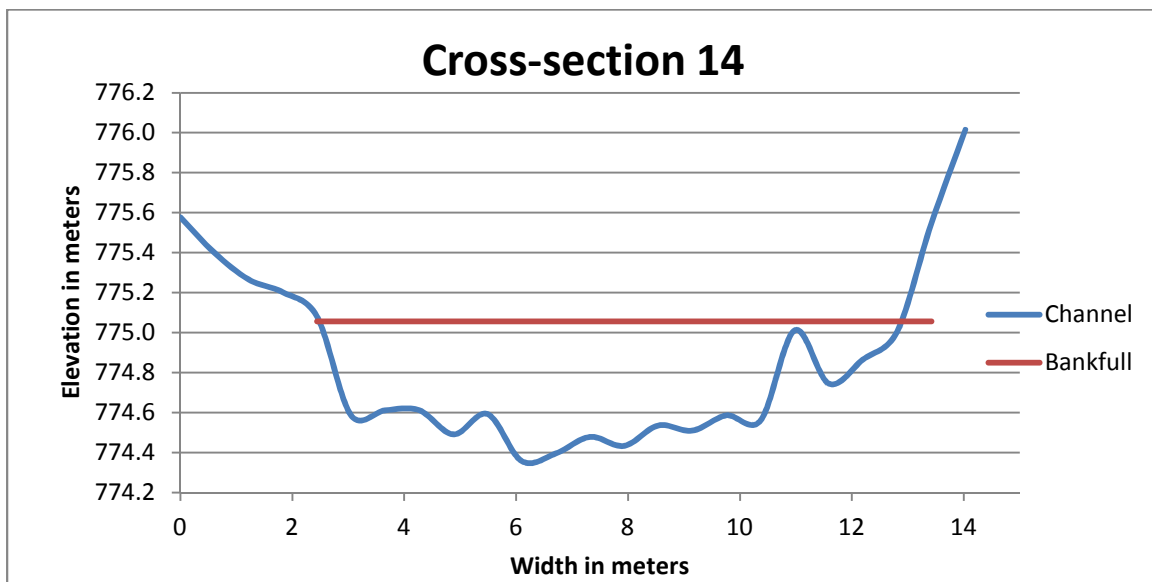


Figure 49. Cross-section 14, the red line represents bankfull conditions.

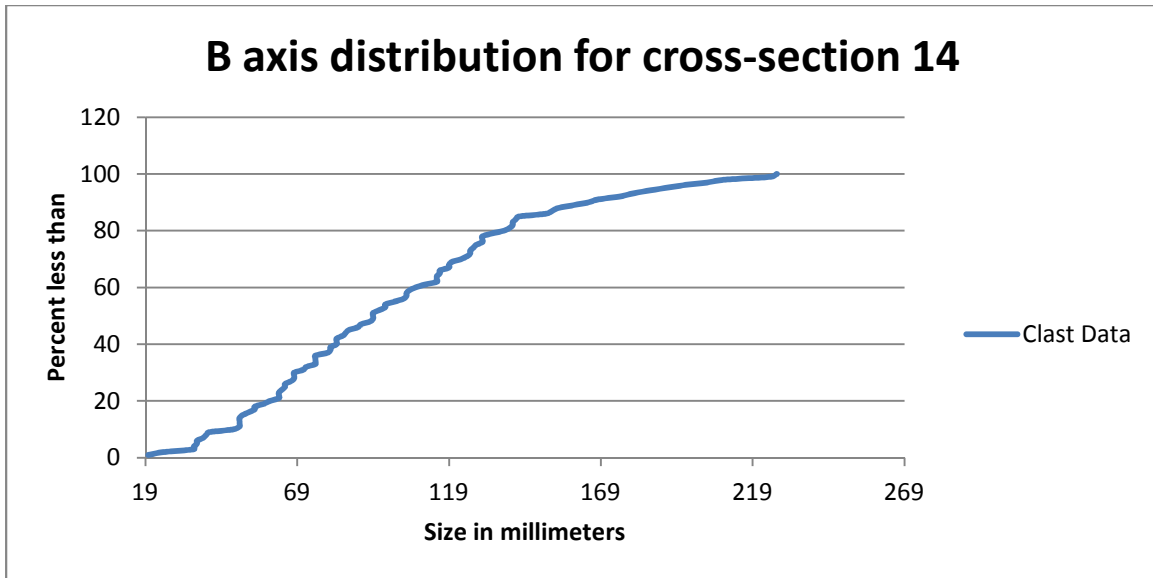


Figure 50. B axis distribution of cross-section 14.



Figure 51. Photo of cross-section 14, view is upstream.

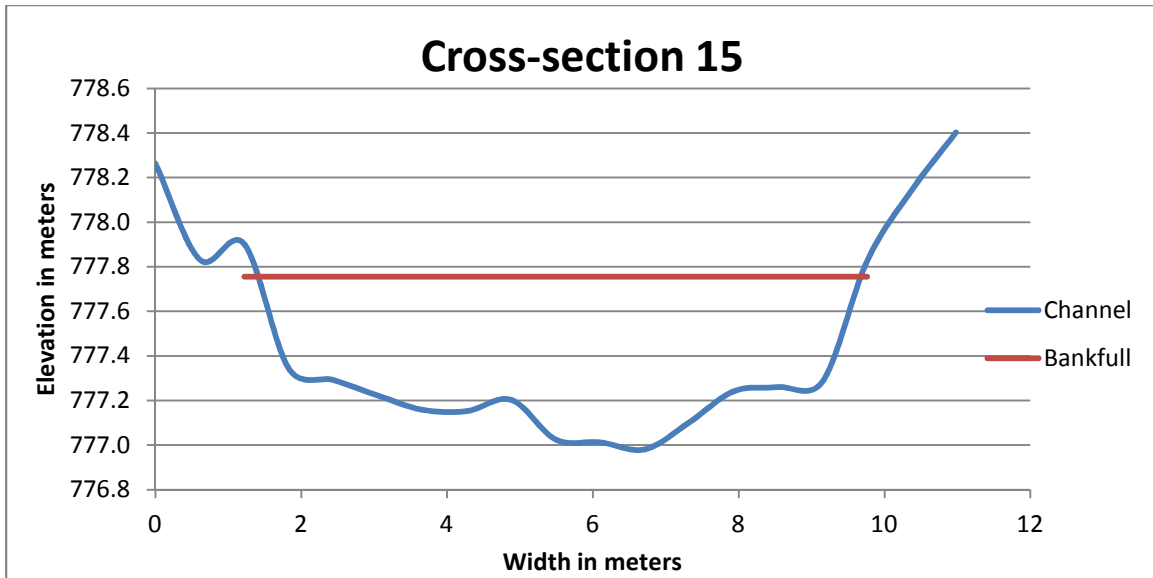


Figure 52. Cross-section 15, the red line represents bankfull conditions.

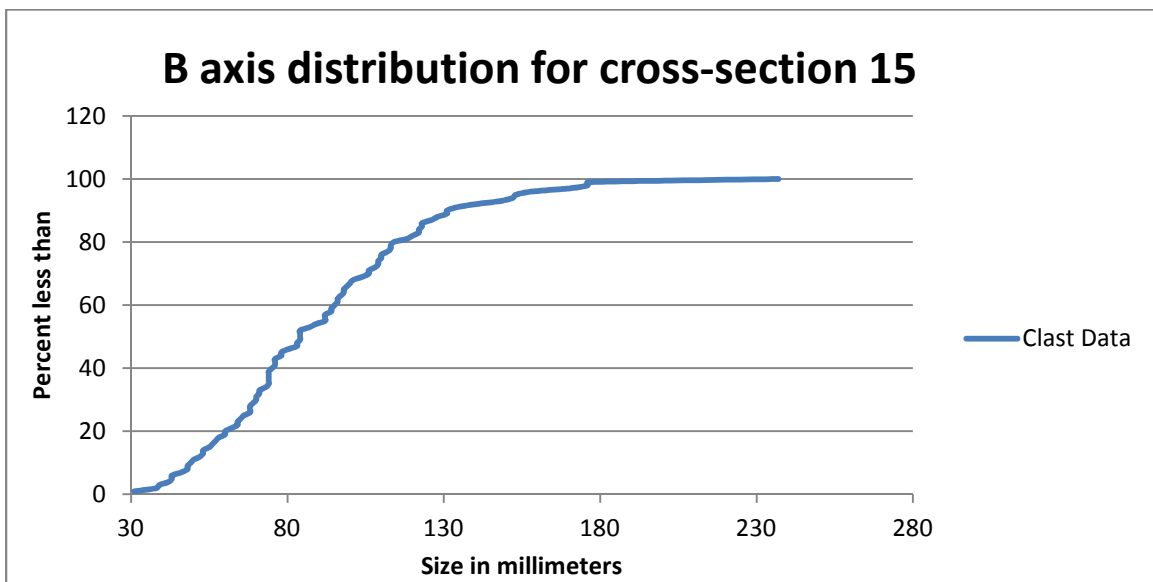


Figure 53. B axis distribution of cross-section 15.



Figure 54. Photo of cross-section 15, view is upstream and the tree at the bottom of the frame is above bankfull stage.

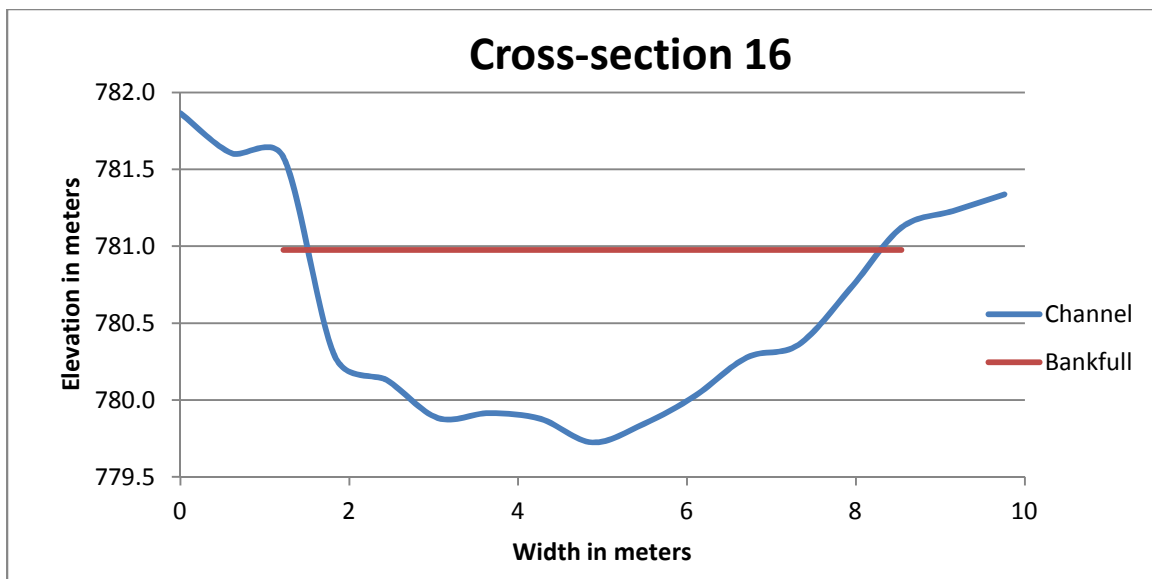


Figure 55. Cross-section 16, the red line represents bankfull conditions.

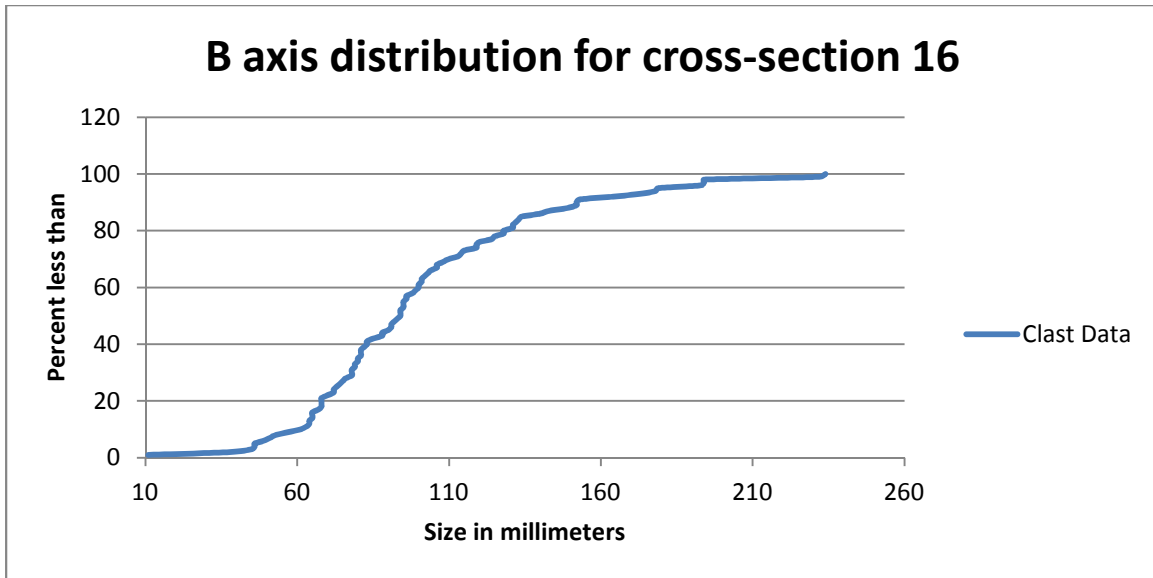


Figure 56. B axis distribution of cross-section 16.



Figure 57. Photo of cross-section 16, view is upstream.

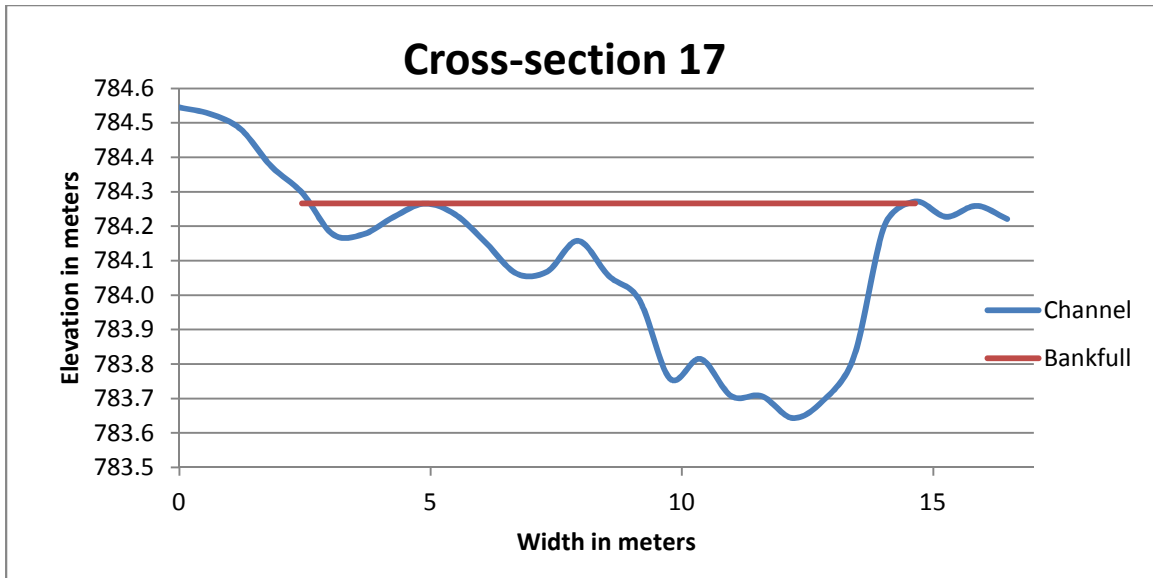


Figure 58. Cross-section 17, the red line represents bankfull conditions.

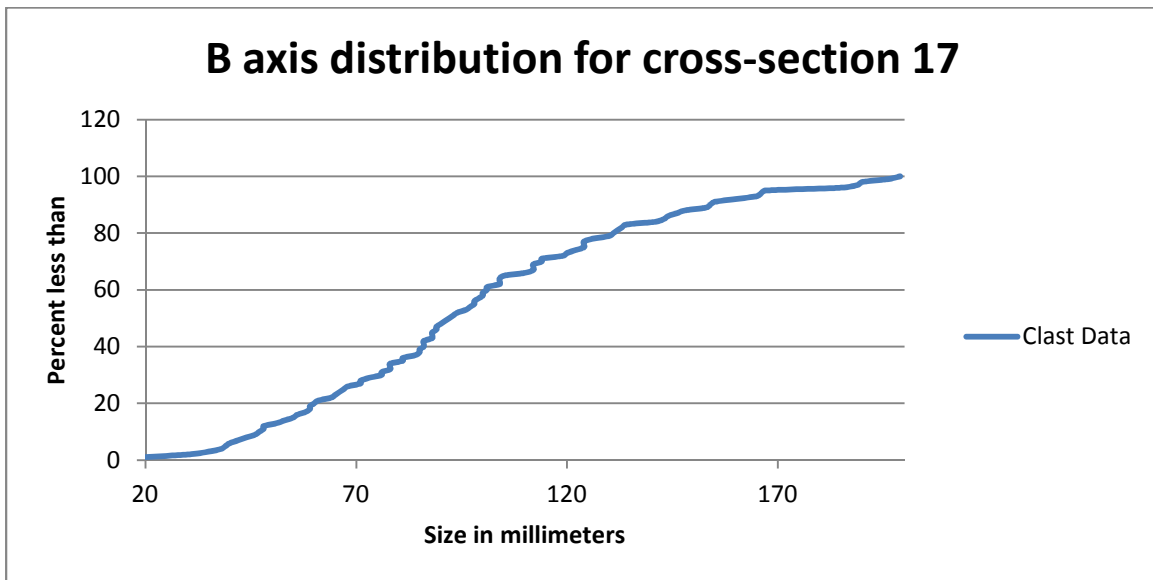


Figure 59. B axis distribution of cross-section 17.



Figure 60. Photo of cross-section 17, view is upstream.

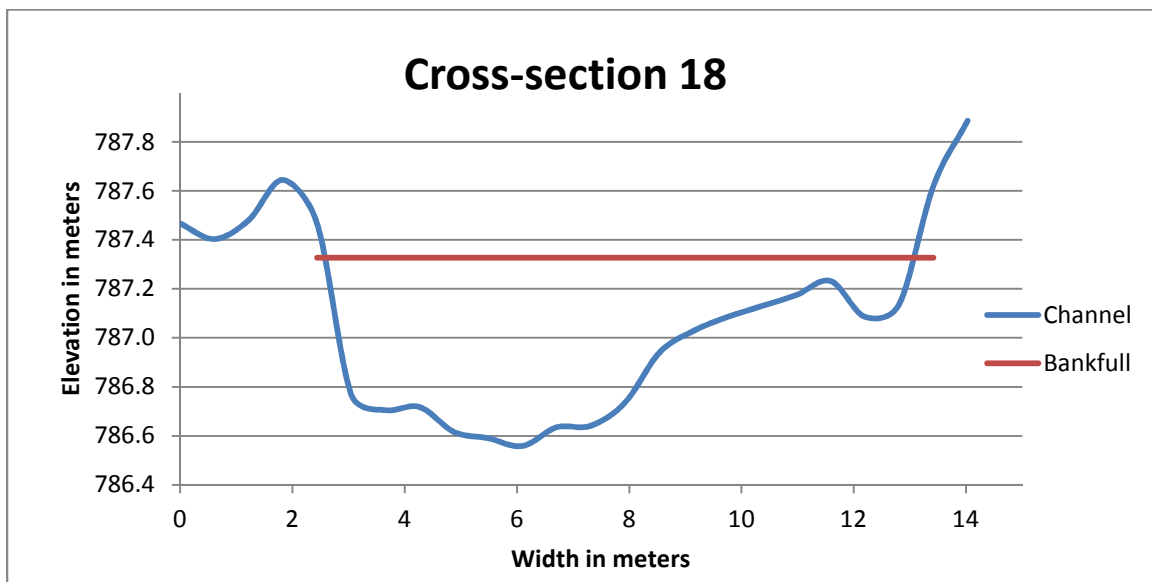


Figure 61. Cross-section 18, the red line represents bankfull conditions.

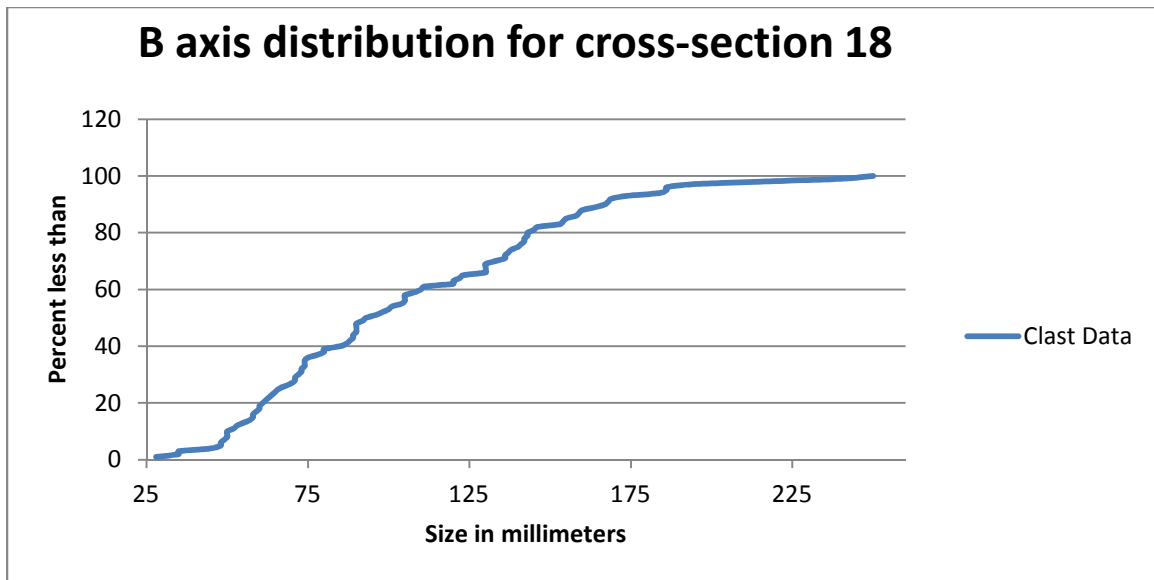


Figure 62. B axis distribution of cross-section 18.



Figure 63. Photo of cross-section 18, view is upstream.

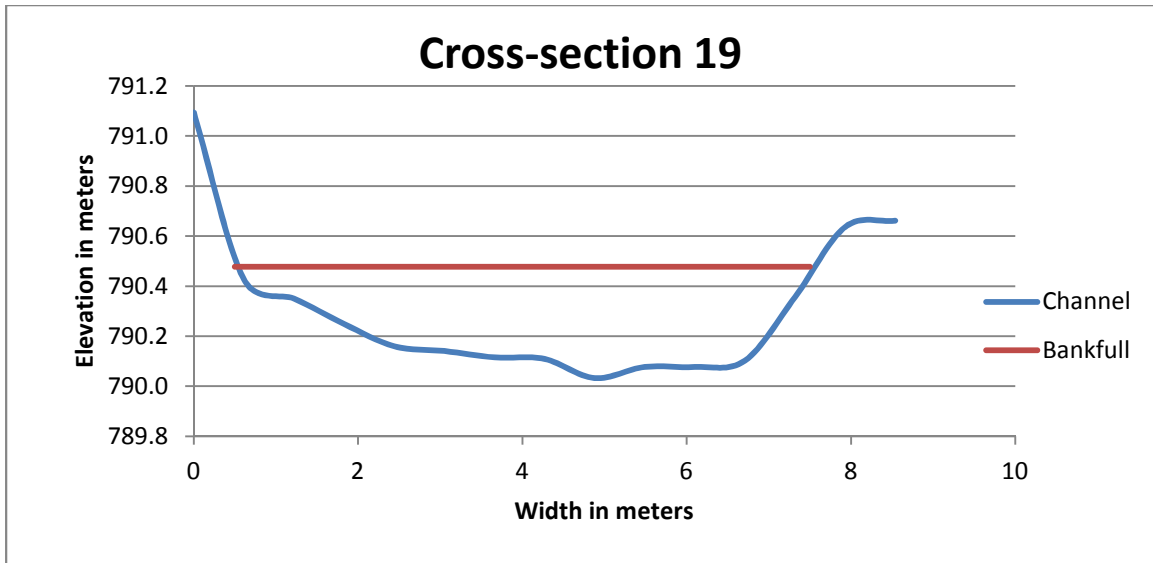


Figure 64. Cross-section 19, the red line represents bankfull conditions.

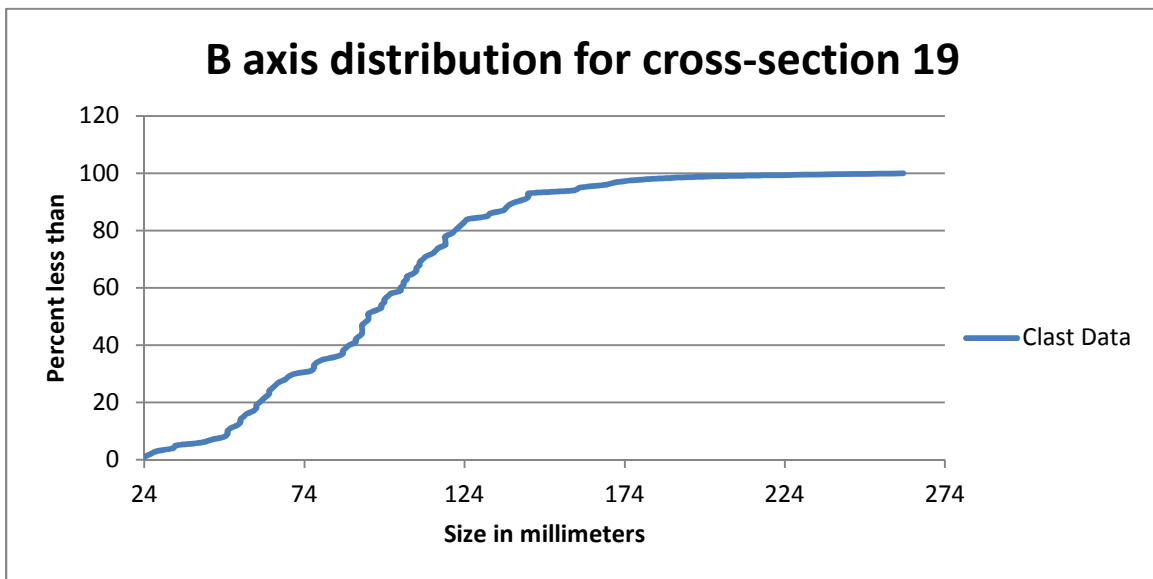


Figure 65. B axis distribution of cross-section 19.



Figure 66. Photo of cross-section 19, view is upstream.

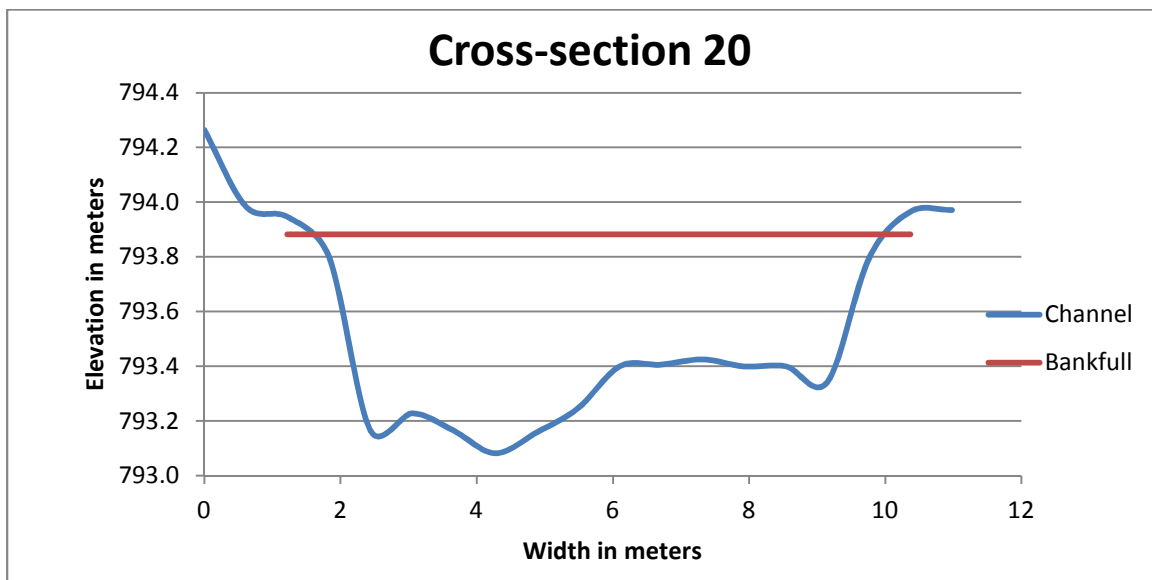


Figure 67. Cross-section 20, red line represents bankfull conditions.

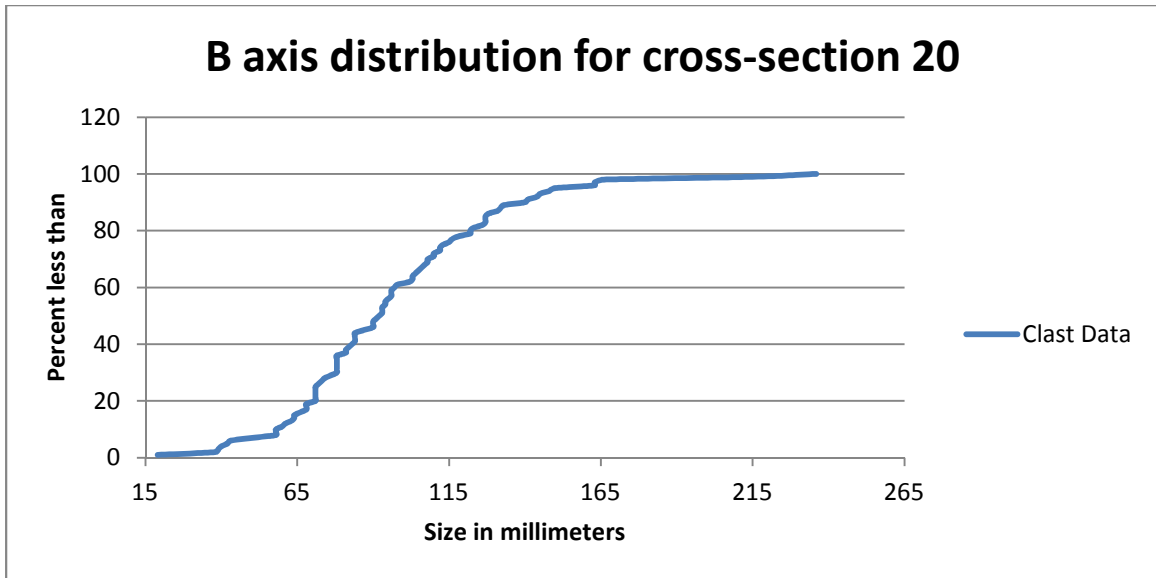


Figure 68. B axis distribution of cross-section 20.



Figure 69. Photo of cross-section 20, view is upstream.

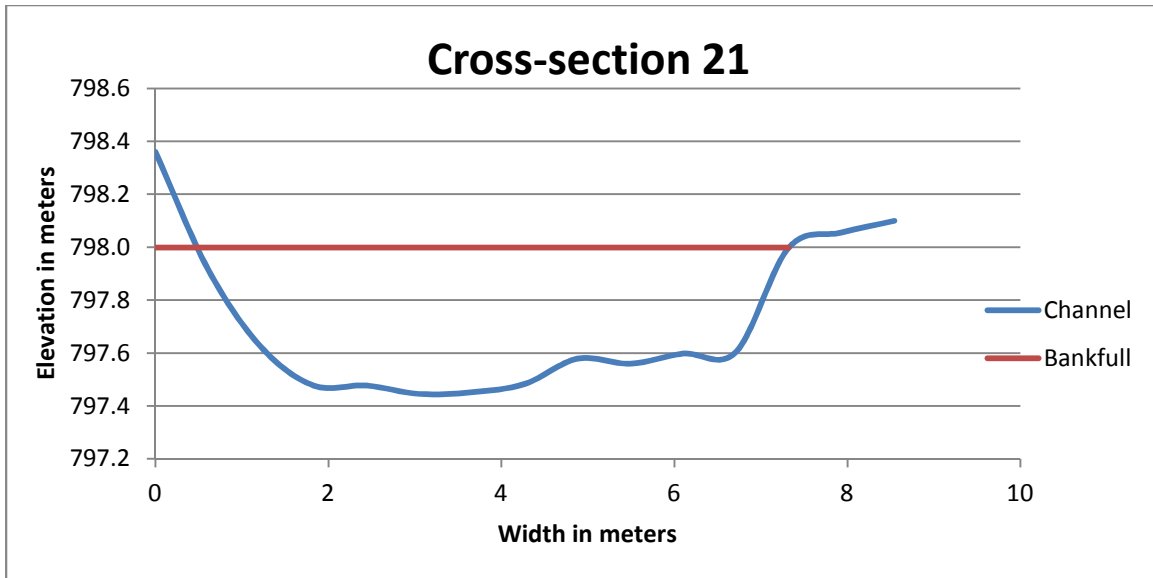


Figure 70. Cross-section 21, the red line represents bankfull conditions.

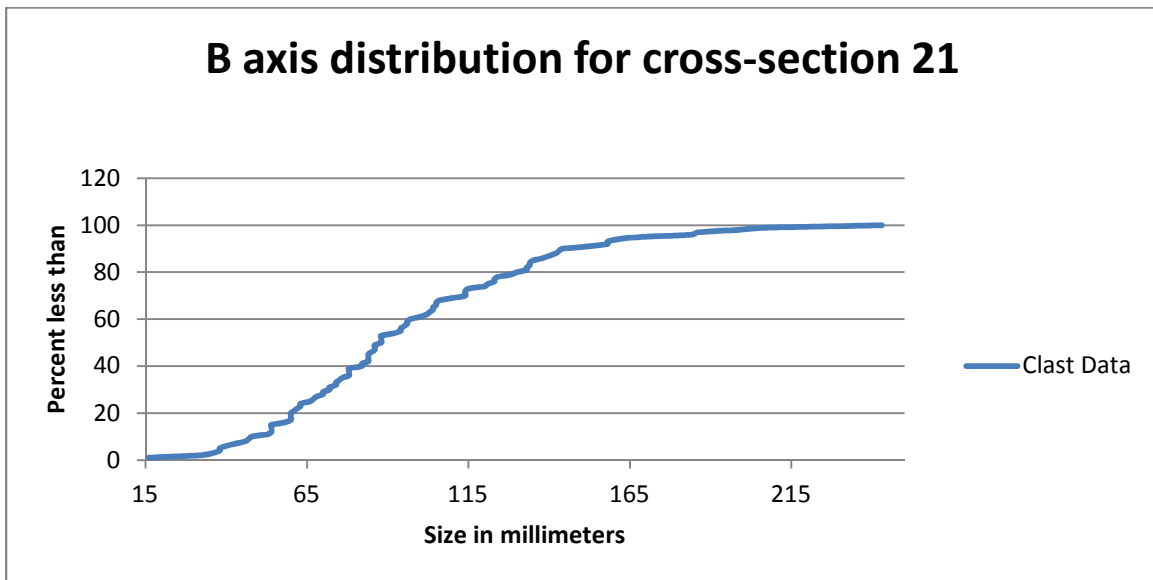


Figure 71. B axis distribution of cross-section 21.



Figure 72. Photo of cross-section 21, view is upstream.

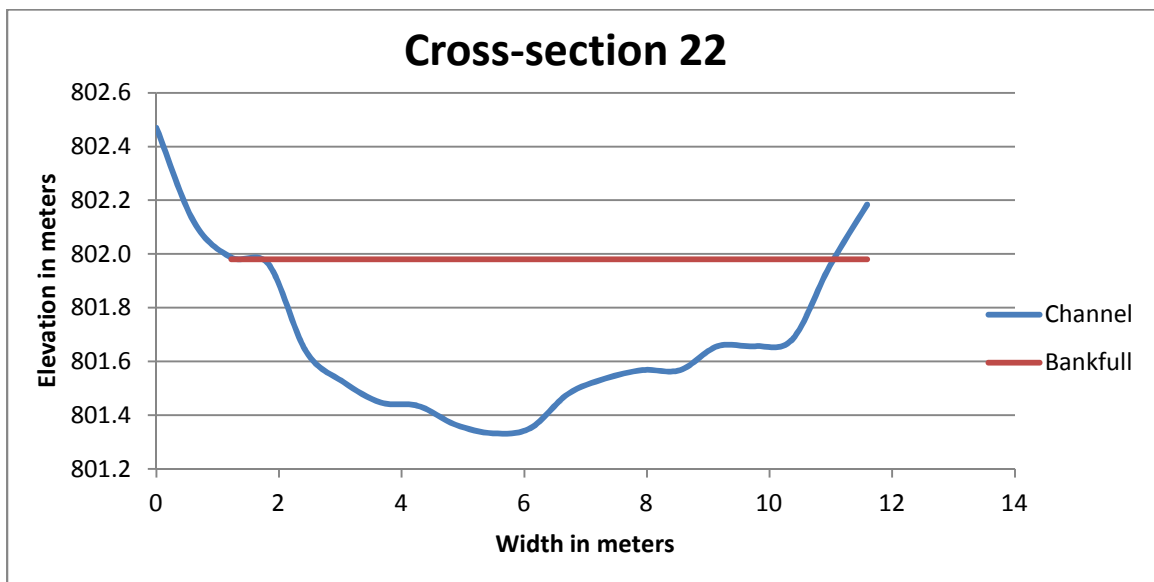


Figure 73. Cross-section 22, the red line represents bankfull conditions.

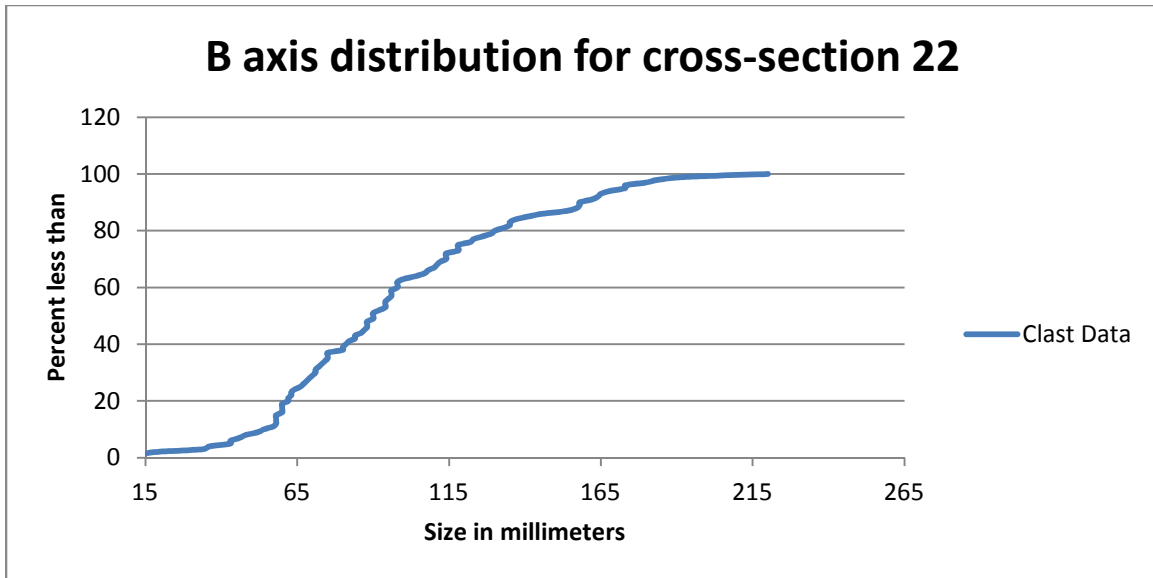


Figure 74. B axis distribution of cross-section 22.



Figure 75. Photo of cross-section 22, view is upstream.



Figure 76. Cross-section 23, the red line represents bankfull conditions.

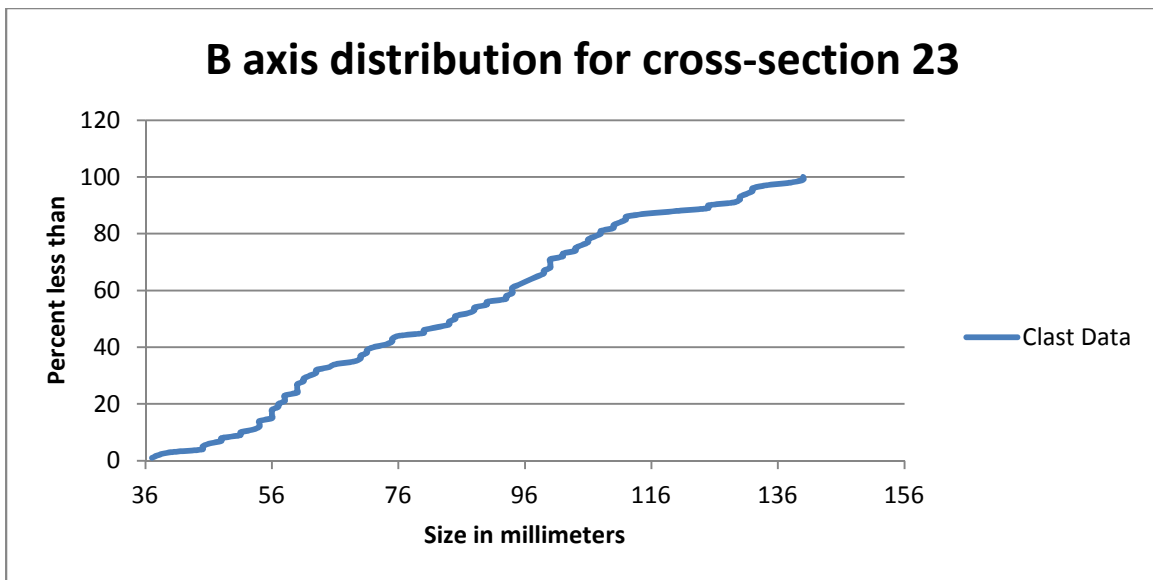


Figure 77. B axis distribution of cross-section 23.



Figure 78. Photo of cross-section 23, view is downstream.

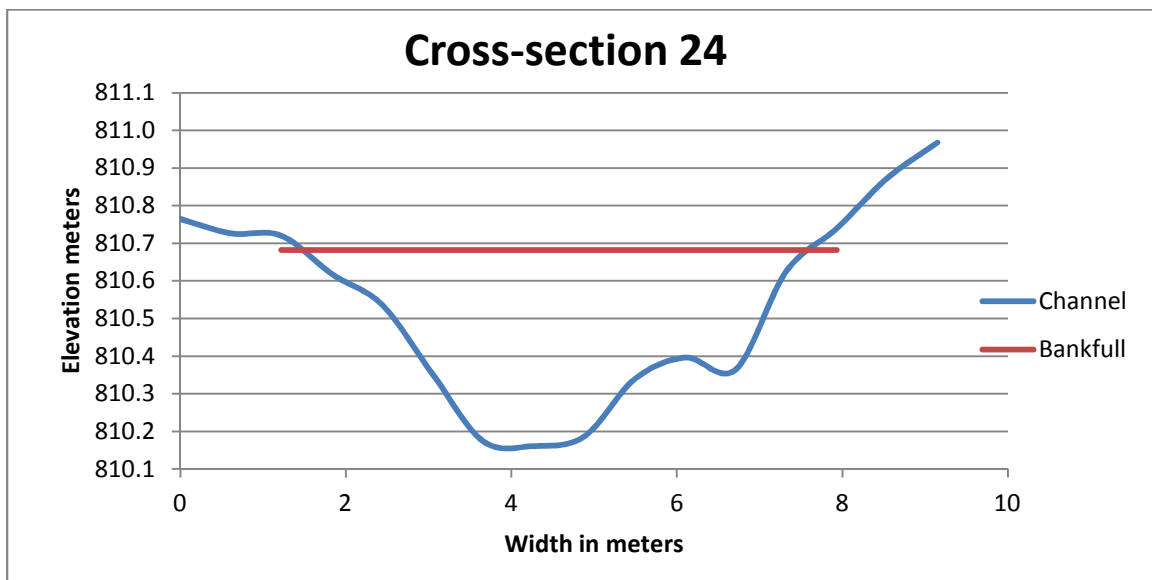


Figure 79. Cross-section 24, the red line represents bankfull conditions.

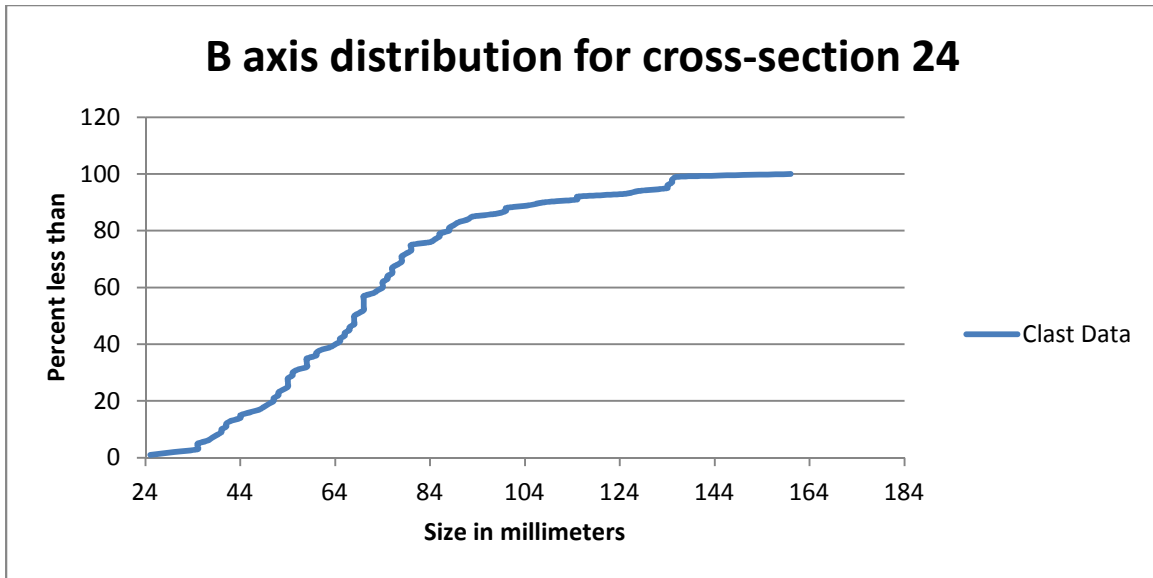


Figure 80. B axis distribution of cross-section 24, the red line represents the D_{90} grain size and the green line represents the D_{50} grain size.



Figure 81. Photo of cross-section 24, view is downstream.

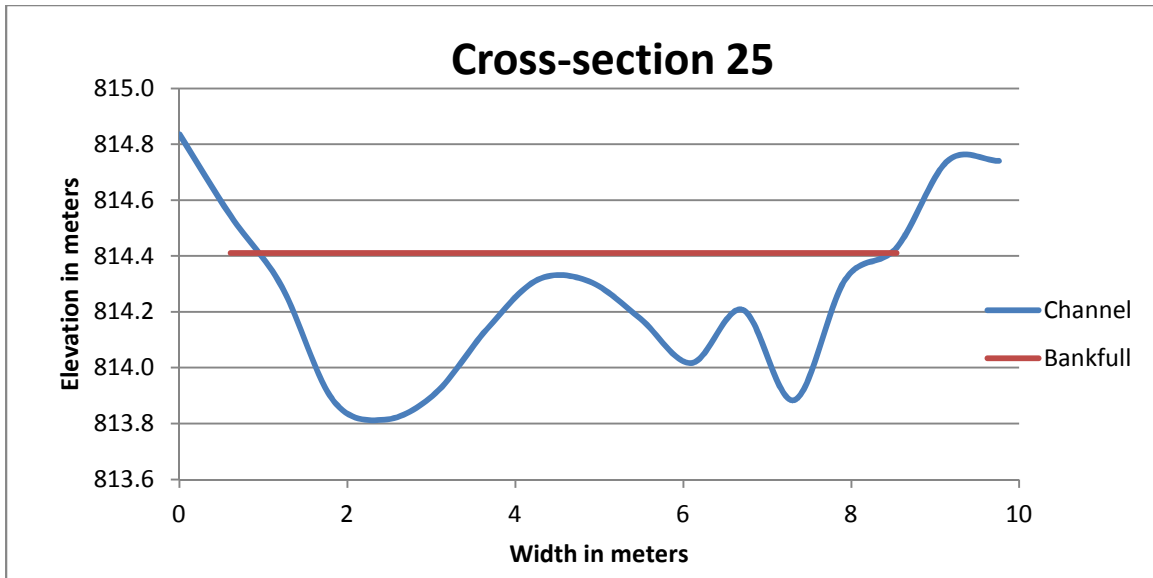


Figure 82. Cross-section 25, the red line represents bankfull conditions.

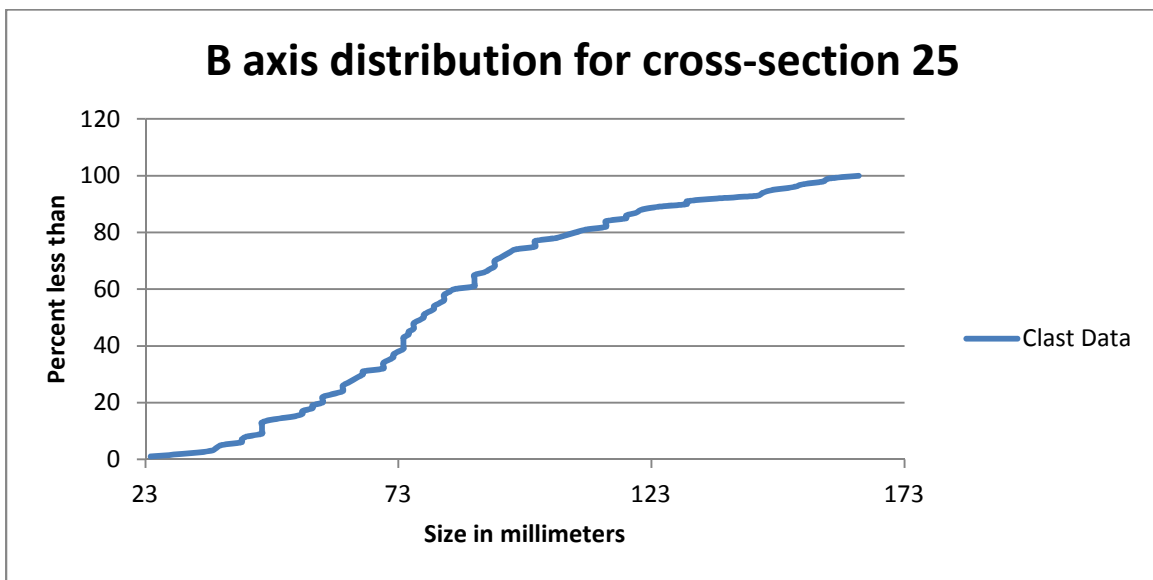


Figure 83. B axis distribution of cross-section 25.



Figure 84. Photo of cross-section 25, view is downstream.

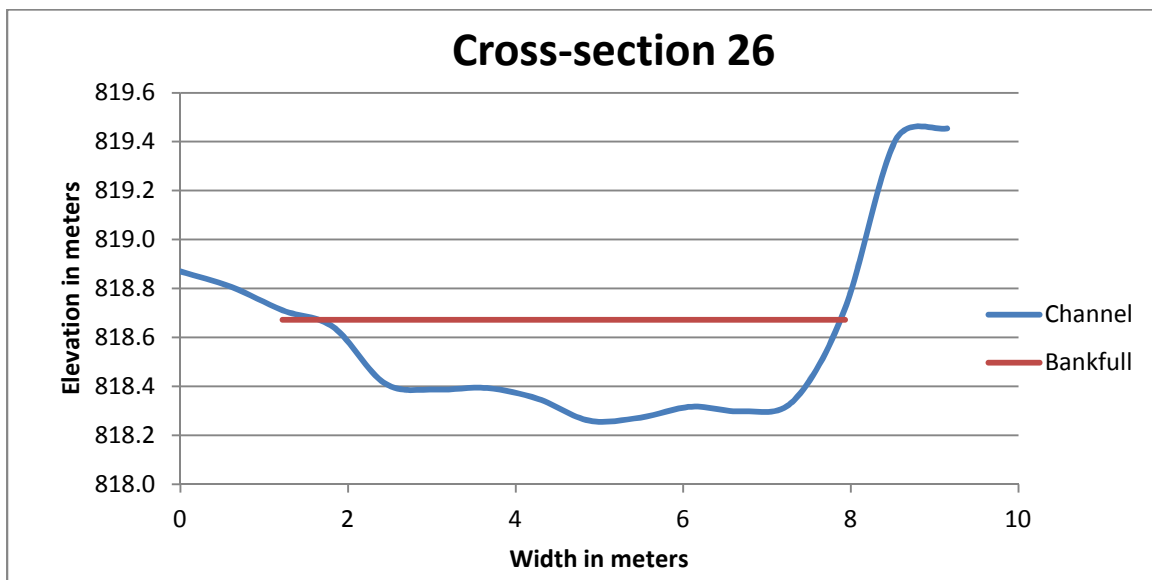


Figure 85. Cross-section 26, the red line represents bankfull conditions.

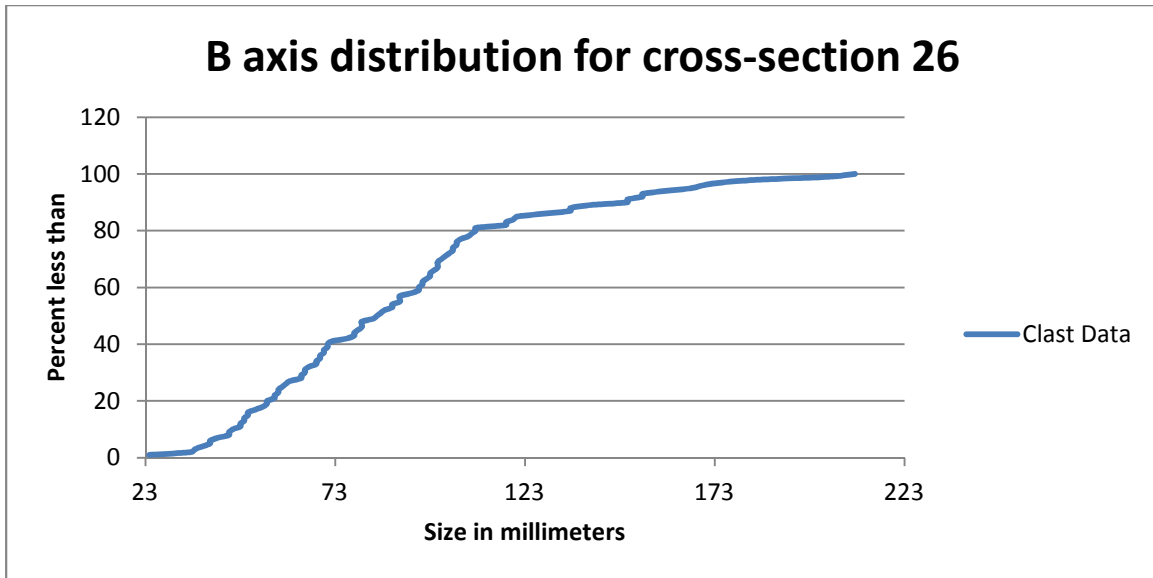


Figure 86. B axis distribution of cross-section 26.



Figure 87. Photo of cross-section 26, view is downstream.

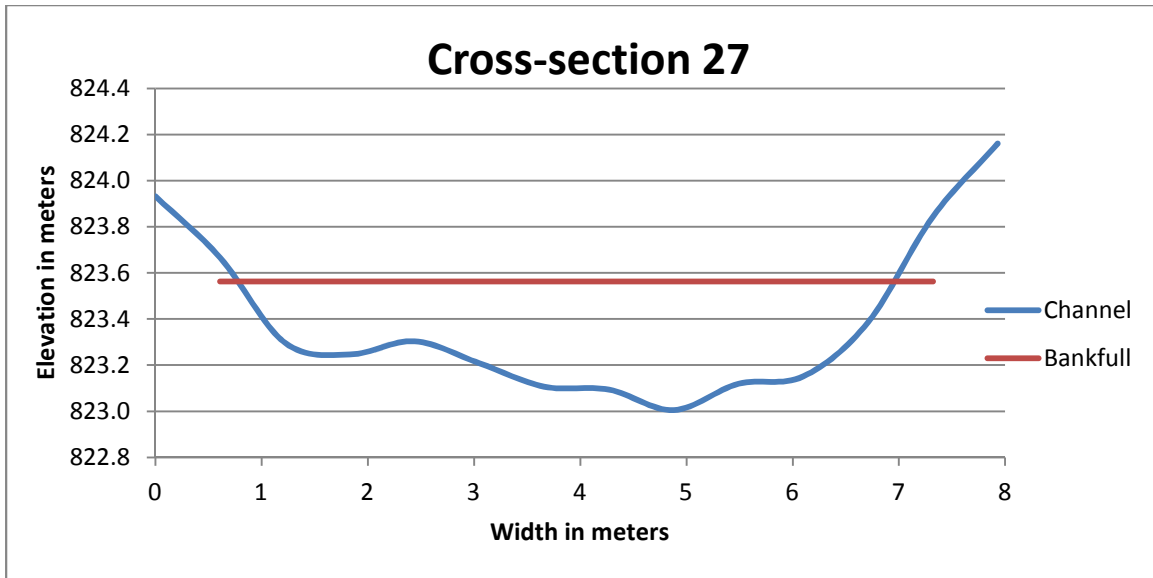


Figure 88. Cross-section 27, the red line represents bankfull conditions.

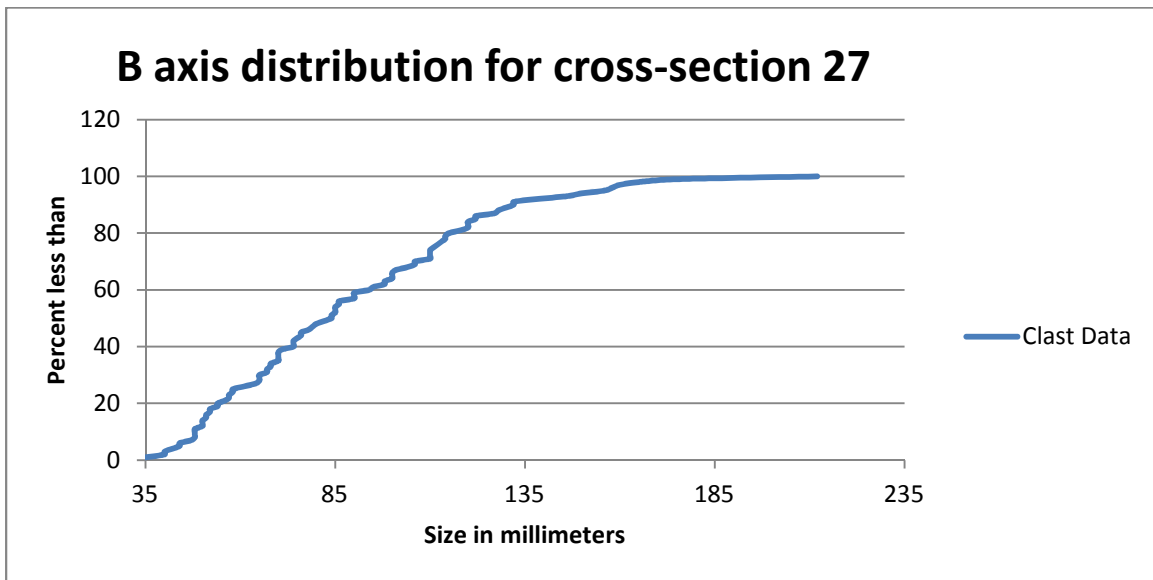


Figure 89. B axis distribution of cross-section 27.



Figure 90. Photo of cross-section 27, view is downstream.

Measuring cross-sections allowed for the measurement and calculation of channel characteristics and allowed calculation of bankfull Shields stress (τ_{bf}^*). Also measuring the slope of the channel at each cross-section allowed for the calculation of reference Shields stress (τ_r^*) along with the calculation of the bankfull Shields stress (τ_{bf}^*). The values for D_{90} , D_{50} bankfull Shields stress (τ_{bf}^*), and reference Shields stress (τ_r^*) for the cross-sections. These measurements and calculations are shown in Table 2.

Table 2. Measurements of D_{90} and D_{50} , bankfull Shields stress (τ_{bf}^*), and reference Shields stress (τ_r^*) for all cross-section. No data is presented for cross-section 6 due to the lack of grain size data resulting from high slope and bedrock surface at the cross-section.

Cross-section D50	τ_{bf}^* D_{90}	τ_{bf}^* D_{50}	τ_r^*	D_{90} in mm	D_{50} in mm
1	0.123	0.208	0.076	120	70
2	0.073	0.134	0.069	110	60
3	0.076	0.136	0.073	90	50
4	0.122	0.198	0.120	190	110
5	0.314	0.479	0.120	110	60
6			0.175		
7	0.033	0.029	0.064	120	50
8	0.055	0.106	0.060	120	60
9	0.051	0.092	0.077	170	90
10	0.129	0.215	0.093	100	60
11	0.139	0.221	0.106	150	80
12	0.031	0.056	0.061	160	90
13	0.078	0.143	0.127	160	80
14	0.077	0.091	0.099	160	90
15	0.050	0.078	0.068	140	80
16	0.111	0.180	0.103	150	90
17	0.019	0.031	0.064	150	90
18	0.050	0.090	0.095	160	90
19	0.023	0.035	0.068	140	90
20	0.037	0.129	0.114	140	90
21	0.038	0.062	0.075	140	80
22	0.058	0.102	0.112	150	90
23	0.012	0.017	0.074	120	80
24	0.063	0.099	0.116	100	60
25	0.046	0.076	0.109	130	70
26	0.030	0.054	0.085	150	80
27	0.055	0.087	0.106	130	80

Important properties of the stream at the cross-sections include the height of the water at bankfull, the slope, and also the width of the stream at each cross section. The slope of the channel is used in Equation 2 to calculate the shear stress of the channel. The height of the water and width of the channel are used in Equation 3 along with the amount of shear stress from Equation 2 to calculate the bankfull Shields stress. Figures 91, 92, 93, and 94 show bankfull height, slope, width, D_{90} and D_{50} measurements for all measured cross-sections, respectively. As the height of the water and the grain size decreased the submergence of those grains increases.

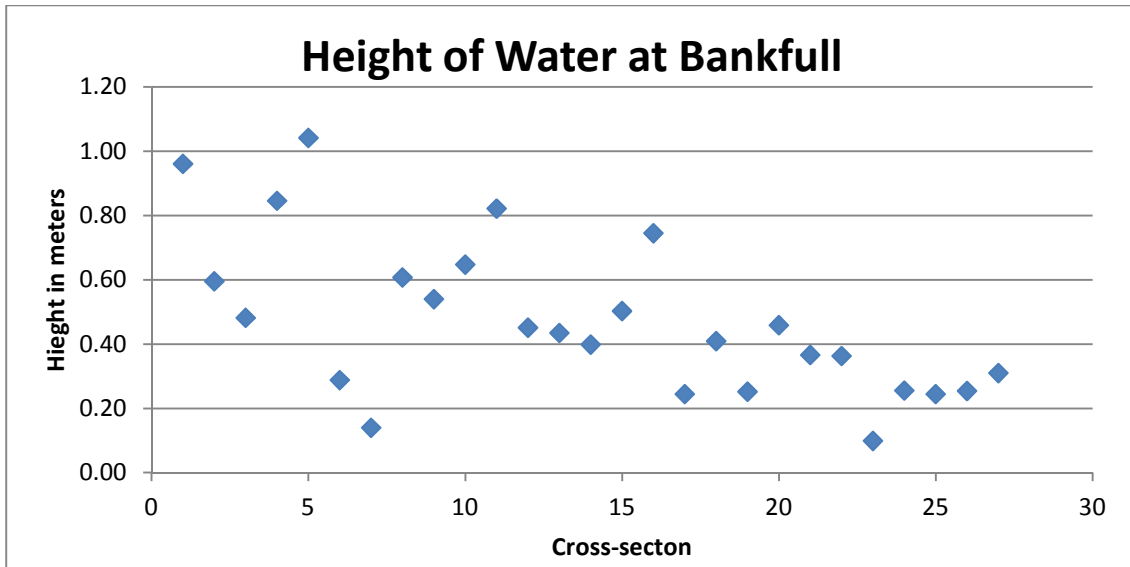


Figure 91. Height of the water at bankfull conditions at each cross-section.

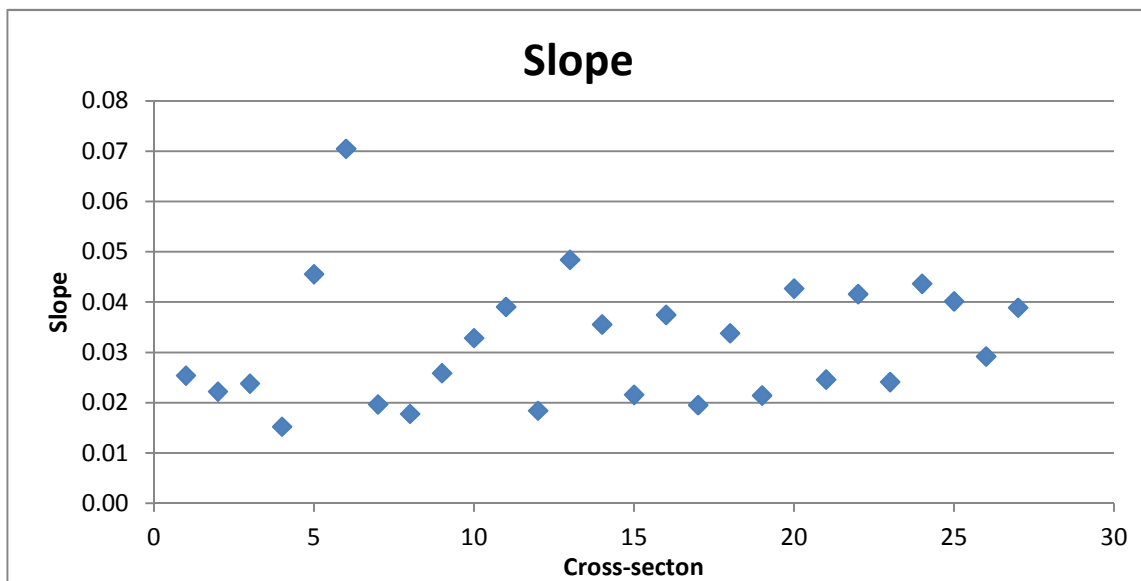


Figure 92. Slope of the channel at each cross-section.

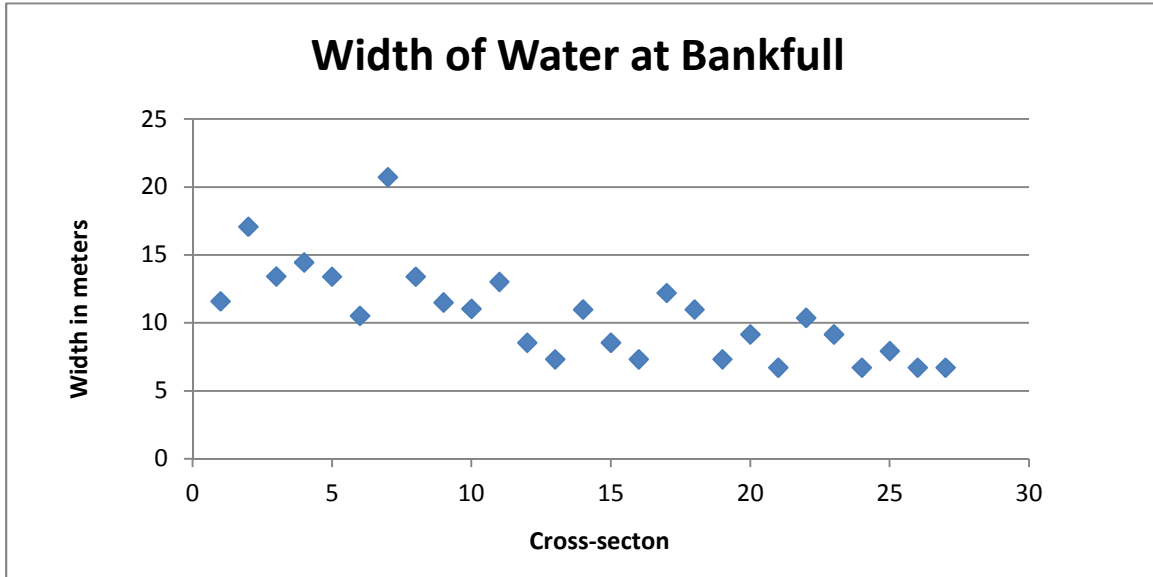


Figure 93. Width of the channel at each cross-section.

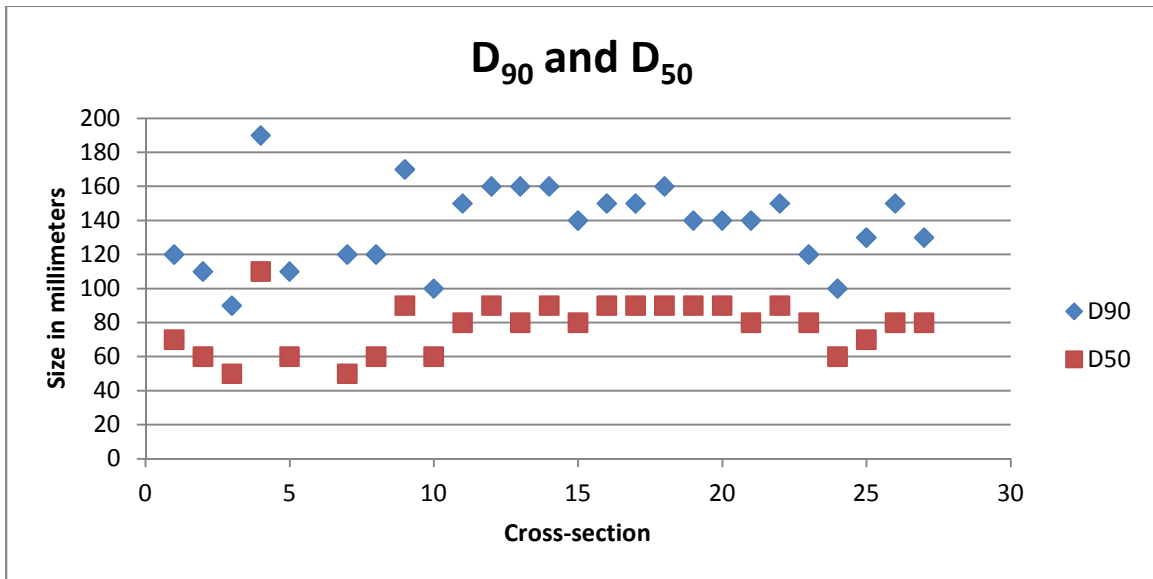


Figure 94. D₉₀ and D₅₀ measurements at each cross-section.

As the study area progressed upstream the slope of the study area remained fairly constant ranging mostly between 0.02 and 0.05 percent. Typical mountain streams have a slope range from about 0.02 to 0.05 (Mueller et al., 2005). This means that the study area falls directly

into the category of a mountain stream. The height of the water at bankfull progressed from seemingly random into a steadily decreasing trend around cross-section 7 and started to become consistent slightly above 0.2 meters in the upper reaches of the study area. The width of the channel also decreased with distance upstream and became consistent at around 7 meters. Submergence of the grains in the study area steadily decreased with distance upstream as seen in Figure 95. Calculations of D_{90} , D_{50} , slope, width, height, and submergence are also presented in Table 3.

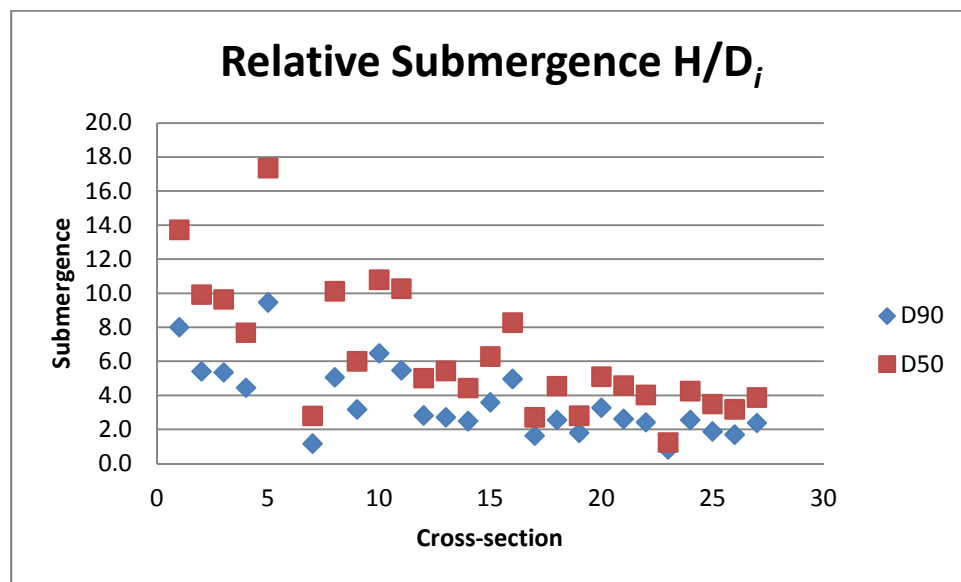


Figure 95. Relative submergence of the D_{90} and D_{50} at each cross-section.

Table 3. Measurements of D_{90} , D_{50} , slope, width, height, and submergence. No grain size or submergence data is presented for cross-section 6 due to the lack of grain size data resulting from high slope and bedrock surface at the cross-section.

Cross section	D90 in mm	D50 in mm	Slope	Width	Height	H/D90	H/D50
1	120	70	0.03	11.59	0.96	8.0	13.7
2	110	60	0.02	17.08	0.60	5.4	9.9
3	90	50	0.02	13.42	0.48	5.4	9.6
4	190	110	0.02	14.45	0.85	4.5	7.7
5	110	60	0.05	13.40	1.04	9.5	17.4
6			0.07	10.52	0.29		
7	120	50	0.02	20.73	0.14	1.2	2.8
8	120	60	0.02	13.40	0.61	5.1	10.1
9	170	90	0.03	11.50	0.54	3.2	6.0
10	100	60	0.03	11.04	0.65	6.5	10.8
11	150	80	0.04	13.02	0.82	5.5	10.3
12	160	90	0.02	8.54	0.45	2.8	5.0
13	160	80	0.05	7.32	0.43	2.7	5.4
14	160	90	0.04	10.98	0.40	2.5	4.4
15	140	80	0.02	8.54	0.50	3.6	6.3
16	150	90	0.04	7.32	0.75	5.0	8.3
17	150	90	0.02	12.20	0.24	1.6	2.7
18	160	90	0.03	10.98	0.41	2.6	4.6
19	140	90	0.02	7.32	0.25	1.8	2.8
20	140	90	0.04	9.15	0.46	3.3	5.1
21	140	80	0.02	6.71	0.37	2.6	4.6
22	150	90	0.04	10.37	0.36	2.4	4.0
23	120	80	0.02	9.15	0.10	0.8	1.2
24	100	60	0.04	6.71	0.26	2.6	4.3
25	130	70	0.04	7.93	0.24	1.9	3.5
26	150	80	0.03	6.71	0.25	1.7	3.2
27	130	80	0.04	6.71	0.31	2.4	3.9

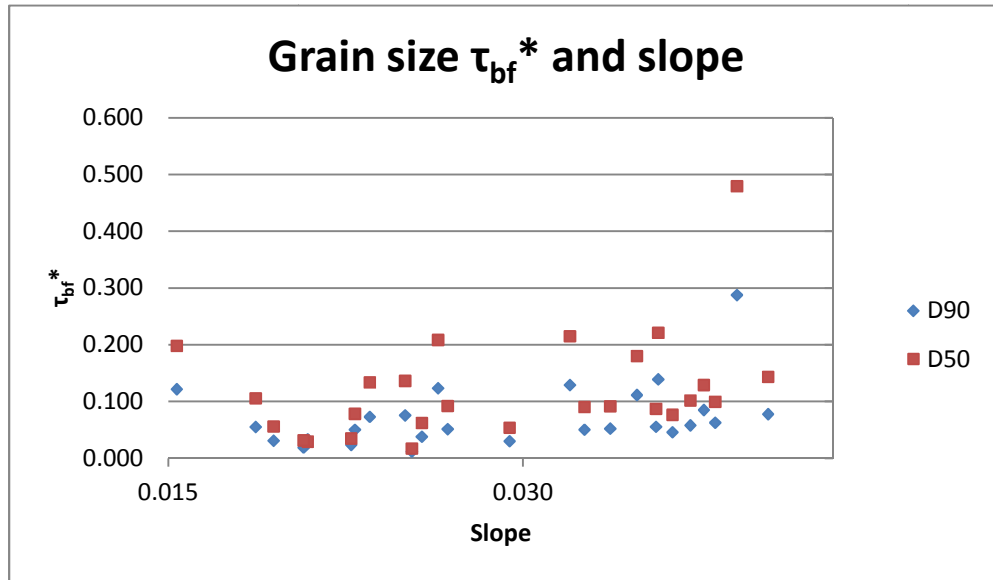


Figure 96. Bankfull Shields stress (τ_{bf}^*) verses slope.

These channel properties becoming consistent also led to a stabilization of bankfull Shields stress (τ_{bf}^*) and reference Shields stress (τ_r^*) with D_{50} bankfull Shields stress around 0.05 and 0.07 for the D_{90} bankfull Shields stress. Figure 96 shows how the ratio between slope and bankfull Shields stress (τ_{bf}^*).

The relationship between amount of bankfull Shields stress (τ_{bf}^*) and slope stays fairly constant for the study area and bankfull Shields stress (τ_{bf}^*) does not range much above 0.2. This shows that the other controls are also in place on the amount of bankfull Shields stress (τ_{bf}^*) namely width, height, and grain size. Figure 96 is exactly what is to be expected since Equation 4 is a relationship between slope and reference Shields stress (τ_r^*).

As shown by Mueller et al. (2005) a stream becomes self-shaping when the ratio of bankfull Shields stress (τ_{bf}^*) and reference Shields stress (τ_r^*) is slightly greater than 1. And in areas of the stream bed where the ratio of bankfull Shields stress (τ_{bf}^*) and reference Shields stress (τ_r^*) is less than 1 the stream should not be self-shaping. Figure 97 shows the ratio between bankfull Shields stress (τ_{bf}^*) and reference Shields stress (τ_r^*) for the D_{90} and D_{50} clast sizes at each cross-section. Figure 98 difference between bankfull Shields stress (τ_{bf}^*) and reference Shields stress (τ_r^*) at the respective cross-sections. Progression from cross-section 1 to through cross-section 27 shows that the ratio decreases and falls below 1 at cross-section 17 for both D_{90} and D_{50} . After this cross-section only one other cross-section for the D_{50} has a ratio above 1. Figure 98 shows the difference between bankfull Shields stress (τ_{bf}^*) and reference Shields stress (τ_r^*). This figure shows the same relationship as Figure 97 but clearly identifies cross-sections where the ratio is less than 1, by plotting the point below zero on the y axis. Figure 98 is a good visual compliment to Figure 97 to help understand if the stream at a particular cross-section is self-shaping or not. Cross-section where the stream channel is considered self-shaping

in Figure 98 would be plotted above zero on the y axis. Whereas, cross-sections in Figure 98 which are not self-shaping would be plotted below zero on the y axis. Both Figure 97 and Figure 98 clearly show there is a distinct drop below the self-shaping threshold around cross-section 14 for both D_{90} and D_{50} grain sizes.

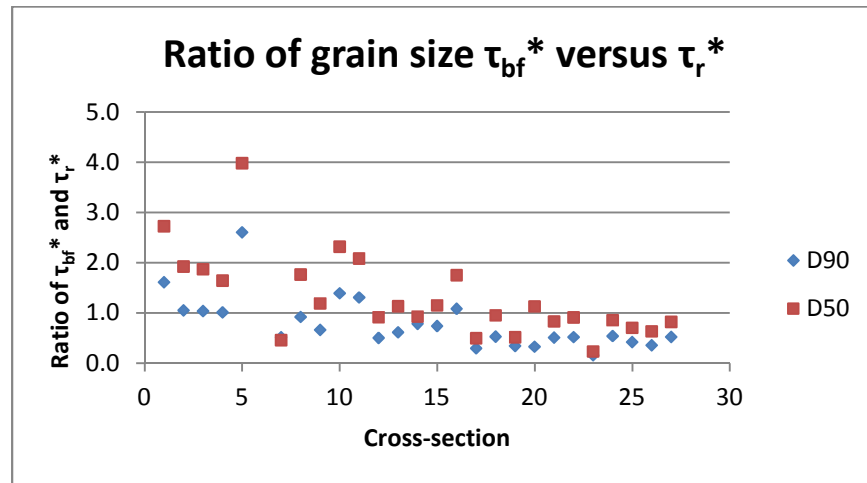


Figure 97. Graphical representation of the ratio between bankfull Shields stress (τ_{bf}^*) and reference Shields stress (τ_r^*) by cross-section.

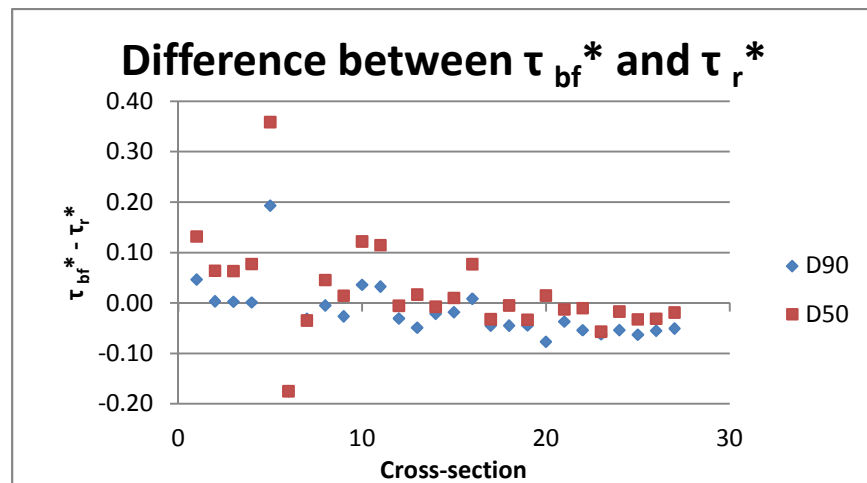


Figure 98. Difference between bankfull Shields stress (τ_{bf}^*) and reference Shields stress (τ_r^*) at each cross-section.

8. DISCUSSION

This study's aim was to determine when a river becomes self-shaping by using the ratio of bankfull Shields stress (τ_{bf}^*) and reference Shields stress (τ_r^*) as shown by Mueller et al. (2005, Fig. 6, included as Figure 2 herein). To overcome the absence of this critical Shields stress data Equation 4 was used to calculate the amount of reference Shields stress for this study. This may have some influence on the results of the study since Equation 4 was not formulated with data from streams in the same area or of the same size. Also the characteristics of the channel made classification of bankfull height hard to determine in portions of the stream bed due to the lack of recent bankfull flows. The main indicator of bankfull height used in this study was the transitional area from gravel clast to fine grain sediment that was stabilized by vegetation on the flood plain. Most of the channel was entrenched and or bound on one side very steep valley sides. The lack of a very well defined bankfull elevation was may lead to some error when calculating bankfull Shields stress (τ_{bf}^*) producing either too little or too much calculated Shields stress.

Mueller et al. (2005) showed that streams that are considered to be self-shaping have a ratio of bankfull Shields stress (τ_{bf}^*) and reference Shields stress (τ_r^*) slightly greater than one, and that this ratio remained roughly consistent across a wide range of channel slopes for gravel rivers. The bankfull Shields stress (τ_{bf}^*) in Mueller et al. (2005) was determined empirically from 159 different stream's grain size and bankfull geometry measurements. The relationship shown in Equation 5 from Mueller et al. (2005) and has been shown to provide an approximation of the bankfull Shields stress.

$$\tau_{bf}^* = (1.91S + 0.037) \quad (5)$$

This measurement of bankfull Shields stress (τ_{bf}^*) and reference Shields stress (τ_r^*) in the

Mueller et al. (2005) study is based off of the slope of the channel using Equation 3 and Equation 4 respectively. Equation 5 use slope to calculate bankfull shields stress and gives a slope dependent measurement. Equation 3 also uses slope to calculate the bankfull Shields stress and the grain size of interest making it a grain size dependent formula. Table 4 shows difference between the grain size dependent bankfull Shields stress (τ_{bf}^*) using Equation 3 and the D_{90} and D_{50} (grain size dependent calculation) and the slope dependent bankfull Shields stress (τ_{bf}^*) from Equation 5 (slope dependent calculation). Buffington et al. (1997) have shown that different of values for Shields stress (τ^*) can be calculated by using different methods in rough, turbulent flow characteristics of gravel-bedded rivers. These different methods of calculating the Shields stress will produce a range of values, not just a single value, for the same section of stream channel.

Table 4 shows that there is a difference between the two different methods of calculating bankfull Shields stress (τ_{bf}^*). The relationship between the grain size dependent bankfull Shields stress (τ_{bf}^*) and slope dependent bankfull Shields stress (τ_{bf}^*) calculations are shown in Figure 99. This figure also shows that the ranges of grain size dependent bankfull Shields stress (τ_{bf}^*) and slope dependent bankfull Shields stress (τ_{bf}^*) fall in similar ranges as the Mueller et al. (2005) study. The values of slope dependent bankfull Shields stress (τ_{bf}^*) from Equation 5 most closely mimic the values of the D_{50} grain size dependent bankfull Shields stress (τ_{bf}^*).

Table 4. Values for grain size dependent bankfull Shields stress, slope dependent bankfull

Shields stress, and ratios for comparison between the different methods. No data is presented for cross-section 6 due to the lack of grain size data resulting from high slope and bedrock surface at the cross-section.

Cross-section	τ_{bf}^* D90	τ_{bf}^* D50	Calculated τ_{bf}^*	τ^*	Ratio of D90 τ_{bf}^* / τ^*	Ratio of D50 τ_{bf}^* / τ^*	Ratio of calculated τ_{bf}^* / τ^*	Ratio of D90 $\tau_{bf}^* /$ calculated τ_{bf}^*	Ratio of D50 $\tau_{bf}^* /$ calculated τ_{bf}^*
1	0.123	0.208	0.086	0.076	1.61	2.73	1.12	1.44	2.44
2	0.073	0.134	0.079	0.069	1.05	1.93	1.14	0.92	1.68
3	0.076	0.136	0.082	0.073	1.04	1.87	1.13	0.92	1.65
4	0.122	0.198	0.066	0.120	1.01	1.65	0.55	1.84	2.99
5	0.314	0.479	0.124	0.120	2.61	3.98	1.03	2.53	3.86
6				0.175					
7	0.033	0.029	0.075	0.064	0.52	0.46	1.17	0.44	0.39
8	0.055	0.106	0.071	0.060	0.92	1.77	1.19	0.78	1.49
9	0.051	0.092	0.086	0.077	0.66	1.19	1.12	0.59	1.07
10	0.129	0.215	0.100	0.093	1.39	2.32	1.08	1.29	2.15
11	0.139	0.221	0.112	0.106	1.31	2.08	1.05	1.25	1.98
12	0.031	0.056	0.072	0.061	0.50	0.92	1.18	0.43	0.78
13	0.078	0.143	0.130	0.127	0.61	1.13	1.02	0.60	1.11
14	0.077	0.091	0.105	0.099	0.79	0.93	1.06	0.74	0.87
15	0.050	0.078	0.078	0.068	0.74	1.15	1.15	0.64	1.00
16	0.111	0.180	0.109	0.103	1.08	1.75	1.06	1.03	1.66
17	0.019	0.031	0.074	0.064	0.30	0.50	1.17	0.25	0.42
18	0.050	0.090	0.102	0.095	0.53	0.95	1.07	0.49	0.89
19	0.023	0.035	0.078	0.068	0.35	0.51	1.15	0.30	0.45
20	0.037	0.129	0.119	0.114	0.33	1.13	1.04	0.32	1.09
21	0.038	0.062	0.084	0.075	0.51	0.83	1.13	0.45	0.74
22	0.058	0.102	0.116	0.112	0.52	0.91	1.04	0.50	0.87
23	0.012	0.017	0.083	0.074	0.16	0.23	1.13	0.14	0.21
24	0.063	0.099	0.120	0.116	0.54	0.86	1.04	0.52	0.83
25	0.046	0.076	0.114	0.109	0.42	0.70	1.05	0.40	0.67
26	0.030	0.054	0.093	0.085	0.35	0.63	1.10	0.32	0.58
27	0.055	0.087	0.111	0.106	0.52	0.82	1.05	0.50	0.78

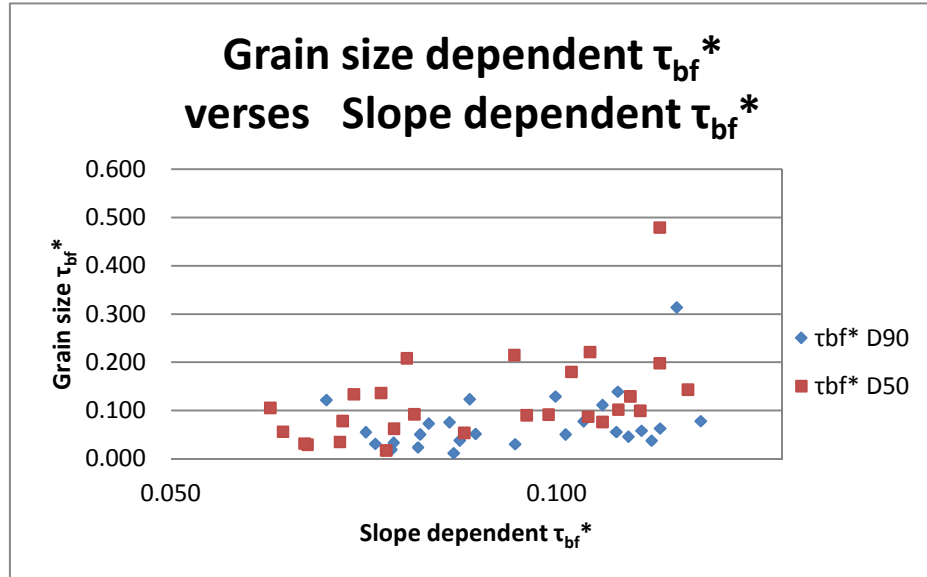


Figure 99. Grain size dependent bankfull Shields stress (τ_{bf}^*) versus slope dependent bankfull Shields stress (τ_{bf}^*) calculation.

As predicted by Mueller et al. (2005) the reference Shields stress (τ_r^*) obtained from Equation 4 does become smaller as the depth of the water at bankfull increases. For this study area the height of the water does increase in the downstream as shown in Figure 91. However, as Ferguson (2012) points out not all of the measurements for reference Shields stress (τ_r^*) fall within the range of 0.030 to 0.086 as shown in Buffington et al. (1997). Ferguson (2012) also identifies that the Mueller et al. (2005) study contains values of reference Shields stress (τ_r^*) outside of the expected range. This study area also matched Mueller et al.'s (2005) results for slope dependent τ_{bf}^* since the amount of bankfull Shields stress is a function of slope. These results show that the slope driven bankfull Shields stress equations still produce consistent values when compared to D_{50} grain size dependent equations for bankfull Shields stress when working with smaller streams that have fully submerged roughness. This is shown by the close values of the predicted and measured D_{50} bankfull Shields stress as seen in Table 4. The ratio between the

slope dependent bankfull Shields stress (τ_{bf}^*) and reference Shields stress (τ_r^*) should be as Mueller et al. (2005) predicted and the bankfull Shields stress (τ_{bf}^*) should be slightly greater than the reference Shields stress (τ_r^*).

For this study area, the slope dependent bankfull Shields stress (τ_{bf}^*) is slightly greater than the reference Shields stress (τ_r^*). By following this convention of using slope as the main predictor for bankfull Shields stress (τ_{bf}^*) and reference Shields stress (τ_r^*) the outcome is as predicted bankfull Shields stress is slightly greater than the reference Shields stress for the entire study area. However, if bankfull Shields stress (τ_{bf}^*) for this study area is calculated using a grain size model, such as Equation 3 and demonstrated by the main approach herein, the predicted pattern is not obtained. The results obtained from this study show that not all of the cross-sections have a ratio of bankfull Shields stress (τ_{bf}^*) and reference Shields stress (τ_r^*) slightly above 1 as shown in Figure 100. A much greater number of them plot below the 1:1 line than what is found in Figure 1. Figure 100 only shows how bankfull Shields stress (τ_{bf}^*) and reference Shields stress (τ_r^*) plot against each other, whereas Figure 97 shows the ratio between bankfull Shields stress (τ_{bf}^*) and reference Shields stress (τ_r^*) plotted at their respective cross-section. On Figure 97 any cross-section where the ratio falls below 1 the amount of bankfull Shields stress (τ_{bf}^*) generated would not be sufficient to overcome the amount of reference Shields stress (τ_r^*) at that cross-section. Cross-sections where the 1:1 relationship is not exceeded are cross-sections 7, 8, 9, 12, 13, 14, 15, and 17 through 27 for D_{90} values and 7, 12, 14, 17, 18, 19, and 21 through 27 for D_{50} values. Figure 101 shows bankfull Shields stress (τ_{bf}^*) and reference Shields stress (τ_r^*) plotted against each other and the points are also shown to be either above or below cross-section 14, the midpoint of the longitudinal survey. This cross-

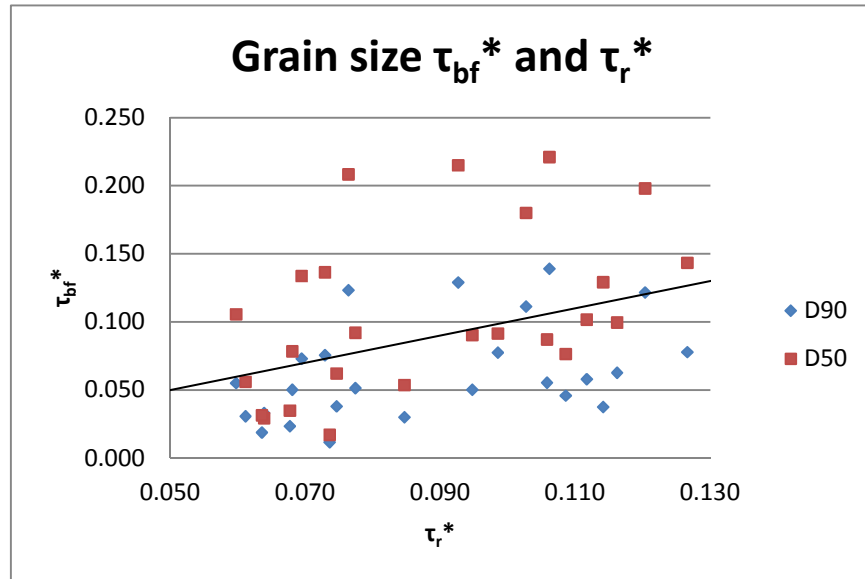


Figure 100. Relationship between grain size bankfull Shields stress (τ_{bf}^*) and reference Shields stress (τ_r^*) and 1:1 reference line.

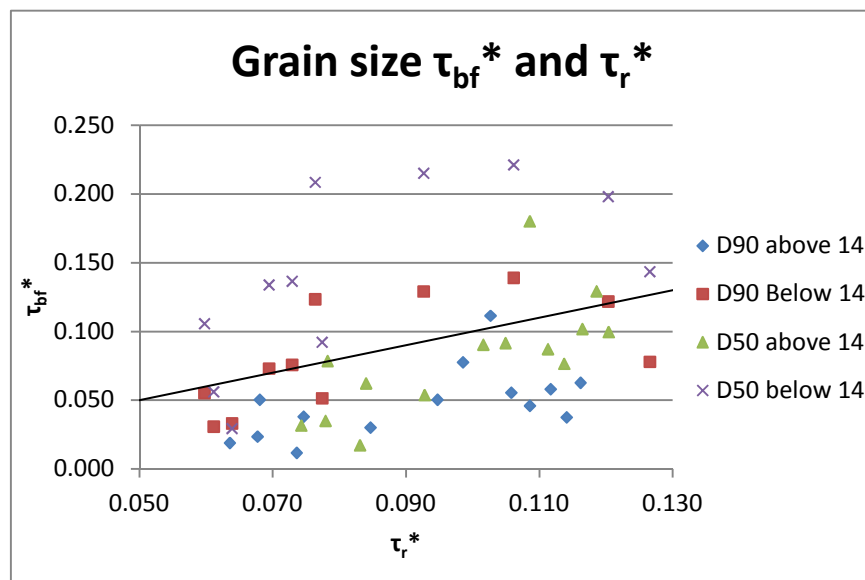


Figure 101. Relationship between grain size bankfull Shields stress (τ_{bf}^*) and reference Shields stress (τ_r^*) with points classed above and below cross-section 14 (midpoint on longitudinal survey) and 1:1 reference line.

section shows an almost perfect break for the D_{50} Shields stress measurements indicating a self-shaping stream.

Figure 97 and Figure 101 both show the stream is self-shaping in lower reaches of the study area and non-self-shaping in the upstream reaches. Figure 97 shows that the ratio of bankfull Shields stress (τ_{bf}^*) and reference Shields stress (τ_r^*) falls below 1 at cross-section 12 for the D_{90} and about cross-section 14 for the D_{50} . Figure 101 shows that for the D_{50} cross-section 14 is an appropriate location to show the break between the stream being self-shaping and being non-self-shaping. The stream after cross-section 14 becomes sufficiently wide and deep enough, have a low slope, and fine contain enough bed material to become self-shaping pass this cross-section. The biased shown to the D_{50} may also result from the data used to produce Equation 4 predominantly consisted of D_{50} measurements. As for the D_{90} measurements of bankfull Shields stress (τ_{bf}^*) this division is not as distinct as it is in the D_{50} measurements of bankfull Shields stress (τ_{bf}^*).

The slope within the study area does not vary much as shown in Figure 92. Consequently the amount of reference Shields stress (τ_r^*) within the channel will not vary much spatially within the study area. However, bankfull Shields stress (τ_{bf}^*) does vary significantly throughout the reach and is due to the increases in width and height of the water at bankfull as shown in Figures 91 and 92. These increases allow the amount of bankfull Shields stress (τ_{bf}^*) to increase moving downstream through the study area and eventually overcoming the amount of reference Shields stress (τ_r^*), and once this occurs the stream is then able to be self-shaping.

As discussed earlier, the amount of relative roughness of a grain also determines the amount of Shields stress on a grain, and the influence of submergence in shallow flows has been demonstrated in previous studies (Neill, 1967; Ashida et al., 1973; Bathurst et al., 1983, 1987;

Misri et al., 1983; Bettess, 1984; Suszka, 1991; Wiberg and Smith, 1991; Armanini, 1999; Lenzi et al., 2006). The depth within a channel increases as discharges increases, along with relative roughness and the ability to entrain larger grains allowing for motion due to reference Shields stress (τ_r^*) becoming smaller is shown in Figure 6 (Lenzi et al., 2006 Fig. 4, included as Figure 6 herein). The study area shows the same relationships between reference Shields stress (τ_r^*) and h/D_{90} or h/D_{50} as shown in Figure 102 for rivers with low slopes in the study conducted by Lenzi et al. (2006).

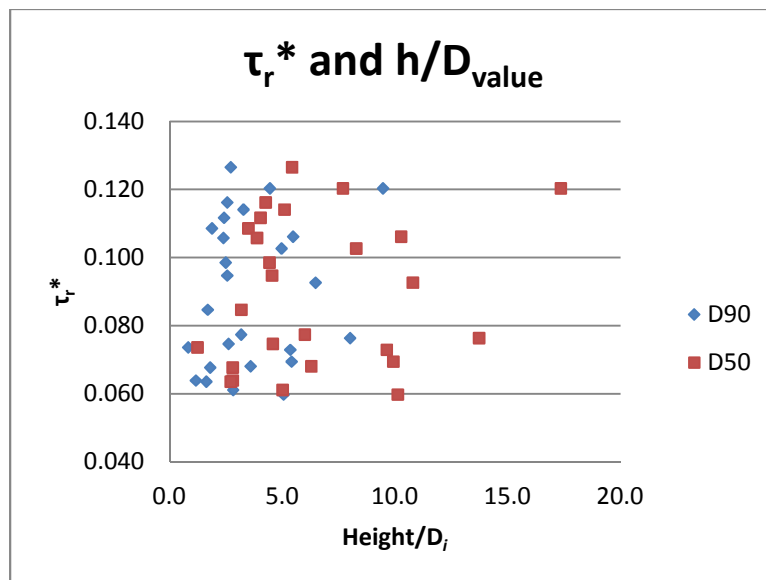


Figure 102. Relationship between τ_r^* and height/ D_{90} or height/ D_{50} .

For this study both D_{90} and D_{50} are used to talk about submergence and are presented in Table 2. Mueller et al. (2005) used data from streams where almost half of the streams were classified as having fully submerged roughness where the ratio of H and D_{84} is greater than 5 and the reference Shields stress (τ_r^*) is higher than 0.06. Figure 103 and 104 both show which cross-sections had fully submerged roughness for the D_{90} and D_{50} grain sizes. This study area mimicked these findings almost exactly. All of the cross sections had a reference Shields stress

(τ_r^*) value greater than 0.06, except for cross-section 8 which had a reference Shields stress (τ_r^*) of 0.06.

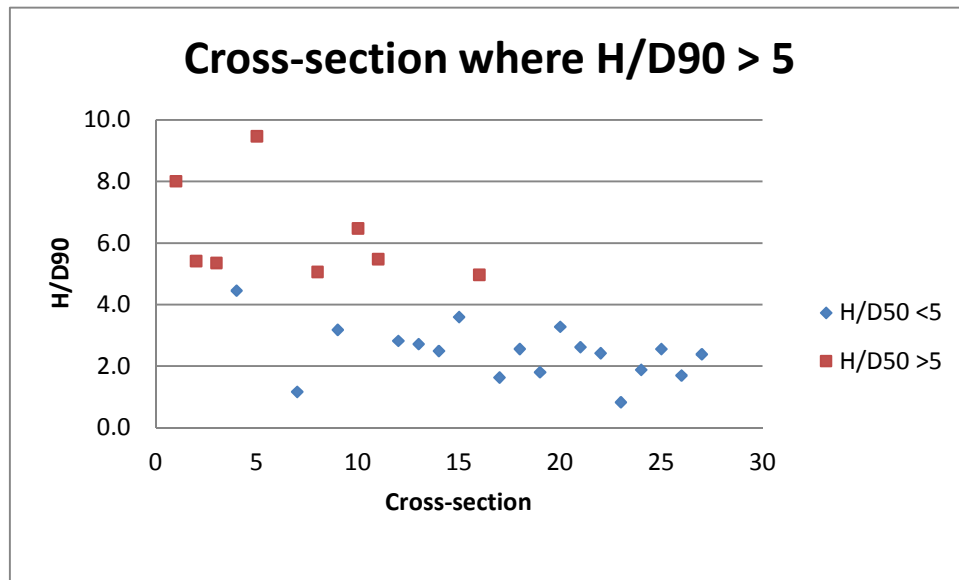


Figure 103. H/D_{90} for each cross-section showing greater than or less than 5.

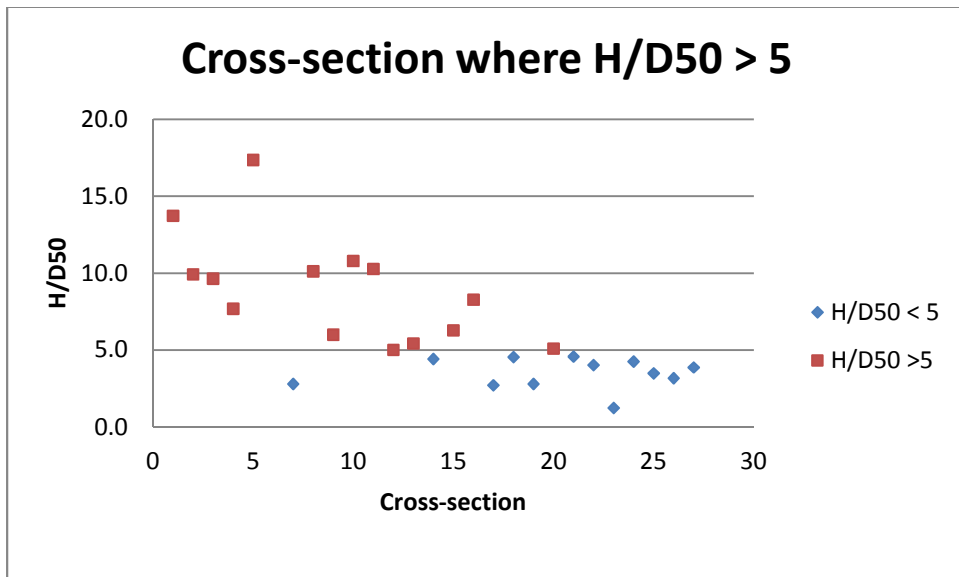


Figure 104. H/D_{50} for each cross-section showing greater than or less than 5.

Lenzi et al.'s (2006) study on when bedload transportation begins in steep streams found that the mobility of different particle sizes (reference Shields stress (τ_r^*)) in steep mountain streams is a function of both relative roughness and relative size, meaning that the transportation of different sizes grains is directly related to their size and the submergence of the grain. In this study cross-sections with fully submerged roughness ($H/D_i > 5$) the bankfull Shields stress (τ_{bf}^*) at that cross-section is greater than the reference Shields stress (τ_r^*) in all of the cross-sections except for 2. This only occurs for the D_{90} grain size at cross-section 8 and for the D_{50} grain size at cross-section 12. At cross-section 8 the H/D_{90} is 5.1 and the bankfull Shields stress (τ_{bf}^*) is lower than the reference Shields stress (τ_r^*) for the same grain size. And at cross-section 12 the H/D_{50} is 5.0 and the bankfull Shields stress (τ_{bf}^*) is lower than the reference Shields stress (τ_r^*) for the same grain size. One other cross-section of note is cross-section 4; at this location the bankfull Shields stress (τ_{bf}^*) is greater than the reference Shields stress (τ_r^*) and the roughness is not fully submerged. Cross-section 4 has an H/D_{90} ratio of 4.5. The study by Mueller et al. (2005) also contained streams where the roughness was not fully submerged and the bankfull Shields stress (τ_{bf}^*) is greater than the reference Shields stress (τ_r^*).

Once a grain becomes submerged other forces besides gravity begin to act on the grain. Figure 105 shows the different forces acting upon a grain on the surface of the channel. For this study only the hydrodynamic lift force, hydrodynamic drag force, and buoyancy are important and could play a role in grain movement (Gregoretti, 2008). In general resistance to flow increased as relative roughness increases and streams become steeper, smaller, and coarser near their headwaters, which affects the amount of reference Shields stress (τ_r^*) (Knighton, 1998; Bathurst, 2002; Mueller et al., 2005). Also in streams where the roughness is not fully

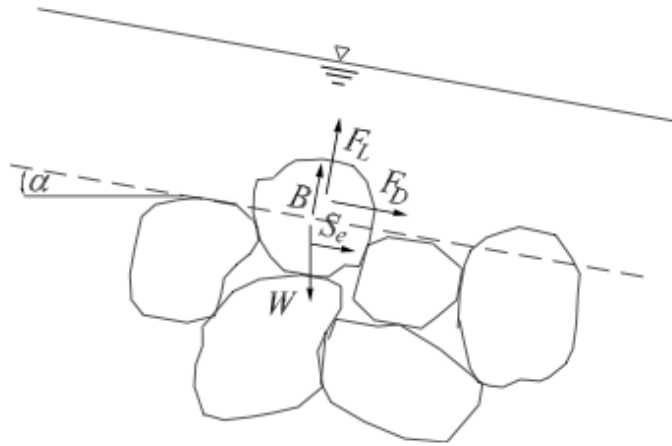


Figure 105. Forces acting upon a single submerged particle are the hydrodynamic drag force F_D , the longitudinal component of the weight $W \sin \alpha$, and the seepage force S_e , and in the normal direction to the flow, the grain is subject to the normal weight component $W \cos \alpha$, the buoyancy B , and the hydrodynamic lift force F_L (from Gregoretti, 2008, Figure 2).

submerged the flow is forced around the large grains and the drag force is exerted on the grain which greatly reduces the momentum of the water (Wiberg and Smith, 1991). Once the roughness of the bed is fully submerged gravity and the drag force are no longer the only forces acting on the particles making up the bed, as shown in Figure 105. The velocity profile also becomes logarithmic and the proportion of the drag force on the entire flow is reduced and the momentum of the water is increased once H/D_{84} becomes greater than 5 (Wiberg et al., 1991).

This study closely mimics the results presented by Mueller et al. (2005) except for some notable differences in the data. The biggest difference in this study occurred when comparing the differences between bankfull Shields stress (τ_{bf}^*) when calculated using a grain size dependent equation and when calculating bankfull Shields stress (τ_{bf}^*) using a slope dependent equation like the one used by Mueller et al. (2005). Buffington et al. (1997) showed that different method

for estimating Shields stress will yield different results when dealing with rough, turbulent flows that occur in gravel-bedded rivers. When using the slope dependent equation for both bankfull and reference Shields stress the results for this study match almost perfectly the results from the Mueller et al. (2005) study where bankfull Shields stress (τ_{bf}^*) is greater than the reference Shields stress (τ_r^*) in the study area.

However, if the grain size dependent equation is used then this relationship breaks down for the study area as seen in Figure 100. Figure 97 shows how the ratio between bankfull Shields stress (τ_{bf}^*) and reference Shields stress (τ_r^*) changes moving upstream through the study area. Eventually the channel is no longer able to maintain the trend of bankfull Shields stress (τ_{bf}^*) being slightly greater than reference Shields stress (τ_r^*) because bankfull Shields stress (τ_{bf}^*) decreases going upstream due to sediment becoming coarser, the slope becomes steeper, and the width and the height of the water at bankfull decreasing. All of these factors lead to a decrease in bankfull Shields stress (τ_{bf}^*) and the increase in the slope of the channel produces greater reference Shields stress (τ_r^*).

There are some discrepancies between this study and the Mueller et al.'s (2005) study with regard to bankfull Shields stress (τ_{bf}^*) calculation and its relation to reference Shields stress (τ_r^*). One possible reason for this could be due to the calculation of reference Shields stress (τ_r^*) used in this study. Ferguson (2012) showed that increases in critical Shields stress (τ_c^*) with slope for a given bed sorting cannot be predicted with a linear or simple power law due to scattering of the results away from actual measured values. The use of another predictor for reference Shields stress (τ_r^*) or actual field measurements of critical Shields stress (τ_c^*) may allow for better comparison to measurements of bankfull Shields stress (τ_{bf}^*) to determine if a stream is self-shaping or not.

The similarity in the data from the Mueller et al. (2005) study shows that the portions of the Conasauga match the conditions of the 45 other streams that are considered to be self-shaping. But the Conasauga is no longer found to be self-shaping in reaches where the relative roughness is not full submerged. The depth and width of the water play a crucial role in determining which reaches of the Conasauga were self-shaping. As the width and height of the stream increased the bankfull Shields stress also increased and eventually overcame the amount of reference Shields stress for the channel. This suggests a link between the ratio of height and width, regardless of submergence, to produce enough bankfull Shields stress to overcome the reference Shields stress. This would explain why Mueller et al. (2005) had streams without fully submerged relative roughness and still produced enough bankfull Shields stress to be self-shaping.

9. CONCLUSIONS

This work leads to a better understanding of river systems and how they become self-shaping. At this point there is a lot of information on self-shaping streams and mountain streams, but there is a lack of information pertaining the transition between the two. The relationship between τ_r^* and τ_{bf}^* , as shown in Figure 1, shows a clear relationship between the two which is indicative of self-shaping streams. This study helps to define a measurable set of parameters that indicate if a stream is self-shaping. The study also has expanded Figure 1 to the point that the relationship breaks down and is no longer maintained.

For the Conasauga River it is said to be self-shaping in areas where the relative roughness of the channel is completely submerged. Once the height of the water drops below the depth needed for full submergence of the relative roughness the bankfull Shields stress (τ_{bf}^*) falls

below the reference Shields stress (τ_r^*) of the channel. In the study conducted by Mueller et al. (2005) roughly half of the streams in the data set did not meet the conditions for fully submerged roughness and still were capable of producing greater amounts bankfull Shields stress (τ_{bf}^*) than the reference Shields stress (τ_r^*) of the channel. Others studies have shown that there is a link between relative submergence and transportation (Neill, 1967; Ashida et al., 1973; Bathurst et al., 1983, 1987; Misri et al., 1983; Bettess, 1984; Suszka, 1991; Wiberg and Smith, 1991; Armanini, 1999; Lenzi et al., 2006). However, this data also suggest that there is a link between width and height of the water at bankfull conditions and transportation of clast in the channel. Relative submergence of the grains may not play a major role in determining if a stream is self-shaping due to the prevalence of self-shaping streams without full submergence found in the data set presented by Mueller et al. (2005).

Due to the scope and time limitations of this project the link between fully submerged roughness and bankfull Shields stress (τ_{bf}^*) being slightly greater than the reference Shields stress (τ_r^*) could not be explored fully. However, there seems to be a link between the increase momentum from the logarithmic flow profile resulting from the fully submerged roughness and possible transportation (Wiberg and Smith, 1991). More work should be conducted on the relationship between fully submerged relative roughness and Shields stress in self-shaping streams. Another possible research avenue to pursue would be the link between height and width of the water at bankfull and transportation rates regardless of submergence. This study also shows more research is needed to be completed so that the relationships between grain size and slope dependent bankfull Shields stress and reference Shields stress (τ_r^*) estimations in mountain streams can be explored more thoroughly.

REFERENCES

- Andrews, E. D. (1983), "Entrainment of gravel from naturally sorted riverbed material." *Geologic Society of America Bulletin*. v. 94, no. 94: 1225–1231.
- Bathurst, J. C., W. H. Graf, and H. H. Cao (1983), "Initiation of sediment transport in steep channels with coarse bed material." *Mechanics of Sediment Transport*. 207 - 213.
- Bathurst, J. C. (2002), "At-a-site variation and minimum flow resistance for mountain rivers." *Journal of Hydrology*. v. 269, no. 1-2: 11 – 26.
- Bettess, R. L. (1984), "Initiation of sediment transport in gravel streams." *Proceedings of the Institution of the Civil Engineers*. Part 2. v. 77: 79 - 88.
- Brummer, C. J., D. R. Montgomery (2003), "Downstream coarsening in headwater channels." *Water Resources Research*. v. 39. no. 10: 1294. doi:10.1029/2003WR001981
- Buffington, J. M., and D. R. Montgomery (1997), "A systematic analysis of eight decades of incipient motion studies, with special reference to gravel-bedded rivers." *Water Resources Research*. v. 33, no. 8: 1993–2029.
- Carling, P. A. (1983), "Threshold of coarse sediment transport in broad and narrow natural streams." *Earth Surface Processes and Landforms*. v. 8, no. 1: 1–18.
- Clayton, J. A., (2010), "Local sorting, bend curvature, and particle mobility in meandering gravel bed rivers." *Water Resources Research*. v. 46, no. 2: W02601. doi:10.1029/2008WR007669
- Day, T. J., (1980), "A study of the transport of graded sediments." *Hydraulic Resources Station*.
- DuBoys, P. (1879), "Le Rhone et les Riveires a Lit Affouillable." *Annales des Ponts et Chaussees*. v. 18, no. 5: 141 - 195.
- Emmett, W. W. (1975), "The channels and waters of the Upper Salmon River area, Idaho." *U.S. Geology Survey Professional Paper*. 870-A.
- Engelund, F., and J. Fredsoe (1976), "A sediment transport model for straight alluvial channels." *Nordic Hydrology*. v. 7 no. 5: 293 - 306. doi:10.2166/nh.1976.019
- Ferguson, R. I. (2012), "River channel slope, flow resistance, and gravel entrainment thresholds." *Water Resources Research*. v. 48, W05517. doi:10.1029/2011WR010850.
- Garde, R. J. and K. G. Ranga Raju (2000), "Mechanics Of Sediment Transportation And Alluvial Stream Problems." Third edition: 183

- Gilbert, G. K. (1914), "The transportation of debris by running water." U.S. Geologic Survey Professional Paper. no. 86
- Grant, G. E., F. J. Swanson, and M. G. Wolman (1990), "Pattern and origin of stepped-bed morphology in high gradient streams, western Cascades, Oregon." Geological Society of America Bulletin. v. 102, no 3: 340 – 352.
- Gregoretti, C. (2008), "Inception Sediment Transport Relationships at High Slopes." Journal Of Hydraulic Engineering. v.134, no.11: 1620-1629.
- Goode, J. R., and E. Wohl (2010), "Substrate controls on the longitudinal profile of bedrock channels: Implications for reach-scale roughness." Journal of Geophysical Research. v. 115, no. F03018. doi: 10.1029/2008JF001188
- Harrelson, C. C., C. L. Rawlins, and J. P. Potyondy (1994), "Stream Channel Reference Sites: An Illustrated Guide to Field Technique." General Technical Report. no. 245
- Jarrett, R. D. (1984), "Hydraulics of high-gradient streams." Journal of Hydraulic Engineering, ASCE. v. 110, no. 11: 1519 - 1539. doi: 10.1061/(ASCE)0733-9429(1984)110:11(1519)
- Jarrett, R. D. (1990), "Hydrologic and hydraulic research in mountain rivers." Water Resource Bulletin. v. 26 no. 3: 419 - 429.
- Jiang, Z., and P. K. Haff (1993), "Multiparticle simulation methods applied to the micromechanics of bed load transport." Water Resources Research. v. 29 no. 2: 399–412. doi: 10.1029/92WR02063
- Knighton, A. D. (1998), "Fluvial Forms and Processes—A New Perspective." 383. Edward Arnold, London.
- Komar, P. D. (1987), "Selective grain entrainment by a current from a bed of mixed sizes: A reanalysis." Journal of Sedimentary Petrology. v. 57, no. 2: 203–211. doi: 10.1306/212F8AE4-2B24-11D7-8648000102C1865D
- Kramer, H. (1935), "Sand mixtures and sand movement in fluvial models." Transactions of the American Society of Civil Engineers. v. 100, no. 1: 798–878.
- Lamb, M.P., W.E. Dietrich, and J.G. Venditti (2008), "Is the critical Shields stress for incipient sediment motion dependent on channel-bed slope?" Journal of Geophysical Research. v. 113, no. F2. doi: 10.1029/2007JF000831

- Lenzi, M. A., L. Mao, and F. Comiti (2006), "When does bed load transport begin in steep boulder-bed streams?" *Hydrological Processes*. v. 20, no. 16: 3517 - 3533. doi: 10.1002/hyp.6168
- Luque, R. F., and R. van Beek (1976), "Erosion and transport of bed-load sediment." *Journal of Hydraulic research*. v. 14, no. 2: 127 - 144. doi:10.1080/00221687609499677
- Meyer, P. E., and R. J. Muller (1948), "Formulas for bed-load transport." *Proceedings 2nd International Association of Hydraulic Research, Stockholm*. 39 - 64.
- Misri, R. L., R. J. Grade, and K. G. Ranfa Raju (1983), "Experiments on bed load transport of nonuniform sands and gravels." *Proceedings 2nd International Symposium on River Sedimentation*. 440 - 450.
- Montgomery, D. R., and J. M. Buffington (1997), "Channel-reach morphology in mountain drainage basins." *Geological Society of America Bulletin*, May, 1997, v. 109, no. 5, p. 596-611, doi:10.1130/0016-7606(1997)109<0596:CRMIMD>2.3.CO;2
- Mueller, E., J. Pitlick, and J. M. Nelson (2005), "Variation in the reference Shields stress for bed load transport in gravel-bed streams and rivers." *Water Resources Research*. v. 41: W04006. doi:10.1029/2004WR003692
- Mueller, E., and J. Pitlick (2005), "Morphologically based model of bed load transport capacity in a headwater stream." *Journal of Geophysical Research*. v.110, no. F02016. doi:10.1029/2003JF000117
- Neill, C. R. (1967), "Mean velocity criterion for scour of coarse uniform bed material." *Proceedings 12th Congress of the International Association of Hydraulics Research*. no. 3: 46 - 54.
- Parker, G., and P. C. Klingeman (1982), "On why gravel bed streams are paved." *Water Resources Research*. v. 18, no. 5: 1409–1423. doi:10.1029/WR018i005p01409
- Parker, G. (1990), "Surface-based bed load transport relation for gravel rivers." *Journal of Hydraulic research*. v. 28, no. 4: 417 - 436. doi:10.1080/00221689009499058
- Parker, G., P. R. Wilcock, C. Paola, W. E. Dietrich, & J. Pitlick (2007), "Physical basis for quasi-universal relations describing bankfull hydraulic geometry of single-thread gravel bed rivers." *Journal of Geophysical Research*. v. 112, no. F4. DOI: 10.1029/2006JF000549
- Petit, F. (1994), "Dimensionless critical shear stress evaluation from flume experiments using different gravel beds." *Earth Surface Processes and Landforms*. v. 19, no. 6: 565 - 576.

- Pitlick, J., Y. Cui, and P. Wilcock (2009) "Manual for computing bed load transport in gravel-bed streams." General Technical Report. RMRS-GTR-223.
- Pizzuto, J. E. (1992) "The morphology of graded gravel rivers: A network perspective." *Geomorphology*. v. 5, no. 3-5: 457 - 474.
- Rice, S., and M. Church (1996) "Bed material texture in low order streams on the Queen Charlotte Islands, British Columbia." *Earth Surface Processes and Landforms*. v. 21, no. 1:1 - 18.
- Reid, Donald E., E. J. Hickin, and S. C. Babakaiff (2010) "Low-flow hydraulic geometry of small, steep mountain streams in southwest British Columbia." *Geomorphology*. v. 122, no. 1-2: 39 - 55. doi: 10.1016/j.geomorph.2010.05.012
- Reid, I., and L. E. Frostick (1984) "Particle interaction and its effects on the thresholds of initial and final bed load motion in coarse alluvial channel." *Sedimentology of Gravel and Conglomerates*. v. 10: 61 - 68.
- Reid, I., and L. E. Frostick (1986) "Dynamics of bed load transport in Turkey Brook, a coarse grained alluvial channel." *Earth Surface Processes and Landforms*. v. 11, no. 2: 143 - 155.
- Schumm, S.A. (1963) "A tentative classification of alluvial river channels." U.S. Geology Survey Circular. v. 477, no. 10.
- Shields, A. (1936) "Application of the Theory of Similarity and Turbulence Research to the Bed load Movement" *Preuss.Vers.Wasserbau Schiffbau*, 26th.
- Suszka, L. (1991) "Modification of transport rate formula for steep channels." *Fluvial Hydraulics of Mountain Regions*. v. 37: 1297 - 1312.
- Sutton, S. J. (1991) "Development of domainal slaty cleavage fabric at Ocoee Gorge, Tennessee." *The Journal of Geology*. v. 99, no. 6: 789 - 800.
- Thompson, C. and J. Croke (2008) "Channel Flow Competence and sediment transport in upland streams in southeast Australia." *Earth Surface Processes and Landforms*. v. 33, no. 3: 329 - 352. doi: 10.1002/esp.1558
- University of Georgia Automated Environmental Monitoring Network (2013) "Climate Averages." <http://www.griffin.uga.edu/aemn/cgi-bin/AEMN.pl?site=GAEL&report=cl> accessed on: January 15, 2013.

- United States Geological Survey (2012) "USGS 02384540 MILL CREEK NEAR CRANDALL, GA." http://waterdata.usgs.gov/usa/nwis/uv?site_no=02384540 accessed on: August 20, 2012
- White, C. M. (1940) "The equilibrium of grains on the bed of a stream." *Proceedings of the Royal Society of London A*. v. 174, no. 958: 322–338.
- Whiting, P. J., J. F. Stamm, D. B. Moog, and R. L. Orndorff (1999), "Sediment-transporting flows in headwater streams." *Geological Society of America Bulletin*. v. 111, no. 3: 450 - 466. doi: 10.1130/0016-7606(1999)111<0450:STFIHS>2.3.CO;2
- Wiberg, P. L., and J. D. Smith (1987) "Calculations of the critical shear stress for motion of uniform and heterogeneous sediments." *Water Resources Research*. v. 23, no. 8: 1471–1480. doi: 10.1029/WR023i008p01471
- Wiberg, P. L., and J. D. Smith (1991), "Velocity distribution and bed roughness in high-gradient streams." *Water Resources Research*. v. 27, no. 5: 825–838. doi: 10.1029/90WR02770
- Wilcock, P.R., and J.C. Crowe (2003), "Surface-based transport model for mixed-size sediment." *Journal of Hydraulic Engineering*. v. 129, no. 2: 120 - 128. doi: 10.1061/(ASCE)0733-9429(2003)129:2(120)
- Wohl, E. E., and A. Wilcox (2005), "Channel geometry of mountain streams in New Zealand." *Journal of Hydrology*. v. 300, no. 1-4: 252 - 266. doi:10.1016/j.jhydrol.2004.06.006
- Wohl, E. E. (2007), "Channel-unit hydraulics on a pool-riffle channel." *Physical Geography*. v. 28, no. 3: 233 – 248. doi: 10.2747/0272-3646.28.3.233
- Yalin, M. S., and E. Karahan,(1979) "Inception of sediment transport." *Journal of the Hydraulic Division Proceedings of the American Society of Civil Engineers*. v. 105, no 11: 1433–1443.